U.S. DEPARTMENT OF COMMERCE
National Technical Information Service

PB-256 925

A Generalized Water Quality Model for Eutrophic Lakes and Reservoirs

Battelle Pacific Northwest Labs.

Prepared For
Environmental Protection Agency

November 1974

001191

246068

PB 256 925

A GENERALIZED WATER QUALITY MODEL FOR EUTROPHIC LAKES AND RESERVOIRS

RECEIVED
APR 2 8 197
LIBRARY
Environmental Protection Agency
CINCINNATI, OHIO

(Revised)

NOVEMBER 1974

Battelle
Pacific Northwest Laboratories
Richland, Washington 99352

REPRODUCED BY
NATIONAL TECHNICAL
INFORMATION SERVICE
U. S. DEPARTMENT OF COMMERCE
SPRINGFIELD, VA. 22161

BIBLIOGRAPHIC DATA SHEET	1. Report No.	2.	3. Recipient's Accession No. PB-256 925

4. Title and Subtitle
A Generalized Water Quality Model for Eutrophic Lakes and Reservoirs

5. Report Date
Nov 74

6.

7. Author(s) R.G. Baca, M.W. Lorenzen, R.D. Mudd, and L.V. Kimmel

8. Performing Organization Rept. No.

9. Performing Organization Name and Address
Battelle Pacific Northwest Labs.
Richland, Washington

10. Project/Task/Work Unit No.

11. Contract/Grant No.

12. Sponsoring Organization Name and Address
Environmental Protection Agency
Washington, D.C.
Office of Research and Monitoring

13. Type of Report & Period Covered

14.

15. Supplementary Notes Sponsored in part by Environmental Protection Agency, Washington, D.C. Office of Research and Monitoring.

16. Abstracts

The project reported was undertaken in order to provide a multisegment deep reservoir water quality simulation model for the Environmental Protection Agency. The goals of the project were to modify and develop the multisegment deep reservoir hydrothermal and water quality models and to demonstrate their capabilities with data from American Falls Reservoir, Idaho.

17. Key Words and Document Analysis. 17a. Descriptors

*Water pollution,
*Lakes,
*Reservoirs,

Water quality management,
Mathematical models,
Thermal conductivity,
Dissolved oxygen,
Temperature,
Algae,
Nutrients,
Mathematical prediction,
Biochemical oxygen demand,
Decision making,
Seasonal variations,
Idaho.

17b. Identifiers/Open-Ended Terms

*Eutrophication,
Trophi- level,
Model studies,
*American Falls Reservoir.

17c. COSATI Field/Group 13 B

18. Availability Statement National Technical Information Service Springfield, Virginia 22161	19. Security Class (This Report) UNCLASSIFIED	21. No. of Pages 150p
	20. Security Class (This Page UNCLASSIFIED	22. Price 6.00/2.25

INSTRUCTIONS FOR COMPLETING FORM NTIS-35 (10-70) (Bibliographic Data Sheet based on COSATI Guidelines to Format Standards for Scientific and Technical Reports Prepared by or for the Federal Government, PB-180 600).

1. **Report Number.** Each individually bound report shall carry a unique alphanumeric designation selected by the performing organization or provided by the sponsoring organization. Use uppercase letters and Arabic numerals only. Examples FASEB-NS-87 and FAA-RD-68-09.

2. Leave blank.

3. **Recipient's Accession Number.** Reserved for use by each report recipient.

4. **Title and Subtitle.** Title should indicate clearly and briefly the subject coverage of the report, and be displayed prominently. Set subtitle, if used, in smaller type or otherwise subordinate it to main title. When a report is prepared in more than one volume, repeat the primary title, add volume number and include subtitle for the specific volume.

5. **Report Date.** Each report shall carry a date indicating at least month and year. Indicate the basis on which it was selected (e.g., date of issue, date of approval, date of preparation.

6. **Performing Organization Code.** Leave blank.

7. **Author(s).** Give name(s) in conventional order (e.g., John R. Doe, or J.Robert Doe). List author's affiliation if it differs from the performing organization.

8. **Performing Organization Report Number.** Insert if performing organization wishes to assign this number.

9. **Performing Organization Name and Address.** Give name, street, city, state, and zip code. List no more than two levels of an organizational hierarchy. Display the name of the organization exactly as it should appear in Government indexes such as USGRDR-I.

10. **Project/Task/Work Unit Number.** Use the project, task and work unit numbers under which the report was prepared.

11. **Contract/Grant Number.** Insert contract or grant number under which report was prepared.

12. **Sponsoring Agency Name and Address.** Include zip code.

13. **Type of Report and Period Covered.** Indicate interim, final, etc., and, if applicable, dates covered.

14. **Sponsoring Agency Code.** Leave blank.

15. **Supplementary Notes.** Enter information not included elsewhere but useful, such as: Prepared in cooperation with . . . Translation of . . . Presented at conference of . . . To be published in . . . Supersedes . . . Supplements . . .

16. **Abstract.** Include a brief (200 words or less) factual summary of the most significant information contained in the report. If the report contains a significant bibliography or literature survey, mention it here.

17. **Key Words and Document Analysis. (a). Descriptors.** Select from the Thesaurus of Engineering and Scientific Terms the proper authorized terms that identify the major concept of the research and are sufficiently specific and precise to be used as index entries for cataloging.
    (b). Identifiers and Open-Ended Terms. Use identifiers for project names, code names, equipment designators, etc. Use open-ended terms written in descriptor form for those subjects for which no descriptor exists.
    (c). COSATI Field/Group. Field and Group assignments are to be taken from the 1965 COSATI Subject Category List. Since the majority of documents are multidisciplinary in nature, the primary Field/Group assignment(s) will be the specific discipline, area of human endeavor, or type of physical object. The application(s) will be cross-referenced with secondary Field/Group assignments that will follow the primary posting(s).

18. **Distribution Statement.** Denote releasability to the public or limitation for reasons other than security for example "Release unlimited". Cite any availability to the public, with address and price.

19 & 20. **Security Classification.** Do not submit classified reports to the National Technical

21. **Number of Pages.** Insert the total number of pages, including this one and unnumbered pages, but excluding distribution list, if any.

22. **Price.** Insert the price set by the National Technical Information Service or the Government Printing Office, if known.

A GENERALIZED WATER QUALITY MODEL FOR EUTROPHIC LAKES AND RESERVOIRS

211B01602

By

R. G. Baca
M. W. Lorenzen
R. D. Mudd
L. V. Kimmel
PACIFIC NORTHWEST LABORATORIES
a Division of
BATTELLE MEMORIAL INSTITUTE
P. O. Box 999
Richland, Washington 99352

November 1974
(Revised)

Prepared for
OFFICE OF RESEARCH AND MONITORING
U.S. ENVIRONMENTAL PROTECTION AGENCY
WASHINGTON, DC 20460

ABSTRACT

The project reported herein was undertaken in order to provide a multisegment deep reservoir water quality simulation model for the Environmental Protection Agency. The goals of the project were to modify and develop the multisegment deep reservoir hydrothermal and water quality models and to demonstrate their capabilities with data from American Falls Reservoir, Idaho.

The computer models developed in this project provide a detailed portrayal of the dynamic processes which determine the trophic states in lakes and reservoirs. The models are formulated in terms of several key environmental variables: dissolved oxygen, biochemical oxygen demand, coliform bacteria, toxic material, algal populations and nutrient materials, and the major controlling factors: light, temperature, stream flows, and loading rates.

In this report the theoretical basis for the models is described in detail. The data collected for American Falls are summarized and compared to calculated results. Results of sensitivity analyses and model performance are also presented.

The model has produced excellent temperature simulations and good water quality simulations. Dissolved oxygen profiles were modeled quite well. However, more complete testing and verification of the nitrogen and phosphorus models would be desirable.

It was found that the model results are more sensitive to values of algal sinking velocities, benthic BOD, and diffusion coefficients than to other model parameters.

A separate document entitled "User's Manual: Hydrothermal and Water Quality Models" provides detailed instruction for model use.

Preceding page blank

CONTENTS

Page

ABSTRACT ii

FIGURES. iv

SECTION I: CONCLUSIONS. 1

SECTION II: RECOMMENDATIONS 2

  FUTURE MODEL REFINEMENT 2

  ADDITIONAL DATA COLLECTION. 3

  FURTHER CALIBRATION AND SENSITIVITY 3

SECTION III: INTRODUCTION 5

  GENERAL 5

  OBJECTIVE 5

SECTION IV: HYDROTHERMAL MODEL. 7

  MODELING APPROACH 7

  ENERGY TRANSPORT. 8

  ATMOSPHERIC HEAT EXCHANGES. 11

  FORMATION OF ICE COVER. 20

  HYDRAULICS OF STRATIFIED FLOWS. 22

  NUMERICAL SOLUTION TECHNIQUES 32

  COMPUTER PROGRAMS 34

SECTION V: WATER QUALITY MODEL. 36

  MODELING APPROACH 36

  CONSTITUENT TRANSPORT 39

  BIOCHEMICAL OXYGEN DEMAND 40

  NITROGEN. 40

  PHOSPHORUS. 42

  TOXIC SUBSTANCES. 44

  ALGAE 44

  ZOOPLANKTON 46

  REAERATION. 47

  DISSOLVED OXYGEN. 47

  COLIFORM BACTERIA 48

SUMMARY OF SUBMODEL CONSTANTS. 49
NUMERICAL SOLUTION METHODS 51
COMPUTER PROGRAM 53
SECTION VI: AMERICAN FALLS DATA. 55
SITE DESCRIPTION 55
DATA COLLECTION. 56
SECTION VII: MODEL APPLICATION AND RESULTS 68
APPLICATION OF THE HYDROTHERMAL MODEL. 68
APPLICATIONS OF THE WATER QUALITY MODEL. 68
DISCUSSION OF RESULTS. 80
Temperature 80
Dissolved Oxygen. 80
Phosphorus. 89
Nitrogen. 89
SECTION VIII: SENSITIVITY ANALYSIS 97
HYDROTHERMAL MODEL 98
Diffusion Constants 98
Element Thickness 102
WATER QUALITY MODEL. 102
Time Step 102
Algal Growth and Death Rates. 103
Sinking Velocities. 104
Diffusion Coefficients. 104
Reaeration. 105
Denitrification 105
Benthic BOD 105
Phosphorus Loss to Sediment 106
SECTION IX: FINAL REMARKS. 107
REFERENCES. 108
ACKNOWLEDGMENTS 112
APPENDIX A: SUMMARY OF AMERICAN FALLS DATA A-1

FIGURES

Figure **Page**

1 Geometric Representation for the Deep Reservoir Hydrothermal Model 8

2 Typical Control Volume. 8

3 Illustration of Densimetric Flow. 23

4 Conceptualization of a Withdrawal Zone. 27

5 Illustration of Withdrawal Layer Configurations. 29

6 Temperature and Density Structure for Application of Craya's Criteria 31

7 Summary of Water Quality Model Processes. 38

8 Study Area Showing Location of American Falls Reservoir. 55

9 Aerial Photograph of American Falls Dam 56

10 Plan View of American Falls Reservoir 57

11 Capacity Area Curves for American Falls Reservoir 58

12 Diagram of American Falls Segmentation. 58

13 Wind Speed, American Falls Reservoir, 1968. . . . 60

14 Atmospheric Vapor Pressure. 61

15 Dry Bulb Temperature. 62

16 Net Short Wave Solar Radiation. 63

17 Long Wave Atmospheric Radiation 64

18 Atmospheric Pressure. 65

19 Surface Elevation Versus Time, Observed and Initial Mass Balance 66

20 Segment 1-Surface Temperature Versus Time 69

21 Segment 2-Surface Temperature Versus Time 70

22 Segment 3-Surface Temperature Versus Time 71

23 Segment 1-Temperature Profiles for Given Julian Day. 72

24 Segment 1-Temperature Profiles for Given Julian Day. 73

25 Segment 2-Temperature Profiles for Given Julian Day. 74

26 Segment 2-Temperature Profiles for Given Julian Day. 75

27 Segment 2-Temperature Profiles for Given Julian Day. 76

28 Segment 3-Temperature Profiles for Given Julian Day. 77

29 Segment 3-Temperature Profiles for Given Julian Day. 78

30 Segment 3-Temperature Profiles for Given Julian Day. 79

31 Segments 2 and 3 Dissolved Oxygen Surface Concentrations History. 81

32 Dissolved Oxygen Profiles - Segment 1 82

33 Dissolved Oxygen Profiles - Segment 2 83

34 Dissolved Oxygen Profiles - Segment 3 86

35 Phosphorus Concentration Histories for Surface Layer - Segment 3 90

36 Phosphorus Profiles - Segment 3 91

37 Nitrogen History for Surface Layer - Segment 1 93

38 Nitrate Profiles - Segment 1. 94

39 Phytoplankton and Zooplankton Histories for Surface Layer - Segment 1 95

40 Phytoplankton and Zooplankton Profiles - Segment 1 96

41 Segment 3 - Diffusion Coefficient Variation Surface Temperature Versus Time 99

42 Temperature Versus Depth on Indicated Julian Day for Three Different Diffusion Coefficients. . . 100

A-1 Snake River Oxygen and BOD, 1968. . . . . A-1

A-2 Snake River Ammonia and Nitrite, 1968 . . . . A-2

A-3 Snake River Nitrate and Organic Nitrogen, 1968. . . . . A-3

A-4 Snake River Soluble and Organic Phosphorus, 1968. . . . . A-4

A-5 Snake River Phytoplankton and Zooplankton, 1968 . . . . A-5

A-6 Snake River *E. coli* and Toxic Compound, 1968. . . . . A-6

A-7 Tributary 1-Flow and Temperature, 1968. . . . . . A-7

A-8 Tributary 1-Dissolved Oxygen and BOD, 1968 . . . . A-8

A-9 Tributary 1-Ammonia and Nitrite, 1968 . . . . . . A-9

A-10 Tributary 1-Nitrate and Organic Nitrogen, 1968. . . . . A-10

A-11 Tributary 1-Soluble and Organic Phosphorus, 1968. . . . . A-11

A-12 Tributary 1-Phytoplankton and Zooplankton, 1968 . . . . A-12

A-13 Tributary 1-*E. coli* and Toxic Compound, 1968. . . . . A-13

A-14 Tributary 2-Flow and Temperature, 1968. . . . . . A-14

A-15 Tributary 2-Dissolved Oxygen and BOD, 1968 . . . . A-15

A-16 Tributary 2-Ammonia and Nitrite, 1968 . . . . . . A-16

A-17 Tributary 2-Nitrate and Organic Nitrogen, 1968. . . . . A-17

A-18 Tributary 2-Soluble and Organic Phosphorus, 1968. . . . . A-18

A-19 Tributary 2-Phytoplankton and Zooplankton, 1968 . . . . A-19

A-20 Tributary 2-*E. coli* and Toxic Compound, 1968. . . . . A-20

A-21 Tributary 3-Flow and Temperature, 1968. . . . . . A-21

A-22 Tributary 3-Dissolved Oxygen and BOD, 1968 . . . . A-22

A-23 Tributary 3-Ammonia and Nitrite, 1968 . . . . . . A-23

A-24 Tributary 3-Nitrate and Organic Nitrogen, 1968. . . . . A-24

A-25 Tributary 3-Soluble and Organic Phosphorus, 1968. . . . . A-25

A-26 Tributary 3-Phytoplankton and Zooplankton, 1968 . . . . A-26

A-27 Tributary 3-*E. coli* and Toxic Compound, 1968. . . . . A-27

A-28 Segment 1-Surface Temperature Versus Time A-28

SECTION I

CONCLUSIONS

The objectives of this project have been achieved with the development and demonstration of the multisegment Deep Reservoir Models. Both the hydrothermal and water quality modules have been shown to be completely operational and ready for general use in water resource studies. Application of the models to American Falls Reservoir yielded these major conclusions:

- The multisegment hydrothermal model can accurately predict vertical temperature profiles in a reservoir with little or no subjective effort.
- The hydrothermal model requires only standard meteorological data to accurately predict seasonal temperature variations.
- The multisegment water quality model can realistically simulate the natural seasonal patterns of algal growth and death and nutrient cycling.
- The water quality model can reasonably predict the DO-BOD dynamics in reservoirs and impoundments.

It is anticipated that these computer models will provide an important decision-making tool for assessing future trophic states of reservoirs and lakes as functions of nutrient inputs, waste loadings, and hydraulic and hydrologic site characteristics. Other potential applications of these models are:

- Waste allocation studies
- Evaluation of waste discharge impacts
- Management of reservoir operations
- Preimpoundment analyses
- Nutrient diversion and lake recovery studies

These models, when applied by experienced analysts, can be used to find sound and economical solutions to the complex problems of water resources management.

SECTION II

RECOMMENDATIONS

Three areas of further work are recommended in order to enhance the general reliability and usefulness of the water quality model: 1) model refinements, 2) additional data collection, and 3) further calibration and sensitivity runs.

In addition to these recommendations, qualified suggestions can be made for improving water quality at American Falls Reservoir.

FUTURE MODEL REFINEMENT

The present model as applied to American Falls Reservoir requires relatively large amounts of computer time (7 minutes for a 3-segment, 7-1/2-month simulation on Univac 1108) for the quality model alone. This time is not entirely intrinsic to the code but results from special problems at American Falls. However, it is felt that further modifications to the numerical solution algorithm would allow longer time steps reducing computer time requirements.

It is also recommended that more than one species of algae be added to the quality model. The large concentrations of algae calculated for American Falls result partially from the buoyant properties of Aphanizomenon during part of the growth phase. It would be valuable for general application to evaluate simultaneously the effect of different growth rates, nutrient requirements, and physical properties of algal cells on predicted results.

It would also be desirable to add an additional zooplankton species with different growth parameters and feeding habits.

ADDITIONAL DATA COLLECTION

Growth and decay of algae are important processes which significantly affect water quality. Unfortunately, very limited data on observed algal populations were available. It is strongly recommended that weekly chlorophyll profiles be measured at a minimum of three locations in the reservoir for an entire summer. This information is needed to properly calibrate the water quality model. In addition, the attenuation coefficient of the water should be determined and light profiles should be measured in conjunction with the chlorophyll determinations.

The methods used to estimate ice cover are somewhat crude, and thus require sufficient field data for refinement. It is therefore recommended that surveys of ice thickness be made throughout the winter. Oxygen profiles should also be collected during these surveys.

The fate of nitrogen and phosphorus input to the reservoir is not clear. There are apparently large losses of both nitrogen and phosphorus. The losses were modeled by increasing denitrification rates and phosphorus losses to the sediments. It would be beneficial to analyze several sediment core samples for both phosphorus and nitrogen concentrations.

FURTHER CALIBRATION AND SENSITIVITY

All water quality simulation models improve with use. As additional information about important processes and reaction rates, as well as boundary conditions, is collected further refinements in calculations can be made. With refined computational procedures and more complete field data, confidence in model predictions improves.

Additional sensitivity analysis will indicate the parameters and processes which should be studied in more detail. It is suggested that the sensitivity of model predictions to changed flow regimes and waste loads be investigated.

Since the thermal regime in American Falls Reservoir is predominantly nonstratified, it would be valuable to examine the performance of the hydrothermal model on other systems more strongly stratified. There are several lakes and reservoirs such as Lake Washington, Lake Mendota, Lake Tahoe, and Detroit Reservoir (Oregon) with complete data. Application of the model to two or three of these lakes would provide an excellent basis for a benchmark study.

SECTION III

INTRODUCTION

GENERAL

Under a previous contract[1] with the Environmental Protection Agency, Battelle-Northwest developed a general water quality model for river basins. The objective of the previous project was to incorporate the best available models for each phenomenon or water quality parameter into an integrated model which could be generally applied to river basins. The model was designed to handle river reaches, stratified reservoirs, and tidally influenced estuaries. The portions of the model designed for rivers and estuaries were calibrated and verified on the Willamette River Basin in Oregon. However, the portion of the model designed for application to stratified reservoirs was not completed.

The multisegment deep reservoir hydrothermal model, which was to be integrated with a multisegment water quality model, was found to be inoperable. Due to time and funding limitations the problems encountered were not successfully overcome.

The project reported herein was undertaken in order to have a multisegment deep reservoir water quality model available to the EPA.

The computer models developed in this project are capable of realistically simulating the thermal regime and water quality dynamics of stratified lakes and reservoirs. The principal environmental variables used in the models include: 1) water flows, 2) temperature, 3) solar radiation, 4) dissolved oxygen, 5) total and benthic BOD, 6) phytoplankton, 7) zooplankton, 8) nitrogen and phosphorus, 9) toxic material, and 10) coliform bacteria. The hydrothermal and water quality models provide a detailed portrayal of the chemical and biological transformations of an aquatic ecosystem and the main controlling factors.

OBJECTIVE

The purpose of the project was to modify and develop the multisegment deep reservoir hydrothermal and water quality models and to demonstrate their capabilities with data from American Falls Reservoir, Idaho.

This report documents the model development and application to American Falls Reservoir. The theoretical basis of the models developed in this work are presented in Sections IV and V. The data used in modeling American Falls Reservoir are presented in Section VI and model application and results in Section VII. Results of sensitivity analyses are presented in Section VIII.

A separate document entitled "User's Manual: Hydrothermal and Water Quality Models" provides detailed instructions for model use.

SECTION IV

HYDROTHERMAL MODEL

Atmospheric energy exchanges with a water body, coupled with the internal heat transport, are highly significant factors affecting water quality. These heat exchanges are intimately associated with the mass transport properties and hydrodynamic characteristics of the water mass. Aquatic chemistry factors, such as reactivity, solubility, and stabilization, are often temperature-dependent as are most biological processes, all of which interrelate to mass transport processes. The combined effects of temperature and mass properties in turn are interrelated to specific hydrodynamic characteristics such as buoyancy or gravity currents and degrees and types of stratification.

This section presents a description of the hydrothermal component of the deep reservoir model. The computer model is a modified and refined version of the original Water Resources Engineers' multisegment program.[2] The principal merits of this hydrothermal model are its 1) efficiency of computation and 2) quasi-two-dimensional description of flow and temperature patterns.

MODELING APPROACH

The complete mathematical formulation of the hydrothermal model is based on a simple conceptual representation of the system geometry. A three-dimensional body of water is represented by a set of segments, each of which is made up of a set of horizontal layers. Figure 1 illustrates this representation.

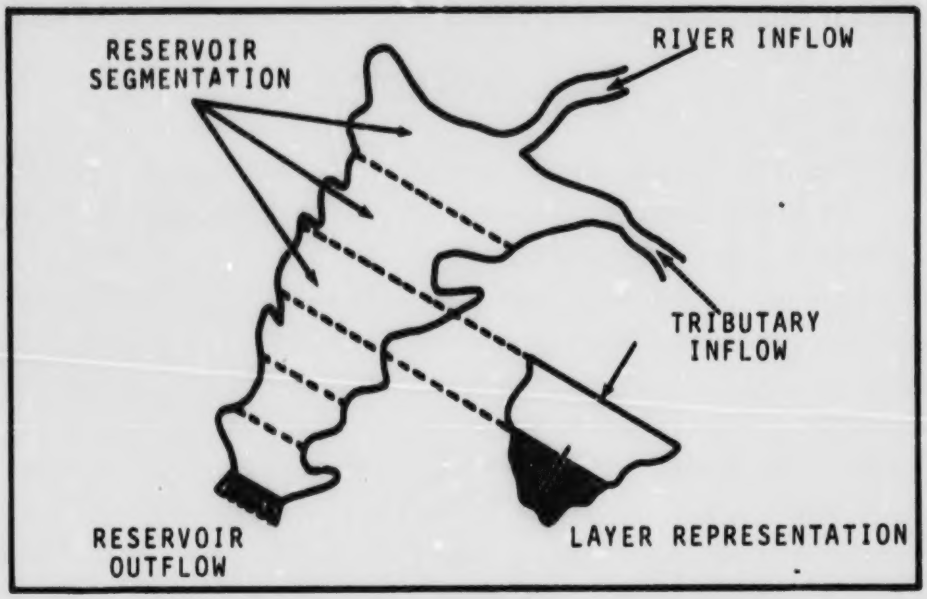
RESERVOIR
SEGMENTATION
RIVER INFLOW
TRIBUTARY
INFLOW
RESERVOIR
OUTFLOW
LAYER REPRESENTATION

FIGURE 1. Geometric Representation for the Deep Reservoir Hydrothermal Model

ENERGY TRANSPORT

On the basis of this segment-layer representation, the transport of thermal energy in the reservoir is expressed by a two-dimensional heat balance in which longitudinal diffusion is neglected. The governing equation describing the spatial and temporal temperature variations may be derived by considering a typical control volume or layer, as shown below:

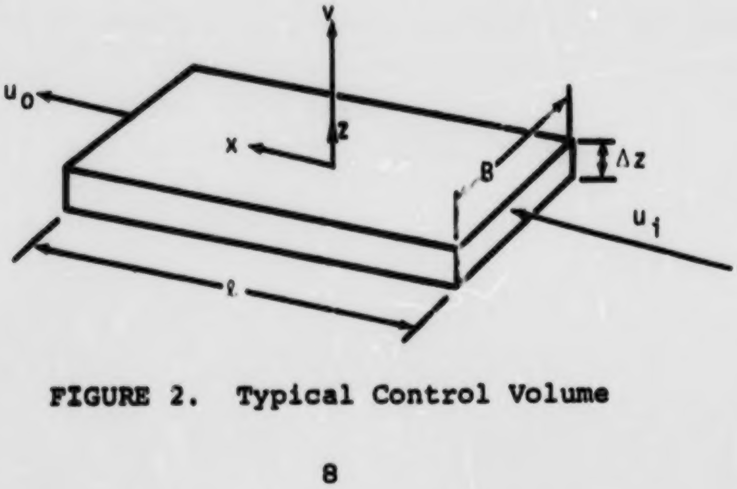
v
u_o
z
x
B
Δz
u_i
ℓ

FIGURE 2. Typical Control Volume

An energy balance on such a control volume would require:

Internal Heat Balance

$$\underset{\text{(accumulation)}}{\rho c \frac{\partial T}{\partial t} B\Delta z \ell} = \underset{\text{(vertical advection)}}{- \rho c\, B\ell \left[(vT)_{z+\Delta z} - (vT)_z \right]}$$

$$\underset{\text{(vertical diffusion)}}{+ B\ell \left[(q)_z - (q)_{z+\Delta z} \right]}$$

$$\underset{\text{(horizontal advection)}}{+ B\Delta z\, (\rho_i c u_i T_i - \rho c u_o T)}$$

$$\underset{\text{(volumetric heat source)}}{+ B\ell \Delta z H'} \qquad (1)$$

where

T = temperature
ρ = water density
c = specific heat
q = diffusion heat flux
H' = internal heat source
u_i, u_o = horizontal inflow and outflow velocities
v = vertical velocity

Dividing through by $B\Delta z\ell$ and taking the limit as $\Delta z \to 0$,

$$\rho c \frac{\partial T}{\partial t} = - \rho c \frac{\partial (vT)}{\partial z} - \frac{\partial q}{\partial z} + \frac{c}{\ell} (\rho_i u_i T_i - \rho u_o T) + H' \qquad (2)$$

If a Fickian form of diffusion is assumed, i.e.,

$$q = - \varepsilon \frac{\partial T}{\partial z} \qquad (3)$$

Then

$$\rho c \frac{DT}{Dt} = - \rho c T \frac{\partial v}{\partial z} + \frac{\partial}{\partial z} (\varepsilon \frac{\partial T}{\partial z}) + \frac{c}{\ell} (\rho_i u_i T_i - \rho u_o T) + H' \qquad (4)$$

The left-hand term is the substantial derivative.

If, in addition,

$$\rho_i = \rho \quad (5)$$

$$\frac{\partial v}{\partial z} = 0 \quad (6)$$

$$\frac{\partial \varepsilon}{\partial z} = 0 \quad (7)$$

The more concise expression is obtained:

$$\rho c \frac{DT}{Dt} = \varepsilon \frac{\partial^2 T}{z^2} + \frac{\rho c}{\ell} (u_i T_i - u_o T) + H' \quad (8)$$

In terms of volumetric flow rates, this equation can be written as

$$\rho c \left[\frac{\partial T}{\partial t} + \frac{Q_v}{B\ell} \frac{\partial T}{\partial z}\right] = \varepsilon \frac{\partial^2 T}{\partial z^2} + \frac{\rho c}{\ell B \Delta z} (Q_{h,i}\, T_i - Q_{h,o}\, T) + H' \quad (9)$$

For convenience let $\alpha = \frac{\varepsilon}{\rho c}$ (diffusivity); then

$$\rho c \left[\frac{\partial T}{\partial t} + \frac{Q_v}{B\ell} \frac{\partial T}{\partial z}\right] = \rho c \alpha \frac{\partial^2 T}{\partial z^2} + \frac{\rho c}{\ell B \Delta z} (Q_{h,k}\, T_i - Q_{h,o}\, T) + H' \quad (10)$$

Dividing through by ρc and using $A = B\ell$ gives the final expression for the heat balance:

Heat Equation

$$\frac{\partial T}{\partial t} + \frac{Q_v}{A} \frac{\partial T}{\partial z} = \alpha \frac{\partial^2 T}{\partial z^2} + \frac{1}{A \Delta z} (Q_{h,i}\, T_i - Q_{h,o}\, T) + \frac{1}{\rho c} H' \quad (11)$$

The vertical mixing and exchange process which is known to occur between epilimnion and hypolimnion is accounted for in the model by the use of a variable diffusivity coefficient:

Diffusivity Coefficient

$$\alpha = a_1 + a_2 v_w e^{-\frac{4.6}{d}(z_s - z)} \quad (12)$$

where

a_1, a_2 = empirical constants m^2/sec,m
v_w = wind speed, m/sec
d = thermocline depth, m
z_s = water surface elevation, m
z = elevation of the j-th element, m

Specific values for the empirical constants were determined for American Falls Reservoir to be $a_1 = 1. \times 10^{-5}$ and $a_2 = 1. \times 10^{-4}$. In the heat equation, the volumetric source term H' represents the sum of component energy sources due to atmospheric heat exchange which are discussed in the next section.

In solving Equation 11 numerically, it is assumed that the top and bottom surfaces of the segment are insulated. Mathematically this means that

$$\left.\frac{\partial T}{\partial z}\right|_{\text{bottom}} = \left.\frac{\partial T}{\partial z}\right|_{\text{surface}} = 0 \qquad (13)$$

In addition, the net atmospheric heat exchange at the air-water interface is converted into a single volumetric heat source and assigned to the top layer (with the exception of net shortwave radiation, which is distributed vertically according to Beer's law). Although these boundary conditions are not entirely satisfactory from a theoretical point of view, they simplify the computational problem considerably; numerical experiments have shown them to be quite workable. Numerical methods employed to solve the heat equation are discussed in later sections.

ATMOSPHERIC HEAT EXCHANGES

Various energy transfer phenomena occur at the interface between the atmosphere and the particular water body. The external transfer of heat energy across the air-water interface is accomplished by three basic mechanisms: radiation (solar and atmospheric), evaporation, and convection. The net external heat exchange may be expressed as the algebraic sum of the several component energy fluxes.

Atmospheric Heat Balance

$$Q_n = Q_s - Q_{sr} + Q_a - Q_{ar} - Q_{br} - Q_e + Q_c \qquad (14)$$

where

Q_n = net surface heat flux , Kcal/m^2-hr

Q_s = shortwave radiation incident to the water surface

Q_{sr} = reflected shortwave radiation

Q_a = incoming longwave radiation from the atmosphere

Q_{ar} = reflected longwave radiation

Q_{br} = back radiation emitted by the body of water

Q_e = energy utilized by evaporation

Q_c = energy convected to or from the body of water at the surface

Most of these components of the atmospheric heat exchange are not routinely measured; however, the work of many investigators has provided a variety of semitheoretical and empirical relationships which predict the individual heat exchanges. Several comprehensive reviews of accepted prediction techniques are available in the technical literature.[3,4] In this section a summary of the specific relationships used in the hydrothermal model is presented.

The net shortwave radiation which is absorbed by a water body is simply the sum of the incident and reflected components, Q_s and Q_{sr}, respectively. Incident radiation is a standard meteorologic parameter measured and recorded by the U.S. Weather Bureau. If data are not available, net shortwave radiation may be computed by the following equation:

Net Shortwave Radiation

$$Q_{sn} = Q_o \left[\frac{a'' + 0.5\ (1 - a' - d)}{1 - 0.5\ R_{s_o}\ (1 - a' + d)} \right] (1 - 0.65C^2)\ (1 - R_s) \qquad (15)$$

where

Q_{sn} = net shortwave radiation flux, kcal/m^2-hour

Q_o = extraterrestrial radiation flux

a" = mean atmospheric transmission coefficient after scattering and absorption, a function of optical air mass and mean daily precipitable water content

a' = mean atmospheric transmission coefficient after scattering, a function of optical air mass and mean daily precipitable water content

d = total dust attenuation, a function of optical air mass, location, and season ($0.03 \leq d \leq 0.13$)

C = percent cloud cover (decimal)

R_{s_o} = reflectivity of the water surface to shortwave radiation under prevailing sky conditions

$$= A \left[\frac{180\ \alpha}{\pi}\right]^B, \quad 0.35 \leq A \leq 1.18, \ -0.97 \leq B \leq -0.45 \tag{16}$$

where

α = altitude of the sun in radians

$$= \arcsin \left[\sin \frac{\pi\phi}{180} \sin \delta t + \cos \frac{\pi\phi}{180} \cos \delta \cos \frac{\pi t}{12}\right] \tag{17}$$

The extraterrestrial radiation, Q_o, is given by:

$$Q_o = \frac{I_o}{r^2} \left[(\sin\phi \sin\delta) \quad (\dagger_e - \dagger_b) + \frac{12}{\pi} (\cos\phi \cos\delta) \right.$$

$$\left. \left(\sin \frac{\pi\dagger_e}{12} - \sin \left(\frac{\pi\dagger_b}{12}\right)\right)\right] \Gamma \tag{18}$$

with

$$r = 1 + 0.017 \cos \left[\frac{2\pi}{365} (186-D)\right] \tag{19}$$

$$\delta = \frac{23.45}{180} \pi \quad \cos\left[\frac{2\pi}{365} \quad (172-D)\right] \tag{20}$$

$$\dagger_b = ST_b - \Delta\dagger_s + ET - 12 \tag{21}$$

$$t_e = ST_e - \Delta t_s + ET - 12 \tag{22}$$

$$\Delta t_s = \frac{\varepsilon}{15} (L_{sm} - L_{lm}) \tag{23}$$

$$ST_r = 12 - \frac{12}{\pi} \arccos \left[\tan \left(\frac{\pi \phi}{180}\right) \ \tan \left(\frac{\pi \delta}{180}\right)\right] + \Delta t_s + \Delta t_{OR} \tag{24}$$

$$ST_s = 24 - ST_r + 2\ \Delta t + \Delta t_{OR} - \Delta t_{OS} \tag{25}$$

where

l_o = solar constant, 1164 kcal/m^2-hr

r = ratio or the actual and mean distances between the sun and the earth

D = number of the day of the year

ϕ = latitude of the site, degrees

δ = declination of the sun, degrees

t_b, t_e = hours angles corresponding to the beginning and end, respectively, of any time interval between sunrise and sunset

Γ = a correction factor for diurnal exposure to radiation flux ($\Gamma = 0$ when $ST_s \leq ST_b$ or $ST_e \leq ST_r$, and $l = 0$ when $ST_r \leq ST_b$ or $ST_e \leq ST_s$)

ST_b, ST_e = standard times at the beginning and end of the time interval chosen for temperature analysis

ET = equation of time from a solar emphemeris, hours

ST_r, ST_s = the standard times of sunrise and sunset, respectively

Δt_s = difference between standard and local civil time in hours

ε = constant ($\varepsilon = -1$ for west longitude, $\varepsilon = +1$ for east longitude)

L_{sm}, L_{lm} = longitude of standard and local meridians, respectively

Δt_{OR}, Δt_{OS} = hour corrections for obstructions of sunrise and sunset, respectively

In addition, the mean atmospheric transmission coefficient, a", is given by:

$$a'' = \exp\left[-(0.465 + 0.134\, w)\,(0.179 - 0.421 \exp(-0.721\, m))\, m\right] \quad (26)$$

where m, the optical air mass, and w, the water content, are given by:

$$m = \frac{10^{-Z^{*}/19,000}}{\sin\alpha + 0.15\left(\frac{180\,\alpha}{\pi} + 3.885\right)^{-1.253}} \quad (27)$$

$$w = 0.86 \exp\left[-0.111 + 0.0614\,\overline{\theta}_d\right] \quad (28)$$

in which

Z^* = altitude of the site in meters

α = sun's altitude in radians

$\overline{\theta}_d$ = mean daily dew point (°C)

Similarly, the mean transmission coefficient, a', is expressed by the empirical equation:

$$a' = \exp\left[-(0.465 + 0.134\, w)\,(0.129 + 0.171 \exp(-0.880 m))\, m\right] \quad (29)$$

All variables are as previously defined.

Long-wave atmospheric radiation which is emitted by the earth's surface is absorbed by layers of the atmosphere and then reradiated to the earth and/or into space. Unlike solar radiation, atmospheric radiation is present at night as well as during the day. Net atmospheric radiation is that part of the long-wave component which is actually absorbed by a water body, accounting for losses by reflection, or simply the algebraic sum of Q_a and Q_{ar}. The net atmospheric flux, Q_{at}, may be expressed in terms of the empirical equation:

Net Atmospheric Radiation

$$Q_{at} = [0.937 \times 10^{-5}]\,\sigma(T_2)^6\,(1 + 0.17C^2)\,(1-R_L) \quad (30)$$

where

Q_{at} = net atmospheric radiation flux, kcal/m^2-hour

σ = Stefan-Boltzman constant, 4.885×10^{-8} kcal/m^2-hour -°Kelvin^4

T_2 = absolute air temperature at a level of 2 meters above the reservoir surface, °K

R_L = reflectivity of the water surface for atmospheric radiation, = 0.03

Long wave back radiation emitted by the water body is characterized by the Stefan-Boltzman fourth-power radiation law. Thus, back radiation is a function of the absolute temperature of the water at the surface.

Water Surface Radiation

$$Q_{br} = 0.873\ \sigma\ T_w^4 \qquad (31)$$

where

Q_{br} = water surface radiation, kcal/m^2-hour

σ = Stefan-Boltzman constant

T_w = absolute temperature of the water surface, °K

Energy utilized by evaporation is a major component of the heat budget and can often account for 40 to 70 percent of the energy flux from the water body. The general formulation of this term is:

Evaporation Energy Loss

$$Q_e = \rho_w\ (597 - 0.57\ T_w)[(a + bU_2)\ (e_o - e_{a2})] \qquad (32)$$

where

Q_e = energy loss by evaporation, kcal/m^2-hour

ρ_w = density of water, kg/m^3

T_w = temperature of water surface, °C

a, b = empirical constants

U_2 = wind velocity at a height of two meters, m/hour

e_o = saturation vapor pressure of the air at the temperature of the water surface, mb

e_{a2} = water vapor pressure at a height of two meters above ground on the upwind shore

and

$$e_{a2} = e_{a2s} - [0.00066(1+0.00115T'_{a2})] (T_{a2}-T'_{a2}) p \qquad (33)$$

in which

e_{a2s} = saturation vapor pressure at the wet bulb temperature of the air mb

T_{a2} = dry bulb air temperature at a height of two meters, °C

T'_{a2} = wet bulb air temperature at a height of two meters, °C

p = local barometric pressure, mb

The convective heat flux, Q_c, or sensible heat is related to the same variables as the evaporation term. This component is computed from the semi-empirical equation:

Convective Energy Flux

$$Q_c = R\, Q_e$$

with

$$R = 6.1 \times 10^{-4} p \frac{T_w - T_a}{e_o - e_a} \qquad (34)$$

where

Q_c = convective heat loss or gain kcal/m^2-hour

R = Bowen ratio

T_w = water surface temperature, °C

T_a = air temperature, °C

e_o = saturated vapor pressure at water surface temperature, mb

e_a = vapor pressure at point of wind speed observation, mb

All other terms are as previously defined.

With the knowledge of nine basic meteorologic parameters: (1) atmospheric pressure, (2) sky cover, (3) wind speed, (4) dry bulb air temperature, (5) wet bulb air temperature, (6) dew point temperature, (7) shortwave solar radiation, (8) relative humidity, and (9) water temperature, the previous analytical relationships are used directly to estimate the overall heat exchange between a water body and the atmosphere. A relative comparison of the amount of heat loss or gain by each component of the heat budget is shown in Table 1.

TABLE 1. Comparison of Amount of Heat Loss and Gain by Various Components of Atmospheric Heat Balance

Component	Symbol	Range of Heat Loss or Gain ($kcal/m^2$-hour)
Shortwave Solar Radiation	Q_s	30 to 300
Reflected Shortwave	Q_{sr}	5 to 25
Net Shortwave	$Q_{sn}=Q_s-Q_{sr}$	25 to 375
Longwave Atmospheric Radiation	Q_a	225 to 360
Reflected Longwave	Q_{ar}	5 to 15
Net Longwave	$Q_{at}=Q_a-Q_{ar}$	220 to 345
Net Surface Radiation	Q_b	225 to 400
Evaporative Heat Loss	Q_e	25 to 900
Convective Heat Loss or Gain	Q_c	-35 to 50

It is important to note that the components Q_s, Q_{sr}, Q_a, and Q_{ar} are independent of water surface temperature while Q_b, Q_e, and Q_c are explicit functions of water temperature.

In addition to the equations previously presented, various miscellaneous relationships are used in the hydrothermal model which are summarized here:

Beer-Lambert Law

$$I_j = I_o e^{-k(H - Z_j)} \tag{35}$$

where

I_j = intensity of solar radiation on a plane at elevation Z_j, Kcal $m^{-2}sec^{-1}$

k = extinction coefficient, m^{-1}

I_o = intensity of solar radiation on a plane at elevation H, Kcal $m^{-2}sec^{-1}$

H = elevation 0.3 m below the reservoir surface, m

Z_j = elevation of plane j, m

Saturation Vapor Pressure

$$e_s = 2.1718 \times 10^8 \exp(-4157.0/(239.09 + T)) \tag{36}$$

where

e_s = saturation vapor pressure, mb

T = water temperature, °C

Heat of Vaporization

$$H_v = 597.0 - 0.57T \tag{37}$$

where

H_v = latent heat of vaporization, Kcal/gm

T = water temperature, °C

Water Density

$$\rho_s = 1000.0 - [(T - 3.98)^2(T + 283.0)/(503.57)(T + 67.26))] \tag{38}$$

where

ρ_s = water density, Kg m^{-3}

T = water temperature, °C

Evaporation Rate

$$E = (a + bU)(e_s - e_a) \tag{39}$$

where

E = evaporation rate, m $\sec^{-1}$

U = wind speed, m $\sec^{-1}$

a,b = input empirical constants $(0, 1 \cdot 10^{-9})$

e_s = saturation vapor pressure at water surface temperature, mb

e_a = vapor pressure at the point of wind speed observation, mb

Vapor Pressure

$$e_a = 2.1718 \times 10^8 \exp[-4157.0/(T_{dp} + 239.09)] \quad (40)$$

where

e_a = vapor pressure, mb

T_{dp} = dew point temperature, °C

Precipitable Water

$$w_c = 0.86(1.26 \times 10^{-5}(T_{db} + 273.0)^2)^{8.33} \quad (41)$$

where

w_c = precipitable water, gm cm^{-3}

T_{db} = dry bulb temperature, °C

FORMATION OF ICE COVER

To properly account for the effects of ice cover on the internal heat balance and on the ecological processes modeled, it was necessary to develop a mathematical model of ice cover formation and its history. Because the exact processes by which ice cover occurs are extremely difficult to model, a simple computational procedure was developed. This procedure consists of monitoring the predicted water surface temperature until a value of 4°C is observed. At this point, a continuous accounting is made of the net heat loss (or gain) across the air-water interface. When the total heat loss to the atmosphere is equivalent to the heat of fusion for 5 cm of ice, an ice cover is assumed to be formed. The ice cover thickness thereafter is computed from the relation

Ice Cover Thickness

$$\Delta = \frac{-Q_T}{H_F} \tag{42}$$

where

Q_T = total heat loss to the atmosphere from the surface layer, Kcal/m^2

H_F = heat of fusion for water, $7.97 \cdot 10^{-4}$ Kcal/m^3

The quantity Q_T is obtained from the summation of the net daily surface heat fluxes

$$Q_T = \sum_{1}^{m} Q_n \Delta t \tag{43}$$

where

m = number of days at 4°C

This summation is carried out for each day the water temperature is at or below 4°C.

Once ice is formed it is assumed that the atmospheric heat exchange is limited to conductance through the ice. The heat flux across the air-ice interface is calculated from the relationship:

Surface Heat Flux

$$Q_n = -k \frac{(T_a - T_s)}{\Delta} \tag{44}$$

where

k = conductivity of ice, 5×10^{-4} Kcal/sec-°C-m

T_a = air temperature, °C

T_s = temperature of surface layer, °C

As a warming trend proceeds, the quantity Q_T will reflect a decrease in the ice cover thickness. When the predicted ice cover is less than 5 cm, the surface heat flux is calculated by the methods described in the previous section.

HYDRAULICS OF STRATIFIED FLOWS

In this model an analytical-empirical approach is used to characterize the complex interflows through the reservoir and the withdrawal patterns at the spillway, gates, and other outlets. The thickness of the withdrawal layer, as well as the interflow thickness, depends functionally on the inflow rates, outflow rates and the degree of stratification. In the case of the withdrawal region, spatial velocity distributions are known functions of the outflow, withdrawal thickness, and width of the reservoir at the outflow; superposition of the horizontal velocity distributions is applied to regions in which withdrawal layers overlap. In the case of reservoir interflows, horizontal velocities are calculated from the horizontal inflow rate and the cross-sectional area at the specific element. Inflows are distributed into a segment according to temperature distributions so that essentially the flow is routed horizontally according to density. Some discussion of the formulations and theoretical basis of this analytical-empirical approach will be found in Reference 2. For completeness, a brief review of the fundamental ideas is presented here.

The rationale employed for characterizing the unsteady, thermally stratified flow is best explained by using the simple example illustrated in Figure 3. Since a pseudo two-dimensional approach (one-dimensional in the vertical) is used, the temperature and flow history of each segment is computed independent of downstream segments. Proceeding from the upstream segment, the outflow history of one segment becomes the inflow history for the next. Horizontal flow between segments is characterized as an interflow (a confined subregion of flow), and the location of the interflow zone is determined on the basis of density compatibility. For example, in segment 1 of Figure 3 the midpoint of the interflow zone is located by scanning the segment temperature profile until the temperature

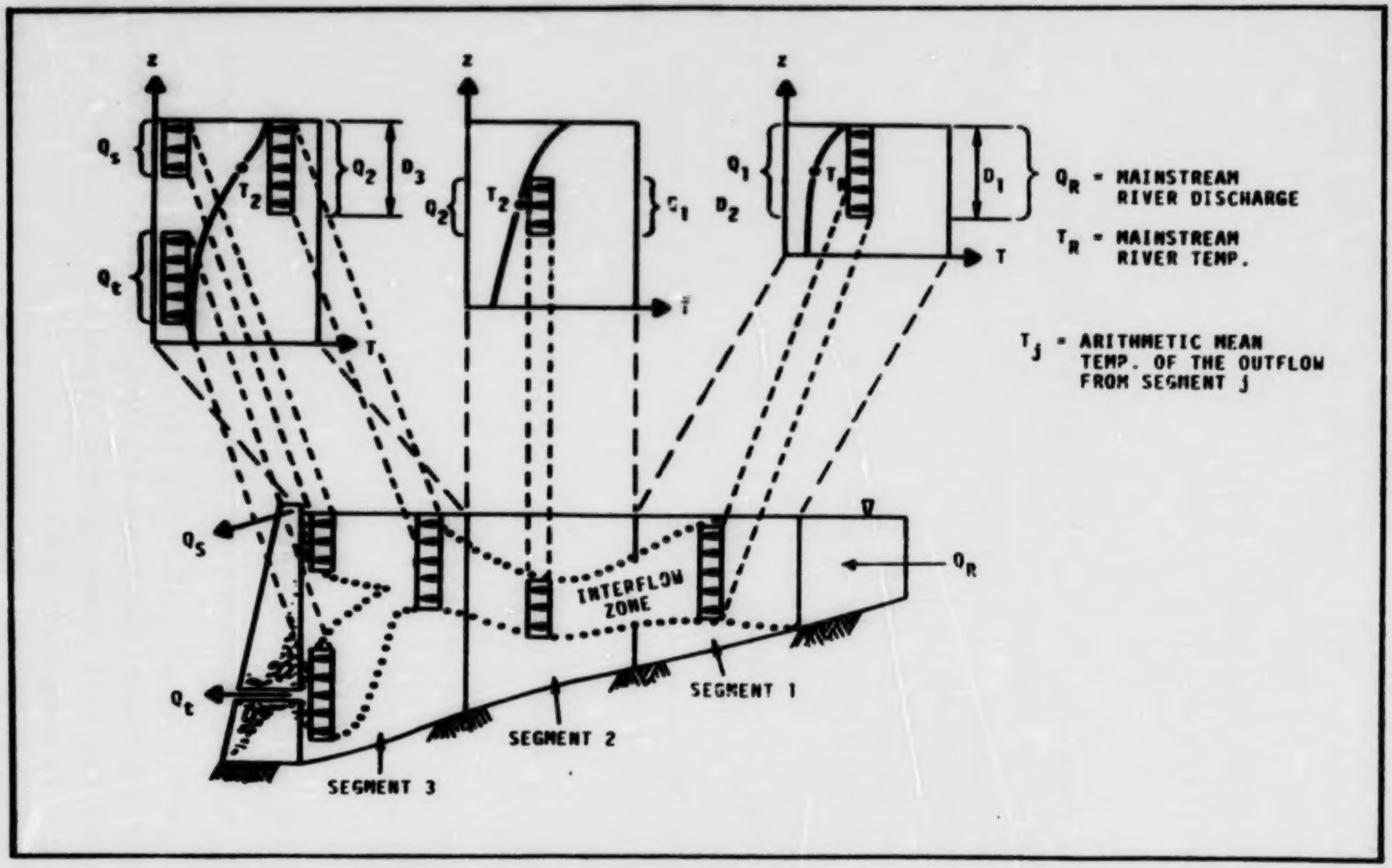
z
z
z
Q_s
Q_t
T_2
Q_2
D_3
T
Q_2
T_2
C_1
D_2
$\bar{T}$
Q_1
T_R
D_1
T
Q_R = MAINSTREAM RIVER DISCHARGE
T_R = MAINSTREAM RIVER TEMP.
T_j = ARITHMETIC MEAN TEMP. OF THE OUTFLOW FROM SEGMENT j
Q_S
Q_t
Q_R
INTERFLOW ZONE
SEGMENT 1
SEGMENT 2
SEGMENT 3

FIGURE 3. Illustration of Densimetric Flow[2]

equals the arithmetic mean temperature of the outflow from the upstream segment. The interflow thickness, D, is computed from Debler's[5] criteria:

Interflow Thickness

$$D = 2.88 \left[\frac{Q}{W\sqrt{gE}}\right] \qquad (35)$$

where

Q = total flow across the upstream interface

W = segment width

g = acceleration of gravity

E = stability $\left(\frac{\beta}{\rho_o}\right)$

β = density gradient $\left(\frac{-\partial\rho}{\partial z}\right)$

ρ_o = density at the channel bottom

Thus the inflow is said to be confined between upper and lower elevation bounds: $z_c + 1/2D$ and $z_c - 1/2D$. For cases in which these elevation bounds exceed the physical bounds, the interflow thickness is shifted up or down. The horizontal velocity distribution is assumed to be constant over the interflow zone.

Mass continuity within a reservoir segment is specified by the equation

Continuity

$$\frac{\Delta\overline{V}_j}{\Delta t} = Q_{ij} - Q_{oj} \qquad (36)$$

with

$\frac{\Delta\overline{V}_j}{\Delta t}$ = volume differential (change in storage)

Q_{ij}, Q_{oj} = total horizontal inflow and outflow for segment j

Since the total inflow and water surface elevations for segment j are known functions of time, the total horizontal outflow is computed directly from Equation 36. Next, the flow ratio, Q_r, is computed from

$$Q_r = \frac{Q_{oj}}{Q_{ij}} \qquad (37)$$

Once the distribution of horizontal inflows is determined (see Equations 41 through 44) the horizontal outflow of each layer (element) is computed from

$$Q_{oj}^{(k)} = Q_r Q_{ij}^{(k)} \qquad k = 1,2,3,\ldots m \text{ layers} \qquad (38)$$

Vertical flows into and out of each layer are computed from a direct flow balance, see Equations 53 and 54.

The vertical temperature profile will generally differ from segment to segment; consequently, the thickness of interflow D will also vary. To maintain energy continuity of horizontally advected heat across adjacent segments it is required that

$$\sum_{n}^{\ell} \rho c Q_{i,j}^{(k)} T_j^{(k)} = \sum_{n'}^{\ell'} \rho c Q_{o,j-1}^{(k)} T_{j-1}^{(k)} \qquad (39)$$

where

ρ = density of water

c = heat capacity of water

$Q_{i,j}^{(k)}$ = horizontal inflow to layer k of segment j

$Q_{o,j-1}^{(k)}$ = horizontal outflow from layer k of segment j-1 (upstream segment)

$T_j^{(k)}, T_{j-1}^{(k)}$ = temperature of the layer k for segment j and j-1

n, n' = layer indices of lower interflow bound

ℓ, ℓ' = layer indices of upper interflow bound

j, k = segment and layer indices, respectively

For computational convenience, the temperature profile within the interflow zone is approximated by a linear function of elevation, namely:

$$T_k = m(z_k - z_o) + b \tag{40}$$

where

$b = T_o$

$z_o = z_c - 1/2D$

and

T_k = temperature of the kth layer

z_k = elevation of the kth layer

m = slope

The slope term, m, is computed from the relationships between flow and velocity within the interflow zone. If Q is the total flow across the interface of adjacent segments, the velocity, U, within the interflow zone is constant and defined by

$$U_{j-1} = \frac{Q}{A_{j-1}} = \frac{QL_{j-1}}{\overline{V}_{j-1}} = \frac{Q_{o,j-1}^{(k)} L_{j-1}}{\overline{V}_{j-1}^{(k)}} \tag{41}$$

$$U_j = \frac{Q}{A_j} = \frac{QL_j}{\overline{V}_j} = \frac{Q_{i,j}^{(k)} L_j}{\overline{V}_j^{(k)}} \tag{42}$$

and in turn

$$Q_{o,j-1}^{(k)} = \frac{Q\overline{V}_{j-1}^{(k)}}{\overline{V}_{j-1}} \tag{43}$$

$$Q_{i,j}^{(k)} = \frac{Q\overline{V}_j^{(k)}}{\overline{V}_j} \tag{44}$$

where

A_j = mean cross-sectional area of interflow zone

L_j = length of the segment j

$\overline{V}_j$ = total volume of segment j

$\overline{V}_j^{(k)}$ = volume of element k

j = segment index

With the above relationships, the slope term, m, is defined as

$$m = \frac{\overline{V}_{j-1} \quad \sum_{k=n'}^{m'} \overline{V}_{j-1}^{(k)} T_{j-1}^{(k)} - T_o}{\overline{V}_j \quad \sum_{k=n}^{m} \overline{V}_j^{(k)} z_{j,k} - z_{j,o}} \tag{45}$$

The interfacing of adjacent segments is carried out automatically in the Deep Reservoir Hydrothermal Model for all segments except the final one upstream of the dam.

Treatment of the downstream segment is based on similar analytical concepts of densimetric flow. The withdrawal depth, d, as illustrated in Figure 4, is defined as

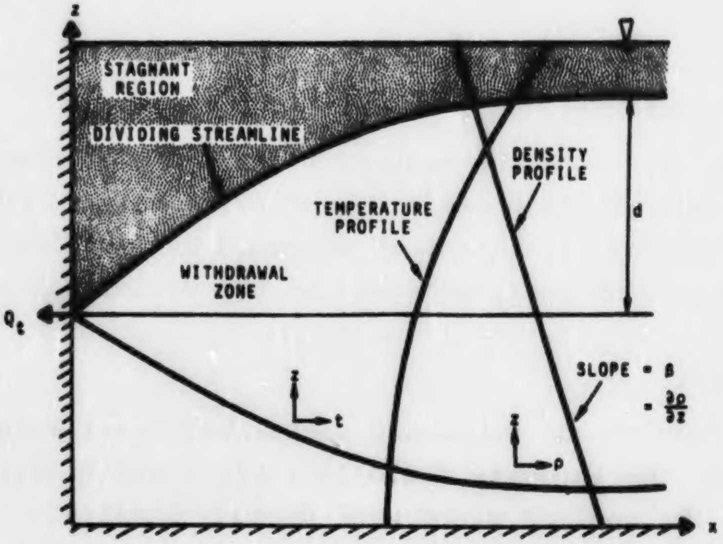
z
STAGNANT REGION
DIVIDING STREAMLINE
DENSITY PROFILE
TEMPERATURE PROFILE
d
WITHDRAWAL ZONE
Q_t
SLOPE = β
= $\frac{\partial \rho}{\partial z}$
z
t
z
ρ
x

FIGURE 4. Conceptualization of a Withdrawal Zone[2]

$$d = 2.0 \left[q \sqrt{\frac{\rho_o}{g\beta}} \right]^{\frac{1}{2}} \tag{46}$$

where

q = volumetric discharge per unit width

ρ_o = density centerline of outlet

g = gravitational constant

$\beta = \frac{-\partial\rho}{\partial z}$ along centerline of outlet

The discharge, q, is computed as

$$q = \frac{Q_s}{w_s} \quad \text{surface outlet} \tag{47}$$

and

$$q = \frac{Q_t}{2w_t} \quad \text{submerged outlets} \tag{48}$$

with

Q_s, Q_t = spillway
w_s, w_t = widths

For regions in which the assumed flow fields overlap, the profiles are simply superimposed. Velocity is assumed constant within the withdrawal layers and is computed by dividing the discharge by the cross-sectional area of the withdrawal zone:

$$U(z) = \frac{Q}{w(2d)} \tag{49}$$

If the bounds of the submerged withdrawal layer exceeds the physical bounds, the velocity field is revised and distributed uniformly over the revised withdrawal depth. Similarly, if the submerged withdrawal zone overlaps the water layers above the thermocline the withdrawal depth is adjusted below the thermocline. Both of these situations are illustrated in Figure 5.

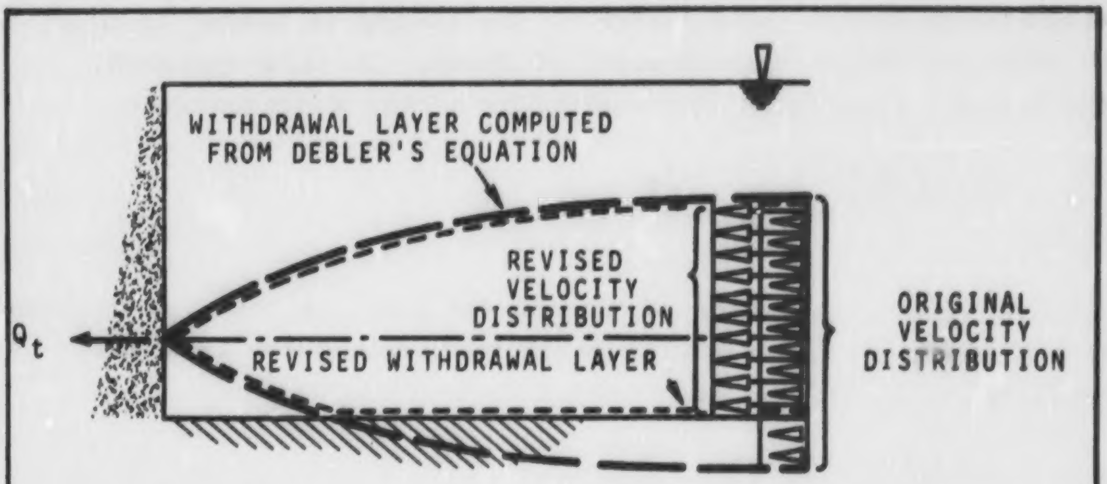
WITHDRAWAL LAYER COMPUTED FROM DEBLER'S EQUATION
REVISED VELOCITY DISTRIBUTION
ORIGINAL VELOCITY DISTRIBUTION
Q_t
REVISED WITHDRAWAL LAYER

A. WITHDRAWAL REGION WITH DIVIDING STREAMLINE CROSSING THE PHYSICAL BOUNDARY

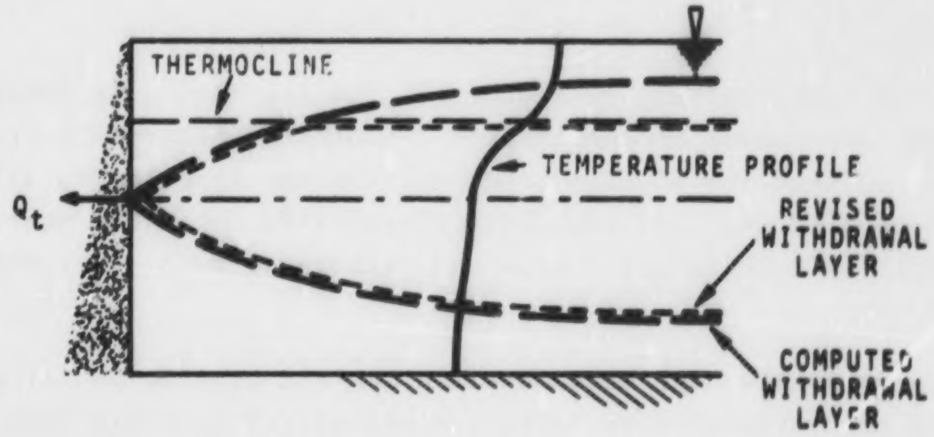
THERMOCLINE
TEMPERATURE PROFILE
Q_t
REVISED WITHDRAWAL LAYER
COMPUTED WITHDRAWAL LAYER

B. WITHDRAWAL REGION WITH DIVIDING STREAMLINE OVERLAPPING THE THERMOCLINE

FIGURE 5. Illustration of Withdrawal Layer Configurations[2]

In cases where natural convective mixing is dominant in the epilimnetic region (see Figure 6) the theory of Craya[6] is used in determining the distribution of flows. In this approach, the density profile is represented by a step function with

$$\rho(z) = \begin{cases} \rho & z > z_t \\ \rho+\Delta\rho & z < z_t \end{cases} \qquad (50)$$

where Z_t is the elevation of the thermocline. A critical epilimnetic discharge at which water will begin to be withdrawn from the hypolimnion is defined as

Surface Outlets

$$q_c = \frac{Q_s}{W_s} = \sqrt{0.75 \quad g\, d_r^3 \frac{\Delta\rho}{\rho}} \qquad (51)$$

Submerged Outlets

$$q_c = \frac{Q_t}{W_t} = \sqrt{1.52 \quad g\, h^3 \frac{\Delta\rho}{\rho}} \quad , \quad 2\,h \le d_r \qquad (52)$$

where d_r and h are defined in Figure 13. If the flow q is greater than q_c for any outlet or combination of outlets, Debler's criterion is used to compute the withdrawal depth from the hypolimnion using for the discharge $q-q_c$ and stability E evaluated below the thermocline. The velocity profile in epilimnion and withdrawal zone are assumed constant.

Having calculated the horizontal inflow and outflow patterns for a segment, the vertical flow rates are calculated directly from the continuity relation:

Continuity

$$Q_{vi} = \sum_{1}^{n-1} (Q_{h,i} - Q_{h,o}) \qquad (53)$$

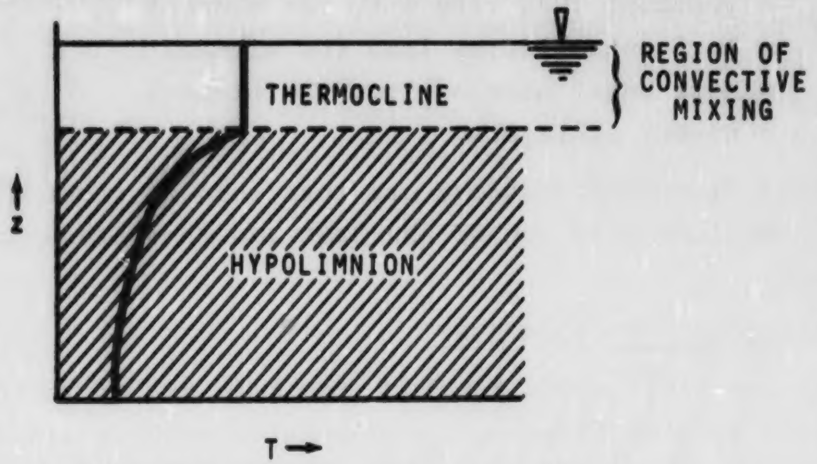
REGION OF
CONVECTIVE
MIXING
THERMOCLINE
z
HYPOLIMNION
T

A. REPRESENTATION OF CONVECTIVE MIXING IN EPILIMNION

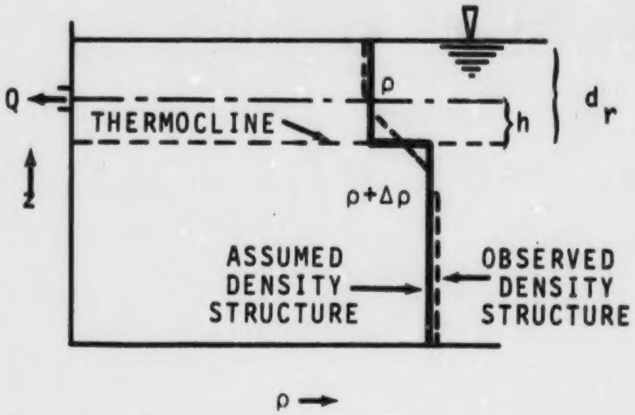
Q
ρ
THERMOCLINE
h
d
r
z
ρ+Δρ
ASSUMED
DENSITY
STRUCTURE
OBSERVED
DENSITY
STRUCTURE
ρ

B. DENSITY PROFILES

FIGURE 6. Temperature and Density Structure for Application of Craya's Criteria[2]

and

$$Q_{vo} = Q_{h,i} + Q_{vi} - Q_{h,o} \tag{54}$$

where

Q_{vo} = vertical flow rate out of the element
Q_{vi} = vertical flow rate into the element
$Q_{h,i}$ = horizontal inflow into the element
$Q_{h,o}$ = horizontal outflow from the element
n = number of layers

These flow distributions are then used as input quantities in the numerical solution of the heat and mass transport equations.

NUMERICAL SOLUTION TECHNIQUES

The governing model equation for heat transport is solved by using a finite-difference method which reduces the differential equation to an algebraic problem. The finite-difference approximation used for the heat equation is:

Finite Difference Approximation

$$\begin{aligned} \frac{A_{j+1}+A_j}{2} \frac{dT_j}{dt} = {} & \frac{A_{j+1}+A_j}{2} \frac{H'_j}{\rho c} + \frac{1}{\Delta z} [Q_{i_j} T_i - Q_{o_j} T_j] \\ & \frac{-1}{\Delta z} [Q_{vo_j} T_j - Q_{vi_j} T_{j-1}] + \frac{A_{j+1}\alpha_{j+1}}{\Delta z^2} T_{j+1} \\ & - \frac{A_{j+1}\alpha_{j+1} + A_j\alpha_j}{\Delta z^2} T_j + \frac{A_j\alpha_j}{\Delta z^2} T_{j-1} \end{aligned} \tag{55}$$

which applies to each element within a segment. Writing the above equation for all elements of interest produces a matrix equation of the form:

$$[P] \left\{\frac{dT}{dt}\right\} = [S] \{T\} + \{R\} \tag{56}$$

where

[P] = a diagonal matrix

[S] = a constant coefficient tridiagonal matrix

{R} = a time varying load vector

To approximate the solution to this system of equations, a second-order Taylor series expansion is used of the form:

$$\{T\}^{n+1} = \{T\}^n + \left\{\frac{dT}{dt}\right\}^n \Delta t + \left\{\frac{d^2T}{dt^2}\right\}^n \frac{\Delta t^2}{2} \qquad (57)$$

Δt = time step

n = time plane index

where the second-order derivative is approximated by

$$\left\{\frac{d^2T}{dt^2}\right\}^n = \frac{1}{\Delta t}\left(\left\{\frac{dT}{dt}\right\}^{n+1} - \left\{\frac{dT}{dt}\right\}^n\right) \qquad (58)$$

Thus Equation 57 may be written as

$$\{T\}^{n+1} = \{T\}^n + \frac{\Delta t}{2}\left\{\frac{dT}{dt}\right\}^n + \frac{\Delta t}{2}\left\{\frac{dT}{dt}\right\}^{n+1} \qquad (59)$$

Since the first term on the right-hand side is known from initial conditions, the second term may be evaluated directly from Equation 56. Substituting the above equation into Equation 56 gives the relation:

$$[P]\left\{\frac{dT}{dt}\right\}^{n+1} = [S]\left(\{T\}^n + \frac{\Delta t}{2}\left\{\frac{dT}{dt}\right\}^n + \frac{\Delta t}{2}\left\{\frac{dT}{dt}\right\}^{n+1}\right) + \{R\} \qquad (60)$$

Rearranging and solving for the time rate of change at the n+1 time plane yields:

$$[\bar{S}]\left\{\frac{dT}{dt}\right\}^{n+1} = \{\bar{R}\}^{n+1} \qquad (61)$$

where

$$[\bar{S}] = [P] - \frac{\Delta t}{2}[S] \qquad (62)$$

$$\{\bar{R}\} = [S]\{T\}^n + \frac{\Delta t}{2}\left\{\frac{dT}{dt}\right\}^n + \{R\} \qquad (63)$$

It is evident from this development that a simple recursion algorithm may be employed to obtain a forward-stepping solution method. The sequence of calculations in the algorithm is:

1. Form the coefficient matrices and load vector.
2. Calculate the modified matrices.
3. Solve for the time rate of change at n+1.
4. Evaluate the relation for T at n+1.
5. Repeat step 1 through 4 for each succeeding time plane.

The algebraic solution of Equation 61 is accomplished by use of the Thomas algorithm[3] which is a modified Gaussian elimination procedure.

COMPUTER PROGRAMS

The hydrothermal model formulation described in previous sections is implemented in two general-purpose computer programs. The first, CLIMA, is a generalized data input program which reads, then organizes, prints and plots, all hydrologic and meteorologic data for the simulation period. The program output allows the user to quickly check a large mass of input data for errors. CLIMA calculates and outputs a standard set of data which is used to initiate the hydrothermal simulations.

The second program, TERMA, was developed in a previous project[1] for EPA from the original WRE Deep Reservoir multi-segment program. Several components of the previous version of TERMA have been improved and streamlined. This computer program simulates the reservoir thermal hydraulics. Vertical temperature profiles and flow distributions are computed and output for the simulation period. The successive simulation of each segment provides a quasi-two-dimensional representation of the temperature and flow patterns. These predicted results are stored on magnetic tape for later input to the water quality simulation model. The current version of TERMA is fully operational for stratified and well-mixed reservoirs and requires little or no subjective effort for proper calibration.

The CLIMA and TERMA programs both have storage requirements of less than 25K decimal words. CLIMA is presently set up to handle 2 meteorologic observations per day for a record of 365 days. The program requires 2 disk or drum files and 1 output tape. Program execution time for a 1-year simulation period is 1 to 2 minutes. TERMA is programmed to accommodate a maximum of 200 elements per segment, and can handle any number of segments. The TERMA program requires 6 disk or drum files, 1 input tape and 1 or 2 output tapes. Execution times are generally under 2 minutes (for a 3-segment representation) for a simulation period of 7-1/2 months.

A user's manual has been prepared to assist the general user in setting up and applying the CLIMA and TERMA programs. Both programs are well commented and easily adaptable to different computer systems.

SECTION V

WATER QUALITY MODEL

Although all water quality models are, by necessity, relatively simple representations of complex physical systems, a wide range of sophistication and detail is possible. An attempt is generally made to develop models which are capable of providing an adequate portrayal of the important biological, chemical, and physical processes while retaining sufficient simplicity to allow efficient numerical application and solution.

MODELING APPROACH

To develop an ecological model capable of simulating the water quality dynamics in stratified reservoirs, many diverse concepts of biology, aquatic chemistry and hydrology must be organized and integrated. The task of formulating a realistic model that is simple enough to use and yet realistic enough to be meaningful often constitutes more than half of the solution of the problem.

The modeling approach employed here is based on the general principle of conservation of mass. This fundamental law is used to derive a differential equation model for constituent transport of biotic and abiotic materials. Chemical and biological transformations are modeled by first and second order kinetic equations. The principal environmental variables used in the complete formulation of the water quality model include:

- Solar radiation
- Temperature
- Dissolved oxygen
- Total and benthic BOD
- Phytoplankton
- Zooplankton

- Nitrogen (organic and inorganic forms)
- Phosphorus (organic and inorganic forms)
- Coliform bacteria
- Toxic material
- Water flows

Figure 7 summarizes these quality parameters and illustrates their interaction. This portrayal of biological and chemical transformations includes the nitrogen and phosphorus cycles linked to algal growth and decay. Zooplankton growth is also coupled to algal production. Production of algal biomass is a function of light, nutrients, temperature, and zooplankton grazing. The effects associated with sinking algae, bottom accumulation and decay of detritus, and release of nutrients are modeled. Organic and inorganic phosphorus loss to sediments is included as well as anaerobic release of soluble phosphorus from the sediments. In addition to photosynthetic production of oxygen, the effects of nitrogen oxidation, BOD exertion and reaeration are modeled. The coliform submodel describes coliform death as a first order decay reaction. A toxic material submodel is linked to algal growth rates and can be modeled either as a conservative parameter or first-order decay. The specific submodel formulations are presented in subsequent sections.

The computational procedure for the complete model consists of two steps. First, the heat transport and fluid flow are simulated for the entire period of interest. Next, these results are input to the water quality model for solution of the equations for constituent transport, which are solved independently for each of 12 constituents. The constituent transport equations are solved implicitly using time steps of about 8 to 12 hours. This partitioned approach was devised for simplicity and convenience of calibrating and applying the computer models. The following sections present the fundamental theory for the generalized water quality model.

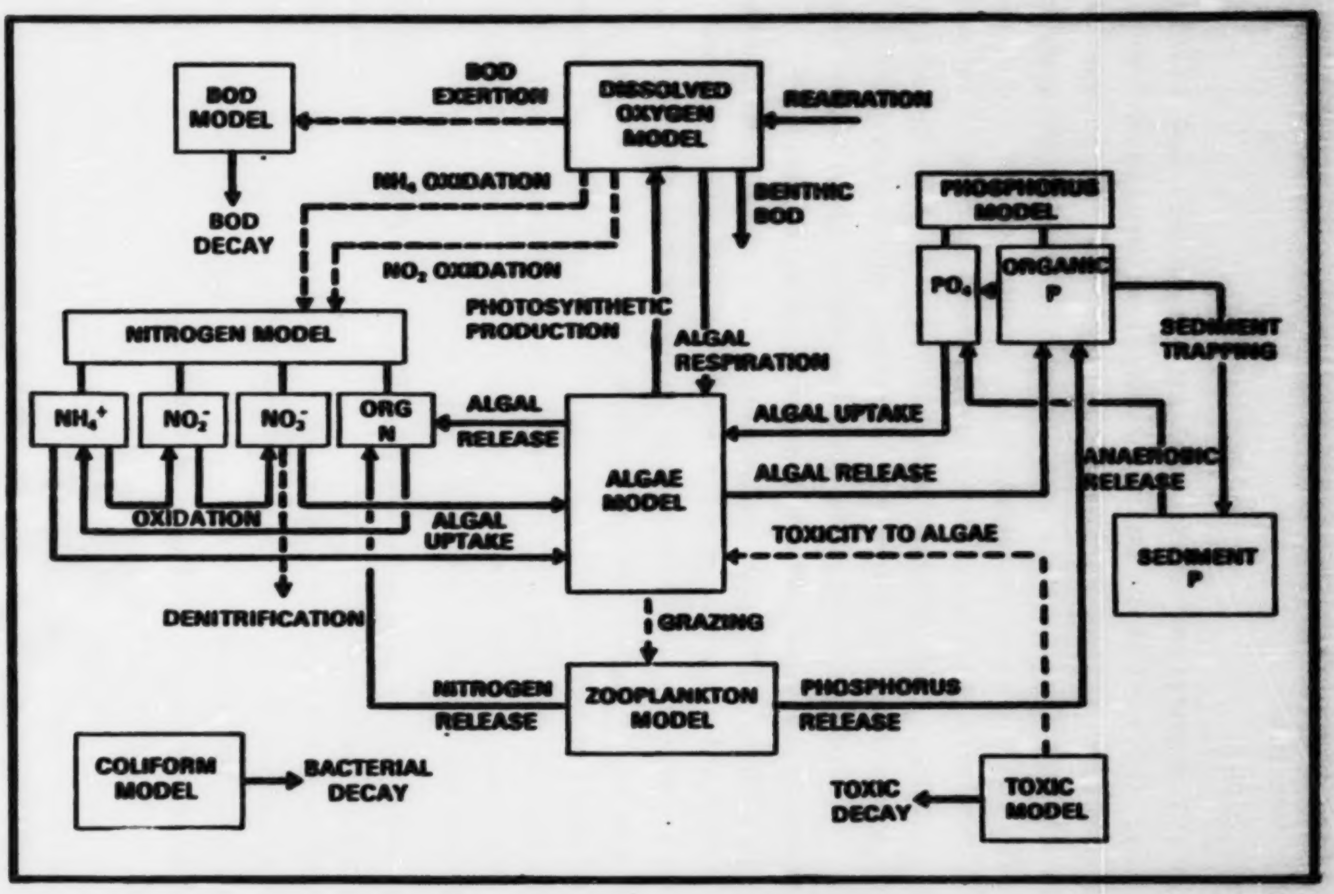
BOD MODEL
BOD DECAY
BOD EXERTION
DISSOLVED OXYGEN MODEL
REAERATION
BENTHIC BOD
NH4 OXIDATION
NO2 OXIDATION
PHOTOSYNTHETIC PRODUCTION
ALGAL RESPIRATION
NITROGEN MODEL
NH4+
NO2-
NO3-
ORG N
OXIDATION
ALGAL RELEASE
ALGAL UPTAKE
DENITRIFICATION
ALGAE MODEL
GRAZING
ZOOPLANKTON MODEL
NITROGEN RELEASE
PHOSPHORUS RELEASE
PHOSPHORUS MODEL
PO4
ORGANIC P
SEDIMENT TRAPPING
ANAEROBIC RELEASE
SEDIMENT P
ALGAL UPTAKE
ALGAL RELEASE
TOXICITY TO ALGAE
COLIFORM MODEL
BACTERIAL DECAY
TOXIC MODEL
TOXIC DECAY

FIGURE 7. Summary of Processes Considered in Water Quality Model

CONSTITUENT TRANSPORT

The transport of a biotic or abiotic constituent through a water system may be represented by a general one-dimensional convection-diffusion equation:

Mass Transport

$$\frac{\partial C^{(k)}}{\partial t} = -\frac{Q_v}{A}\frac{\partial C^{(k)}}{\partial z} + D_z \frac{\partial^2 C^{(k)}}{\partial z^2} + \frac{1}{A\Delta z}\left(Q_{h,i}C_i^{(k)} - Q_{h,o}C^{(k)}\right) + S^{(k)} \quad (64)$$

where

$C^{(k)}$ = concentration of kth constituent, $k = 1,2,\ldots,n$
$C_i^{(k)}$ = concentration of upstream inflow
D_z = effective diffusion coefficient
A = horizontal surface area of water plane for element
Q_v = vertical flow through element (layer)
$Q_{h,i}, Q_{h,o}$ = horizontal inflow and outflow to element
Δz = element thickness
$S^{(k)}$ = source or sink term for kth constituent

This formulation of the conservation of mass principle is applied specifically for the segment layer idealization. The major assumption in this formulation is that lateral and longitudinal gradients are small. This assumption allows mathematical decoupling of the segments; as a result the bulk motion of a constituent within a segment is a primary function of the upstream and tributary boundary conditions and the vertical transport by convection, diffusion and sedimentation. In Equation 64 the sink term, $S^{(k)}$, is used to account for the chemical and biological transformations. The vertical convective term in Equation 64 is modified to include the effect of settling, which is characteristic of suspended constituents such as algae.

BIOCHEMICAL OXYGEN DEMAND

Although BOD is a measure of oxygen demand, it is also a measure of the concentration of biologically decomposable organic mater. The rate of degradation of organic wastes in natural waters depends on the composition of the waste, the types of microorganisms present, and various physical factors. Factors such as temperature, pH, and metal ion concentrations can affect the type and performance of the bacteria available to mediate the oxidation of wastes. The behavior of BOD in natural waters has been described for many years[8] by a first-order rate expression of the form:

$$\frac{dL_c}{dt} = - K_1 L_c \qquad (65)$$

where

L_c = concentration of BOD, mg/l

K_1 = deoxygenation coefficient, 1/day

It should be emphasized that this formulation describes the changes in BOD due to biological oxidation. One of the major problems in modeling carbonaceous BOD arises from the fact that actual field measurements of 5-day BOD include oxygen uptake due to nitrogen oxidation as well as algal respiration and chemical oxidation processes. The model formulations account for these processes separately.

The deoxygenation rate constant, K_1, is known[9] to vary with temperature. The empirical relation

$$K_1^{(T)} = K_1^{(20)} \theta^{(T-20)} \qquad (66)$$

where $K_1^{(20)}$ is the rate constant at 20°C has been used. Values of θ are given in Table 2.

NITROGEN

Compounds of nitrogen are important factors[10] affecting water quality. The oxidation of ammonium and nitrite consumes oxygen. Nitrate and ammonium are nutrient sources for algal growth. Sources[11] of nitrogen species to an aquatic ecosystem are primarily the tributary streams. However, significant nitrogen inputs can come from nitrogen fixation[12,13] by certain filamentous blue-green algae and some bacteria. Nitrogen input and release from the sediments as well as denitrification can also affect nitrogen concentrations.

Four forms of nitrogen are considered in the model: organic-N, NH_4^+-N, NO_2^--N, and NO_3^--N. Ammonium and nitrate are taken up by algae and organic nitrogen is released by algae and zooplankton. The nitrogen taken up by zooplankton in the form of algal cells is transferred through the organic nitrogen compartment for bookkeeping purposes. Variable definitions:

C_1 = NH_4^+-N concentration, mg/l
C_2 = NO_2^--N concentration, mg/l
C_3 = NO_3^--N concentration, mg/l
C_4 = organic nitrogen concentration, mg/l

The rate of change of ammonium nitrogen considers oxidation to nitrate, uptake by algae, and oxidation of organic nitrogen to ammonium.

Ammonium

$$\frac{dC_1}{dt} = - J_1C_1 - PG_pA_{NP}\left(\frac{C_1}{C_1+C_3}\right) + J_4C_4 \qquad (67)$$

where

J_1 = rate constant for ammonium oxidation, 1/day
J_4 = rate constant for organic nitrogen oxidation, 1/day
P = phytoplankton concentration, mg-C/l
G_p = net algal growth rate, 1/day
A_{NP} = ratio of nitrogen to carbon in algal cells, mg-N/mg-C.

The rate of change of nitrite nitrogen considers production from ammonia oxidation and loss from nitrite oxidation.

Nitrite

$$\frac{dC_2}{dt} = J_1C_1 - J_2C_2 \qquad (68)$$

where

J_2 = rate constant for nitrite oxidation, 1/day

The rate of change of nitrate nitrogen considers production from nitrite oxidation, algal uptake, and denitrification as a function of oxygen concentration.

Nitrate

$$\frac{dC_3}{dt} = J_2C_2 - PG_pA_{NP}\left(\frac{C_3}{C_1+C_3}\right) - J_3C_3 \qquad (69)$$

and

$$J_3 = 1.0 - DO/DO_s \text{ (for } DO < DO_s) \qquad (70)$$

where

J_3 = denitrification rate constant, 1/day

The rate of change of organic nitrogen considers oxidation to ammonium, algal release, and zooplankton release.

Organic-Nitrogen

$$\frac{dC_4}{dt} = -J_4C_4 + R_pPA_{NP} + D_zZA_{NZ} \qquad (71)$$

where

R_p = algal respiration rate, 1/day
D_z = zooplankton death rate, 1/day
Z = zooplankton concentration, mg-C/l
A_{NZ} = nitrogen to carbon ratio for zooplankton, mg-N/mg-C

PHOSPHORUS

The major importance of phosphorus[14] in aquatic ecosystems is due to its role in stimulating algal growth. Phosphorus can exist in many organic and inorganic forms. Exchanges[15] with sediments also occur as a result of sedimentation, precipitation, adsorption, and ion exchange.

The model considers algal uptake and release, zooplankton release, degradation of organic phosphorus with consequent release of soluble phosphorus, loss of both organic and soluble phosphorus to the sediments, and anaerobic release from the sediments. The organic phosphorus, like the organic nitrogen, is assumed to be in a particulate form. Settling particulates are accounted for in the transport equations.

$$\frac{dD_1}{dt} = - G_p P A_{pp} + \overbrace{I_3 D_3}^{\text{anaerobic only}} \underbrace{- I_1 D_1}_{\text{bottom layer}} + I_2 D_2 \tag{72}$$

$$\frac{dD_2}{dt} = + R_p P A_{pp} + D_z Z A_{pz} \underbrace{- I_4 D_2}_{\substack{\text{bottom}\\ \text{layer}}} - I_2 D_2 \tag{73}$$

$$\frac{dD_3}{dt} = + I_1 D_1 + \underbrace{I_4 D_2 \overbrace{- I_3 D_3}^{\text{anaerobic only}}}_{\text{bottom layer}} \tag{74}$$

where

D_1 = soluble phosphorus, mg/l

D_2 = organic phosphorus, mg/l

D_3 = sediment phosphorus, mg/l

A_{pp} = phosphorus to carbon ratio in phytoplankton, mg/mg

A_{pz} = phosphorus to carbon ratio in zooplankton, mg/mg

I_1 = rate constant for loss to sediment, 1/day

I_2 = rate constant for release of soluble phosphorus from organic, 1/day

I_3 = rate constant for sediment release, 1/day

I_4 = rate for organic phosphorus loss to sediment, 1/day

All other variables are as previously defined.

TOXIC SUBSTANCES

The behavior of toxic substances in an aquatic environment is very complex and depends significantly on the chemical properties of the substance. The complexity arises from the fact that the bulk transport and distribution of toxic pollutants are affected by several mechanisms of exchange, e.g., chemical transformations, sedimentation and biological uptake. For simplicity a first-order decay model is used where

$$\frac{dT_c}{dt} = -K_t T_c \tag{75}$$

where

T_c = concentration of toxic substance, mg/l
K_t = decay rate constant, 1/day

The effect of a toxic substance can be linked to algal growth rates as described in the next section.

ALGAE

Modeling[16,17,18] of algal population dynamics is inherently complex due to heterogeneous algal populations with different characteristics and the myriad of interacting environmental factors which influence algal growth and decay. One of the most important problems facing limnologists today is to determine why certain types of species predominate in some situations and not in others. A simulation model which considers several species of algae with different nutrient uptake rates, growth rates, cell sizes, sinking velocities and attractiveness to predators could be the basis for an interesting evaluation. However, such a model is beyond the scope of this study. Only a single species of algae is considered and growth constants typical of the predominant species in the system being modeled must be chosen.

The algal growth formulations in this model were adopted from Lorenzen and Mitchell[19] and are given below. Algal growth rates are considered to be a function of light intensity, nitrogen concentration, phosphorus concentration, and temperature. Algal respiration rates are considered to be a function of temperature only. The algae model formulation is:

$$\frac{dP}{dt} = (G_p - D_p)\, P \tag{76}$$

where

G_p = gross specific growth rate, 1/day
D_p = death rate, 1/day
P = phytoplankton concentration, mg-C/l
T = temperature, °C

The gross specific growth rate, G_p, is given by:

$$G_p = \frac{G_m AI\ T}{\sqrt{1 + (AI)^2}} \mathrm{Min}\left[\left(\frac{C_1+C_3}{K_n+C_1+C_3}\right), \left(\frac{D_1}{K_p+D_1}\right)\right]\left(\frac{K_{pt}}{K_{pt}+T_c}\right) \tag{77}$$

where

G_m = maximum specific growth rate, 1/day-°C
A = measure of adaptation to low light, lux^{-1}
I = light intensity, lux
K_n = Michaelis constant for nitrogen, mg/l
K_p = Michaelis constant for phosphorus, mg/l
K_{pt} = toxic compound coefficient, mg/l
T_c = concentration of toxic compound, mg/l

Light intensity as a function of depth is given by

$$I = I_o\, e^{-(\alpha_o + \beta\overline{P})d} \tag{78}$$

where

I = light intensity at depth, d, lux
α_o = attenuation coefficient of water, m^{-1}
β = self-shading factor, m^{-1}/mg/l
$\overline{P}$ = average phytoplankton concentration above depth, d, mg-C/l
I_o = surface light intensity, lux

The surface light intensity, I_o, varies over a 24-hour period according to the following equation suggested by Vollenweider.[20]

$$I_o(t) = 2I_{max} \left(1 + \cos \frac{2\pi}{\lambda} t\right) \text{ for } - \lambda/2 \leq t \leq + \lambda/2 \qquad (79)$$

$I_o(t) = 0$ for other values of t

t = time in hours

λ = number of hours of daylight

The number of hours of daylight, λ, is computed as function of Julian day, latitude and declination (see Equations 19 through 25). The term I_{max} is calculated from the total daily radiation so that the integral of Equation 78 over 1 day equals the total daily radiation. Langleys are converted to lux from the relation 1 lux = 5.7×10^{-6} langleys/min from Westlake.[21]

The decrease in phytoplankton concentration generally occurs through endogenous respiration, zooplankton grazing, and sinking. In the model the effect of sinking is accounted for in the convective term of the transport equation. Respiration and grazing are accounted for in the formulation of the death rate, D_p, given by:

$$D_p = F_1 T + C_g Z \qquad (80)$$

where

F_1 = endogenous respiration rate, 1/day-°C

C_g = zooplankton grazing rate, 1/mg-C-day

Typical values for F_1 and C_g are given in later sections.

ZOOPLANKTON

Zooplankton are important predators on some algal species and their potential effects on algal biomass should be considered. Zooplankton growth and decay are modeled after the formulations of DiToro, et al.[22]

$$\frac{dZ}{dt} = (G_z - D_z)Z \qquad (81)$$

where

G_z = gross growth rate, 1/day

D_z = death rate, 1/day

$$G_z = A_{zp}\ C_g\left(\frac{P}{K_{mp}+P}\right)\ T \tag{82}$$

where

A_{zp} = zooplankton conversion efficiency, decimal
C_g = zooplankton grazing rate, 1/day
K_{mp} = Michaelis constant, mg-C/l
P = phytoplankton concentration, mg-C/l
T = temperature, °C

and

$$D_z = F_2T + F_3 \tag{83}$$

where

F_2 = respiration rate, 1/day-°C
F_3 = death rate due to other causes, 1/day

REAERATION

The rate of reaeration in natural waters is proportional to the oxygen saturation deficit. Numerous studies[23] have been directed to the determination of the constant of proportionality for rivers and streams. However, only minor attention has been given to reaeration processes in impoundments and reservoirs. In these cases, the effects of wind on the reaeration coefficient have been observed but no mathematical correlations are currently available. In this model, a simple linear relation is used.

$$K_r = (a_1 + a_2v_w)\ \theta^{(T-20)} \tag{84}$$

where

v_w = wind speed, m/day
a_1 = 0.5, m/day
$a_2 = 2.5 \times 10^{-6}$

It is estimated that the value of K_r should range between 0.01 to 5.0 per day. Reaeration is confined to the surface layer. Values of θ are given in Table 2.

DISSOLVED OXYGEN

The concentration of dissolved oxygen has often been used as a key indicator of water quality in an aquatic environment. Because of the significance of dissolved oxygen as a major environmental variable, considerable study has been devoted to the processes regulating the balance of oxygen in natural waters. The current knowledge of these processes indicates that dissolved oxygen (DO) levels are influenced by several interrelated factors. The most significant factors are: (1) temperature, (2) bacterial oxidation of suspended and dissolved organic matter, (3) benthic uptake, (4) reaeration, and (5) algal photosynthesis and respiration. The dissolved oxygen model formulated here includes descriptions of all of these factors.

The complete oxygen balance is expressed as:

Dissolved Oxygen Balance

$$\frac{dDO}{dt} = \overset{\left(\substack{\text{Carbonaceous}\\ \text{BOD}}\right)}{- K_1 L_c} \quad \overset{\left(\substack{\text{Ammonium}\\ \text{Oxidation}}\right)}{- \alpha_1 J_1 C_1} \quad \overset{\left(\substack{\text{Nitrite}\\ \text{Oxidation}}\right)}{- \alpha_2 J_2 C_2}$$

$$\underbrace{\overset{\left(\substack{\text{Benthic}\\ \text{Uptake}}\right)}{- \frac{L_b}{\Delta z}}}_{\text{bottom layer}} \quad \underbrace{\overset{(\text{Reaeration})}{+ K_r(DO_s - DO)}}_{\text{surface layer}} \quad \overset{\left(\substack{\text{Algal}\\ \text{Productivity}}\right)}{+ \alpha_3(G_p - D_p)P} \tag{85}$$

where

DO = dissolved oxygen concentration, mg/l
DO_s = dissolved oxygen saturation, mg/l
C_1 = ammonia concentration, mg/l
C_2 = nitrite concentration, mg/l
L_c = carbonaceous BOD, mg/l
L_b = benthic oxygen uptake rate, g/m^2-day

P = phytoplankton concentration, mg-C/l
G_p, D_p = phytoplankton specific growth and death rates, 1/day
$\alpha_1, \alpha_2, \alpha_3$ = stoichiometric constants
K_1, J_1, J_3 = deoxygenation rates, 1/day
K_r = reaeration coefficient, 1/day
Δz = bottom layer thickness, m

The saturation value for dissolved oxygen, DO_s, can be calculated from the equation:[24]

$$DO_s = 14.652 - 0.41022T + 0.007991T^2 - 0.000077774T^3 \qquad (86)$$

Temperature, T, is given in degrees centigrade.

COLIFORM BACTERIA

Early studies[25,26] of the fate of bacteria in an aquatic environment support the generalization that bacteria die off at a relatively constant rate. Although bacterial growth can occur, there are more environmental factors which accelerate the death rate. The mathematical formulation used is

$$\frac{dC}{dt} = -K_c C \qquad (87)$$

where

C = bacteria concentration, No./100 ml
K_c = specific death rate, 1/day

Temperature effects on K_c are accounted for by the empirical relation:

$$K_c = K_c^{(20)} \theta^{(T-20)} \qquad (88)$$

where $K_c^{(20)}$ is the rate at 20°C. The literature[27,28] indicates a tendency for most values to lie in the range 0.01 to 3.5/day.

SUMMARY OF SUBMODEL CONSTANTS

The water quality submodels described above require the complete knowledge of several rate constants, stoichiometric quantities and various conversion factors. Table 2 presents a summary of these quantities and their known range of values. Most of these quantities have been obtained from the technical literature or determined from previous modeling experience.

TABLE 2. Summary of Model Constants

Symbol	Quantity	Range of Values	Units
K_1	BOD decay rate	0.1-2.5	1/day
J_1	Ammonia oxidation rate	0.1-0.5	1/day
J_2	Nitrate oxidation rate	3.0-10.0	1/day
J_3	Denitrification rate	0.0-1.0	1/day
J_4	Ammonification rate	0.02-0.4	1/day
I_1	Phosphorus trapping rate	0.1-0.7	1/day
I_2	Phosphorus release rate	0.1-0.7	1/day
I_3	Organic phosphorus to soluble	0.1-0.7	1/day
K_t	Toxic decay rate	--	1/day
G_m	Maximum specific growth rate	0.05-0.20	1/day-°C
A	Adaptation to low light	0.00054	1/lux
K_n	Nitrogen half saturation constant	0.025-0.3	mg/l
K_p	Phosphorus half saturation constant	0.006-0.03	mg/l
K_{pt}	Toxicity constant	--	mg/l
α_o	Light extinction constant	0.005-0.9	1/m
β	Self-shading factor	0.2-0.6	mg/l-m
F_1	Algal respiration rate	0.005-0.009	1/day-°C
C_g	Zooplankton grazing rate	0.05-0.2	1/mg-C-day
G_p	Phytoplankton growth rate	Eqn.75	1/day-°C
D_p	Phytoplankton death rate	Eqn. 79	1/day-°C
λ	Photoperiod	0.3-0.7	days

TABLE 2 (continued)

A_{zp}	Zooplankton conversion efficiency	0.5-0.7	decimal
v_s	Sinking velocity	0.05-1.0	m/day
A_{np}	Phytoplankton--nitrogen/carbon	0.05-0.17	decimal
A_{dp}	Phytoplankton--phosphorus/carbon	0.024-0.24	decimal
K_{mp}	Michaelis constant	0.06-0.6	mg/l
A_{nz}	Zooplankton--nitrogen/carbon	0.05-0.17	decimal
A_{dz}	Zooplankton--phosphorus/carbon	0.024-0.24	decimal
F_2	Zooplankton respiration rate	0.005-0.03	1/day-°C
F_3	Zooplankton death	--	1/day
G_z	Zooplankton growth rate	Eqn. 81	1/day-°C
K_r	Reaeration constant	0.01-5.0	1/day
α_1	Stoichiometry: O_2/NH_4	3.0-3.43	decimal
α_2	Stoichiometry: O_2/NO_2	1.0-1.14	decimal
α_3	Stoichiometry: O_2/Algae	1.6-2.66	decimal
K_c	Coliform decay rate	0.01-3.5	1/day
θ	Temperature correction coefficient	1.05-1.1	--

NUMERICAL SOLUTION METHODS

There have been several numerical schemes[29,30,31,32] developed for solving the convection-diffusion equation describing constituent transport. Most of these specialized techniques have been devised to overcome the inherent problems of numerical dispersion which occur in convection dominated flows. However, in most physical situations of interest here (stratified reservoirs) vertical convective currents are generally small. Consequently, a standard finite difference procedure is employed to obtain approximate solutions for the constituent transport equations. The procedure is based on the approximation:

Finite Difference Approximation

$$\frac{\partial C^{(k)}}{\partial t} = \frac{D_z}{\Delta z^2}\left(C_{j-1}^{(k)} - 2C_j^{(k)} + C_{j+1}^{(k)}\right)$$

$$- \frac{Q_v}{A\Delta z}\left(C_j^{(k)} - C_{j-1}^{(k)}\right)$$

$$+ \frac{1}{A\Delta z}\left(Q_{h,i}\, C_i^{(k)} - Q_{h,o}\, C_j^{(k)}\right) + S_j^{(k)} \qquad (89)$$

where k is the constituent index and j the layer index. Equation 88 is applicable for each layer in the segment-layer representation (see Figure 2). For a particular segment of m layers, Equation 88 is approximated in time by

$$[P]\,\frac{\{C\}^{n+1} - \{C\}^n}{\Delta t} = \frac{1}{2}\,[S]\,\left(\{C\}^{n+1} + \{C\}^n\right) + \{R\} \qquad (90)$$

This equation can be rearranged by combining terms to form the final algebraic system of equations

System of Equations

$$[\bar{P}]\ \{C\}^{n+1} = [\bar{S}]\ \{C\}^n + \{\bar{R}\} \qquad (91)$$

where

$$[\bar{P}] = [P] + \frac{\Delta t}{2}\,[S] \qquad (92)$$

$$[\bar{S}] = [P] - \frac{\Delta t}{2}\,[S] \qquad (93)$$

$$\{\bar{R}\} = \Delta t\ \{R\} \qquad (94)$$

and

Δt = time increment
n,n+1 = time plane indices

The $[\bar{P}]$ and $[\bar{S}]$ matrices, although unsymmetric, are generally well conditioned, mxm tridiagonal matrices. The Crank-Nicholson[33,34] approximation is unconditionally stable and efficiently solved by Gaussian elimination procedures.[7]

Boundary conditions for the transport equations are assumed to be reflective, which is equivalent to a condition of no mass flux across the surface and bottom boundaries. Constituents which do cross boundaries (oxygen at top and phosphorus exchange with bottom sediments) are modeled by source and sink terms and thus are included directly in the transport equation.

To properly track the diurnal patterns in algal growth and respiration, it was necessary to solve the transport equations for the biotic components at a finer time step than the abiotic constituents.

COMPUTER PROGRAM

The water quality model formulation and solution techniques described in previous sections are implemented in a general-purpose computer program AQUA-II. This computer model is an improved and expanded version of a program developed in a previous project[1] for EPA. The AQUA-II program is a multi-segment model and, as such, can provide a quasi-two-dimensional description of water quality dynamics in a stratified or well-mixed reservoir. Major model improvements have been made in the transport, algal dynamics and nutrient cycle submodels; the present formulations provide more correct portrayals of the physical, chemical and biological processes.

For the convenience of the user, a modular programming approach was used. This approach allows the inexperienced user to easily gain a full understanding of the program structure, computational sequence and the purpose of individual subprograms. All subprograms are well commented and important variables are defined. A special purpose subroutine is included to set default values for the submodel constants. These default values are generally midrange values and are a good starting point in model calibration to different sites. A considerable effort has been made to eliminate the subjectivity generally inherent in complex models.

AQUA-II requires less than 22K decimal words for 200 elements per segment. Any number of segments may be used. The program requires 4 disk or drum files, 1 input tape and 1 output tape. The input data tape is written by TERMA. The output tape is optional and is used for storage file of quality simulation results. These results may be later plotted as desired. Run time for AQUA-II was about 6 to 7 minutes for a 3-segment system over a simulation period of 7-1/2 months.

A user's manual has been prepared to explain the specific steps in data preparation and program application.

SECTION VI

AMERICAN FALLS DATA

SITE DESCRIPTION

American Falls Reservoir is a short detention time reservoir with a maximum volume of 2.1×10^9 cubic meters located on the Snake River in Southeast Idaho. Figure 8 shows the general study area. The American Falls Dam located near the town of American Falls was built and is operated by the U. S. Bureau of Reclamation. Idaho Power Company operates a hydroelectric generating station below the dam. However, the head of the dam is not utilized. Figure 9 is a photograph of the dam area. There are currently plans to replace the existing dam structure and install a new generating facility.

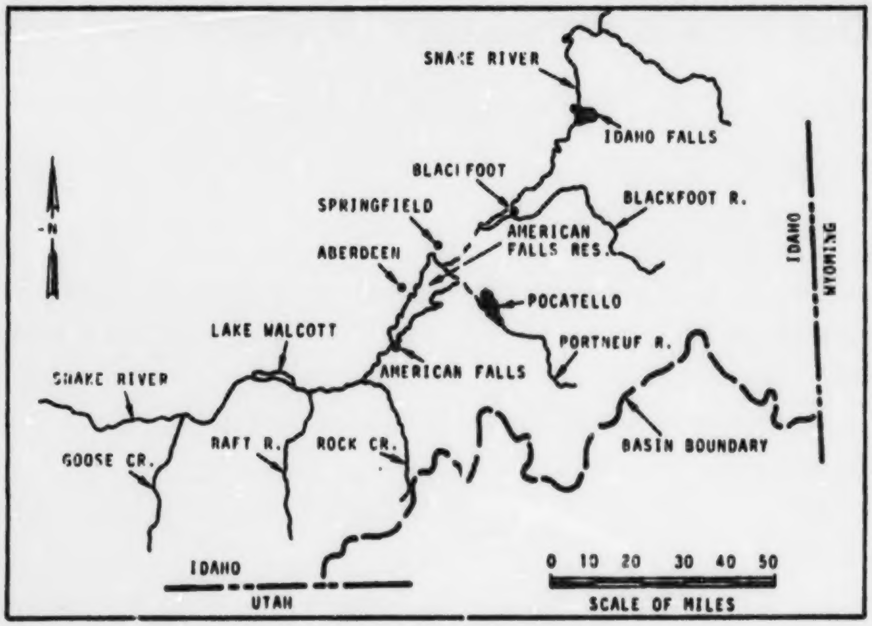
SNAKE RIVER
IDAHO FALLS
BLACKFOOT
SPRINGFIELD
BLACKFOOT R.
N
AMERICAN FALLS RES.
ABERDEEN
POCATELLO
IDAHO
WYOMING
LAKE WALCOTT
PORTNEUF R.
SNAKE RIVER
AMERICAN FALLS
GOOSE CR.
RAFT R.
ROCK CR.
BASIN BOUNDARY
IDAHO
UTAH
0 10 20 30 40 50
SCALE OF MILES

FIGURE 8. Study Area Showing Location of American Falls Reservoir

FIGURE 9. Aerial Photograph of American Falls Dam

There are a number of competing uses for the water resources of the reservoir including agricultural irrigation, waste disposal, recreation and power production. The food processing industry contributes considerable wastes to the tributary rivers during the winter season and irrigation return flows contribute nutrients during the summer.

DATA COLLECTION

The data required for model simulation can be divided into three categories; 1) physical description of the reservoir, 2) meteorologic and hydrologic, and 3) water quality.

After a preliminary review of available data it was decided that 1968 would provide the most complete year of data. Field studies by the EPA[35] and other reports[36] were used for insight into the water quality behavior of the reservoir. However, these data are not complete enough to be used in simulation runs.

The physical description of the reservoir was determined from USGS contour and special river maps as well as information kindly supplied by Mr. Robert Hogg, Idaho Power Company. A plan view of the reservoir is shown in Figure 10. Surface area and volume versus elevation curves are shown in Figure 11. For modeling purposes the reservoir was subdivided into three segments with 0.5 meter elements as shown in Figure 12.

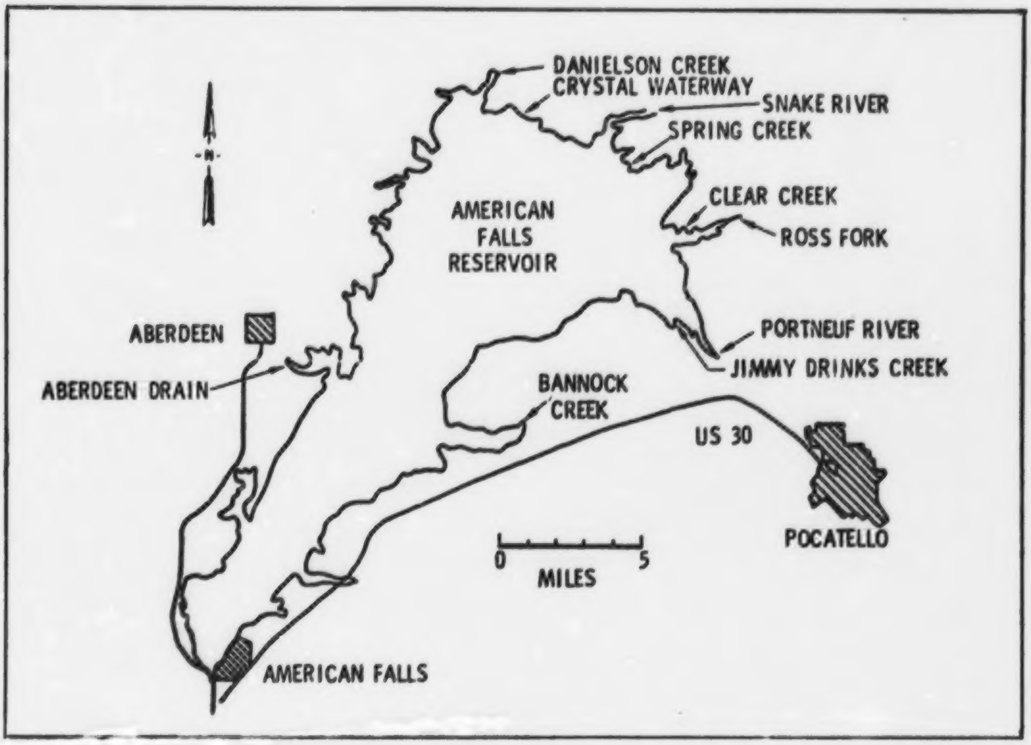
N
DANIELSON CREEK
CRYSTAL WATERWAY
SNAKE RIVER
SPRING CREEK
CLEAR CREEK
ROSS FORK
AMERICAN FALLS RESERVOIR
ABERDEEN
ABERDEEN DRAIN
PORTNEUF RIVER
JIMMY DRINKS CREEK
BANNOCK CREEK
US 30
POCATELLO
0
5
MILES
AMERICAN FALLS

FIGURE 10. Plan View of American Falls Reservoir

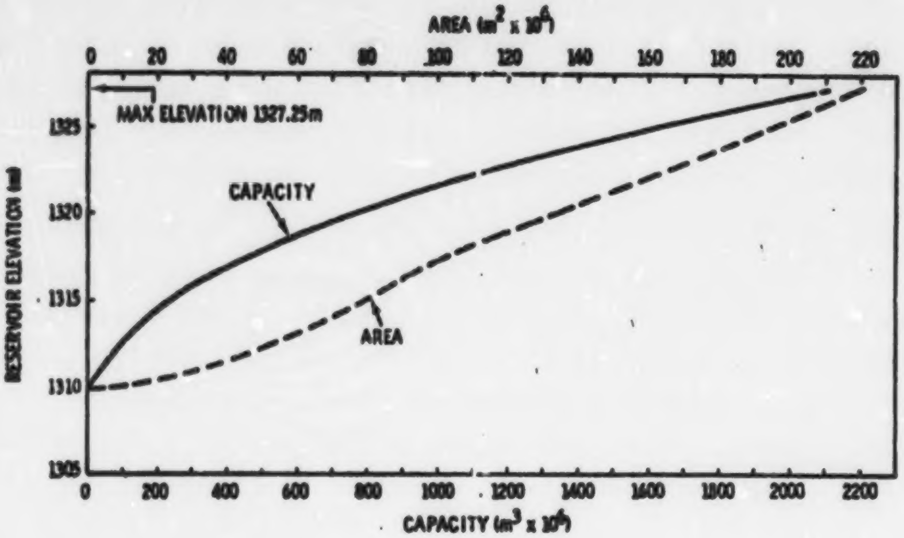

FIGURE 11. Capacity Area Curves for American Falls Reservoir

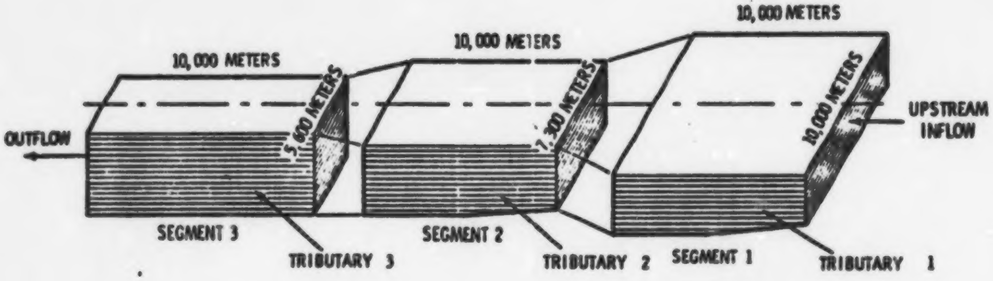
10,000 METERS
10,000 METERS
10,000 METERS
5,800 METERS
7,300 METERS
10,000 METERS
OUTFLOW
UPSTREAM INFLOW
SEGMENT 3
TRIBUTARY 3
SEGMENT 2
TRIBUTARY 2
SEGMENT 1
TRIBUTARY 1

FIGURE 12. Diagram of American Falls Segmentation

Daily meteorological data for 1968 and 1969 were obtained from the National Climatic Center, Asheville, North Carolina. All data except solar radiation were from Pocatello, Idaho. However, the nearest station recording solar radiation was at Boise, Idaho. In addition the solar radiation data from Boise were reported to be questionable in some cases. However, these data were used as they represented the best available. The meteorological data used in the 1968 calculations are shown in Figures 13 through 18.

Hydrologic data were obtained from USGS surface water records and data reported by Bushnell.[36] After obtaining the best estimates of tributary and groundwater inflow and downstream Snake River flow a comparison was made between the calculated surface elevation versus time and the elevation versus time reported by the USGS. The agreement was found to be very poor as shown in Figure 19.

The USGS does report that there are significant irrigation withdrawals which are apparently not accounted for. It was therefore necessary to increase the outflow on a daily basis to maintain a proper water balance as calculated from the observed elevation versus time curve. The proper functioning of the segmented hydrothermal and quality models critically depend on a precise water budget. Slight differences between the observed surface elevation and the surface elevation manifested by a fractionally improper flow balance can produce spurious results in the hydrothermal and quality models.

The American Falls Dam has outlets at the base and spillways at the top. The TERMA program requires the elevation and daily flow for each outlet as input data. No records have been kept at American Falls of daily spillway gate elevations or outlet valve settings to provide a measure of the flow at each of these outlets. The only outflow data available were measured at a gauging station below the reservoir. Mr. Max Vanderberg of the Bureau of Reclamation in Boise, Idaho, indicated that water flowed over the spillway from April 15 to July 20 of 1968.

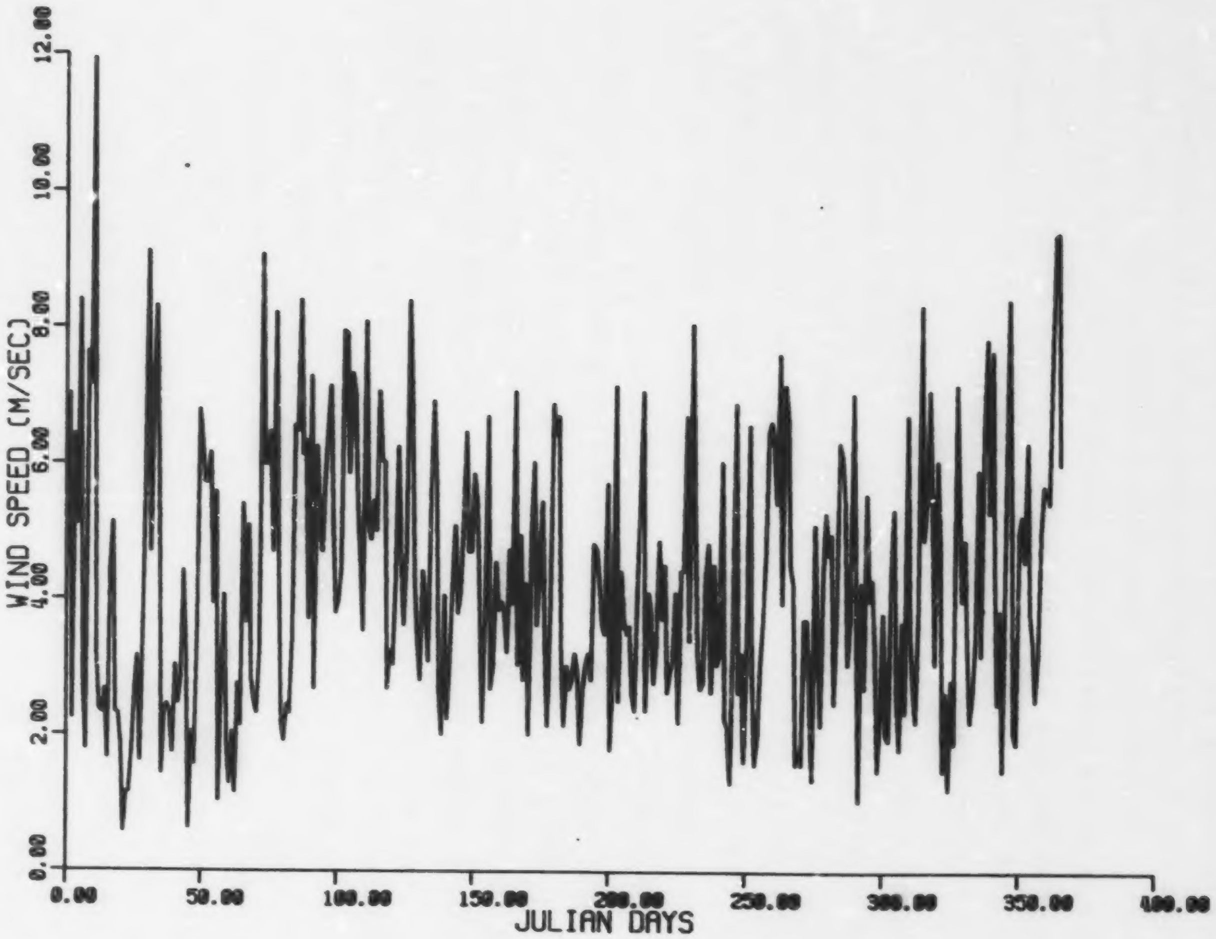

FIGURE 13. Wind Speed, American Falls Reservoir, 1968

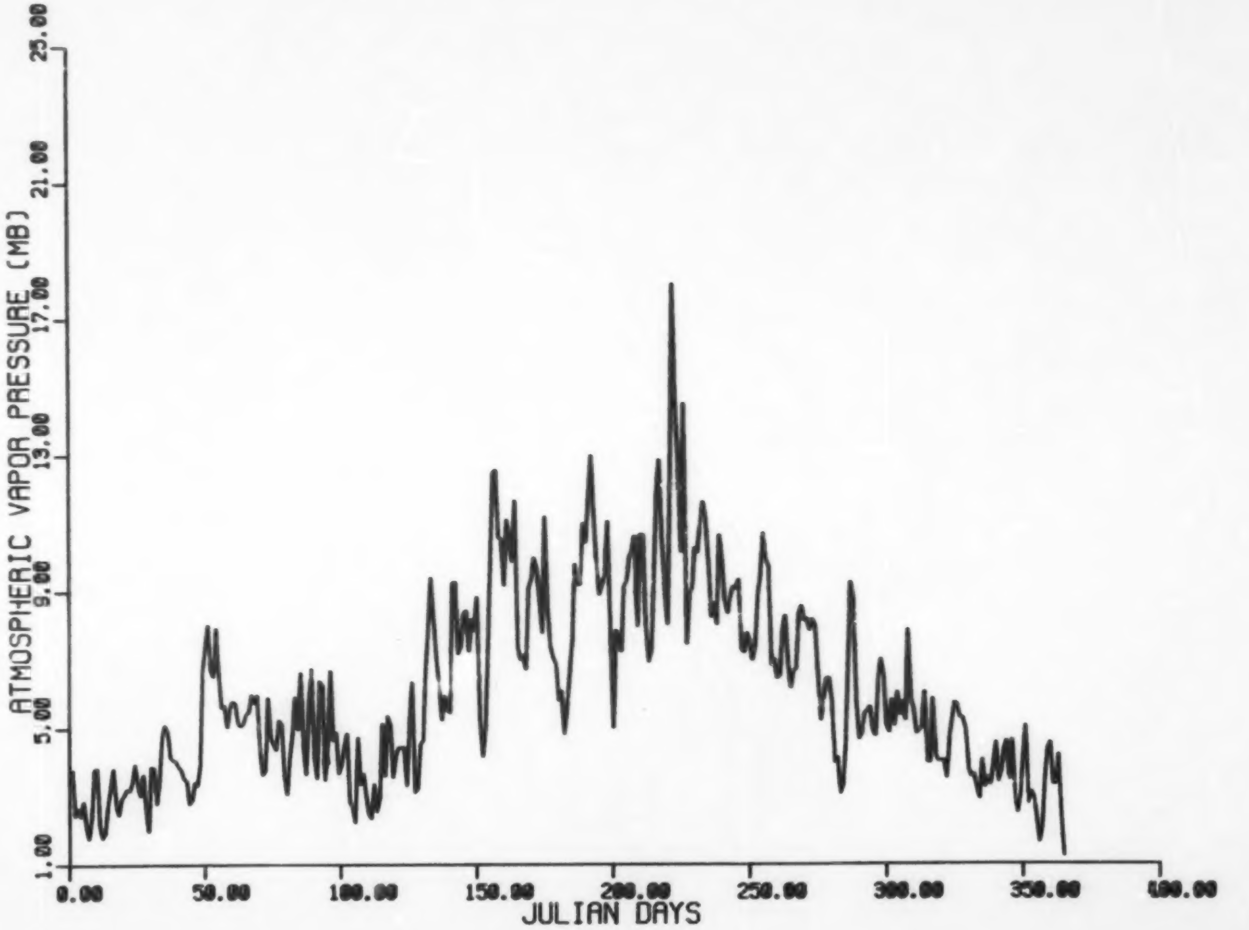

FIGURE 14. Atmospheric Vapor Pressure

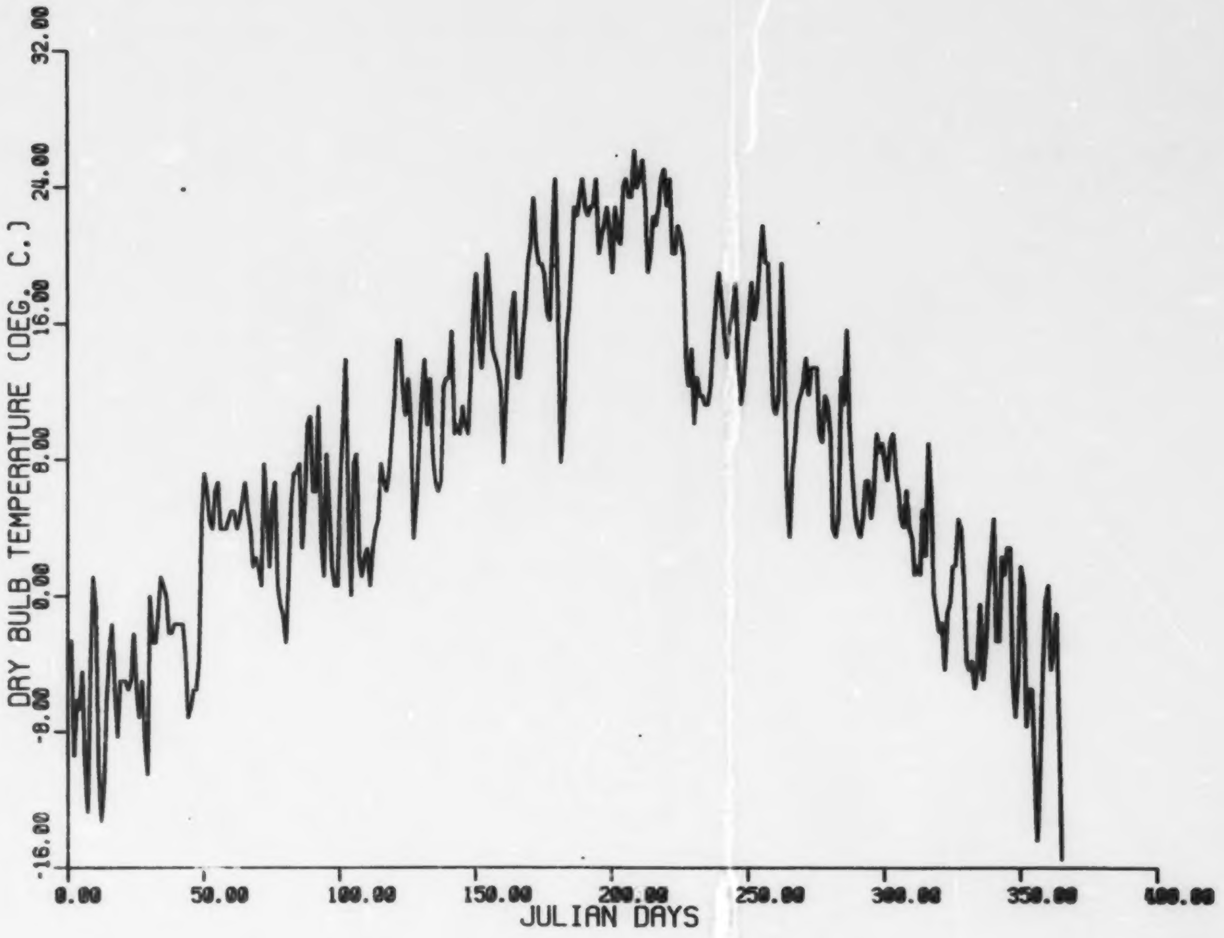

FIGURE 15. Dry Bulb Temperature

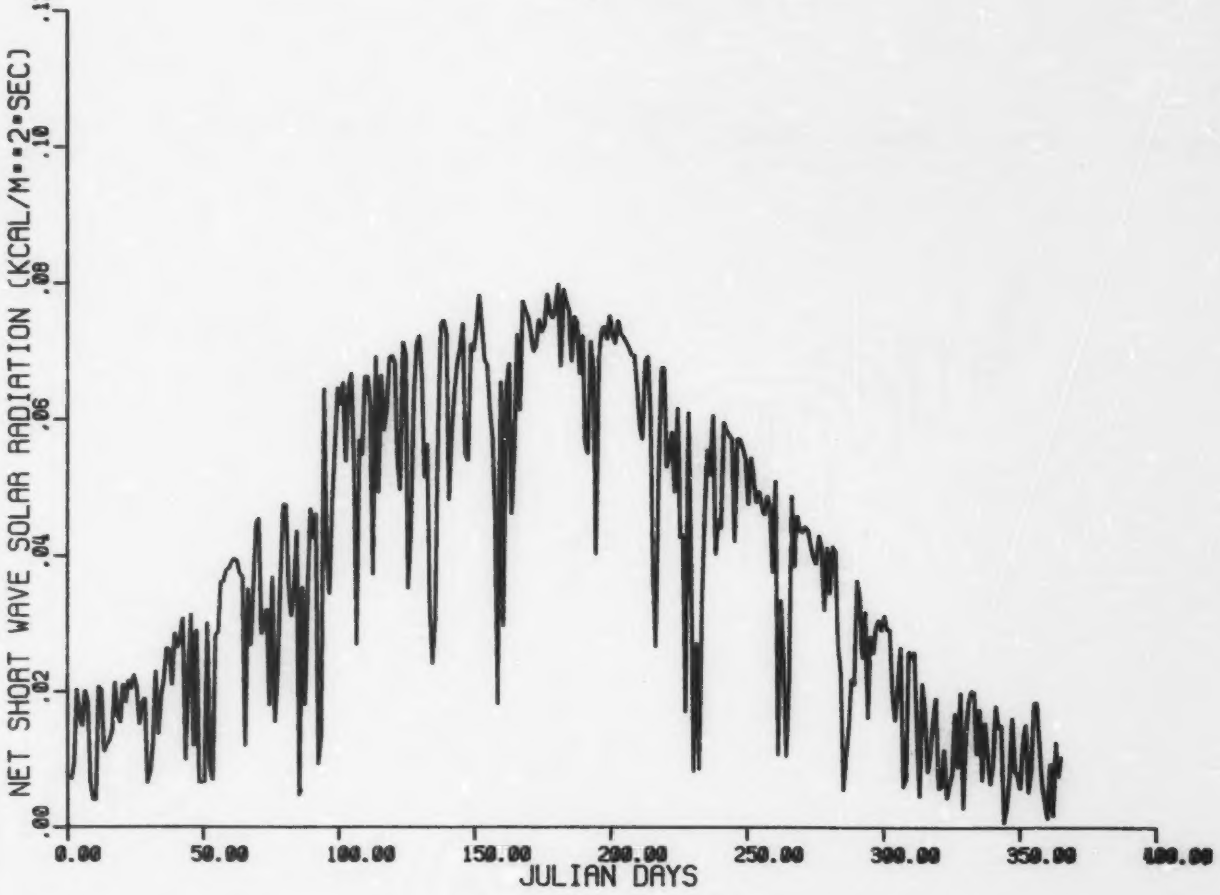

FIGURE 16. Net Short Wave Solar Radiation

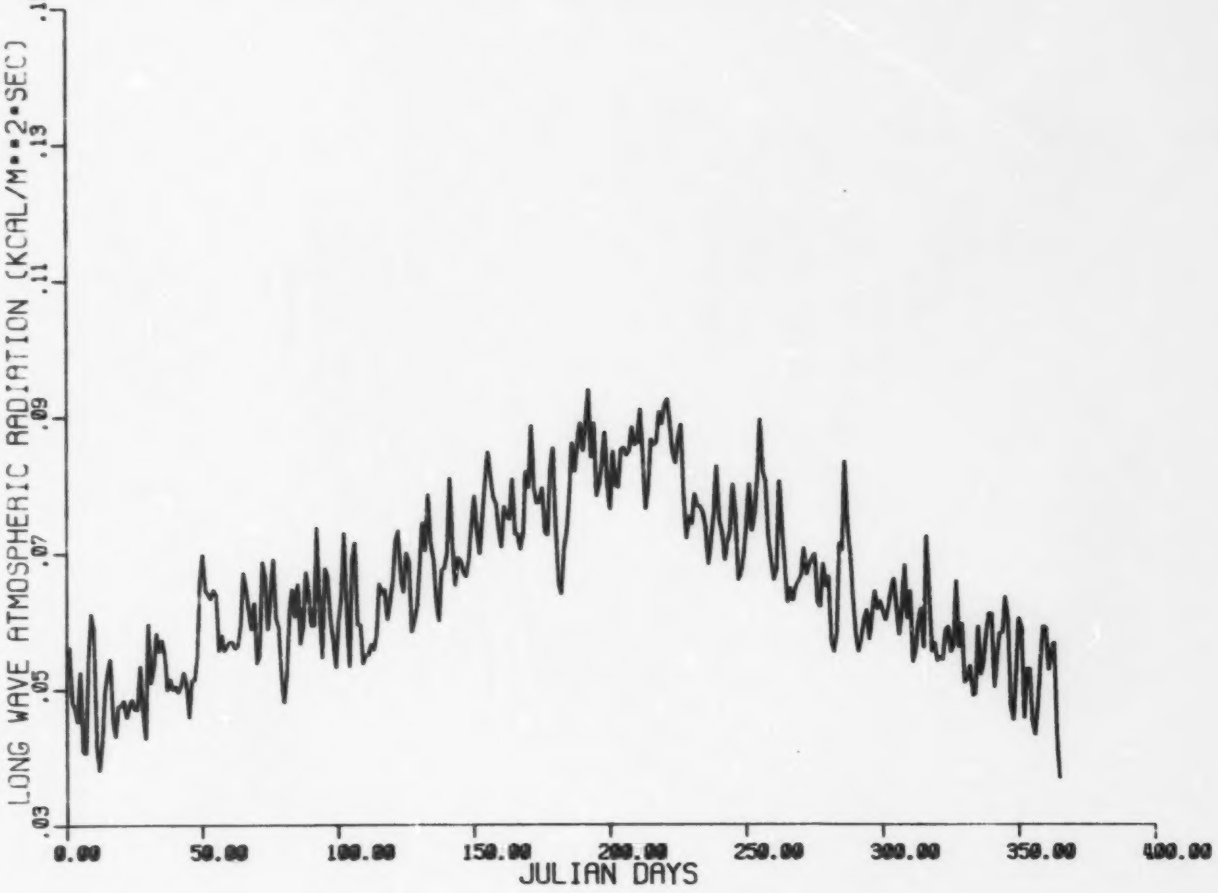

FIGURE 17. Long Wave Atmospheric Radiation

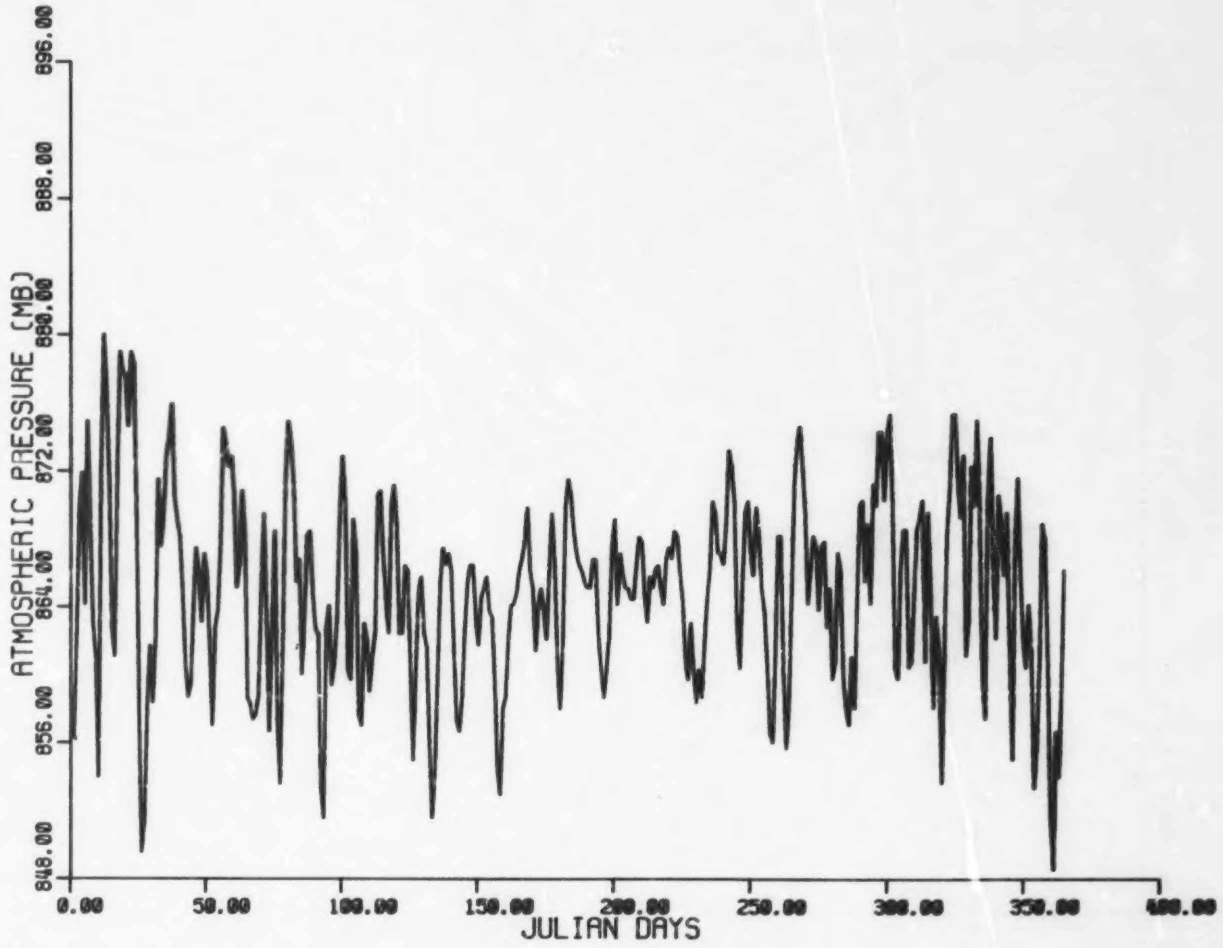

FIGURE 18. Atmospheric Pressure

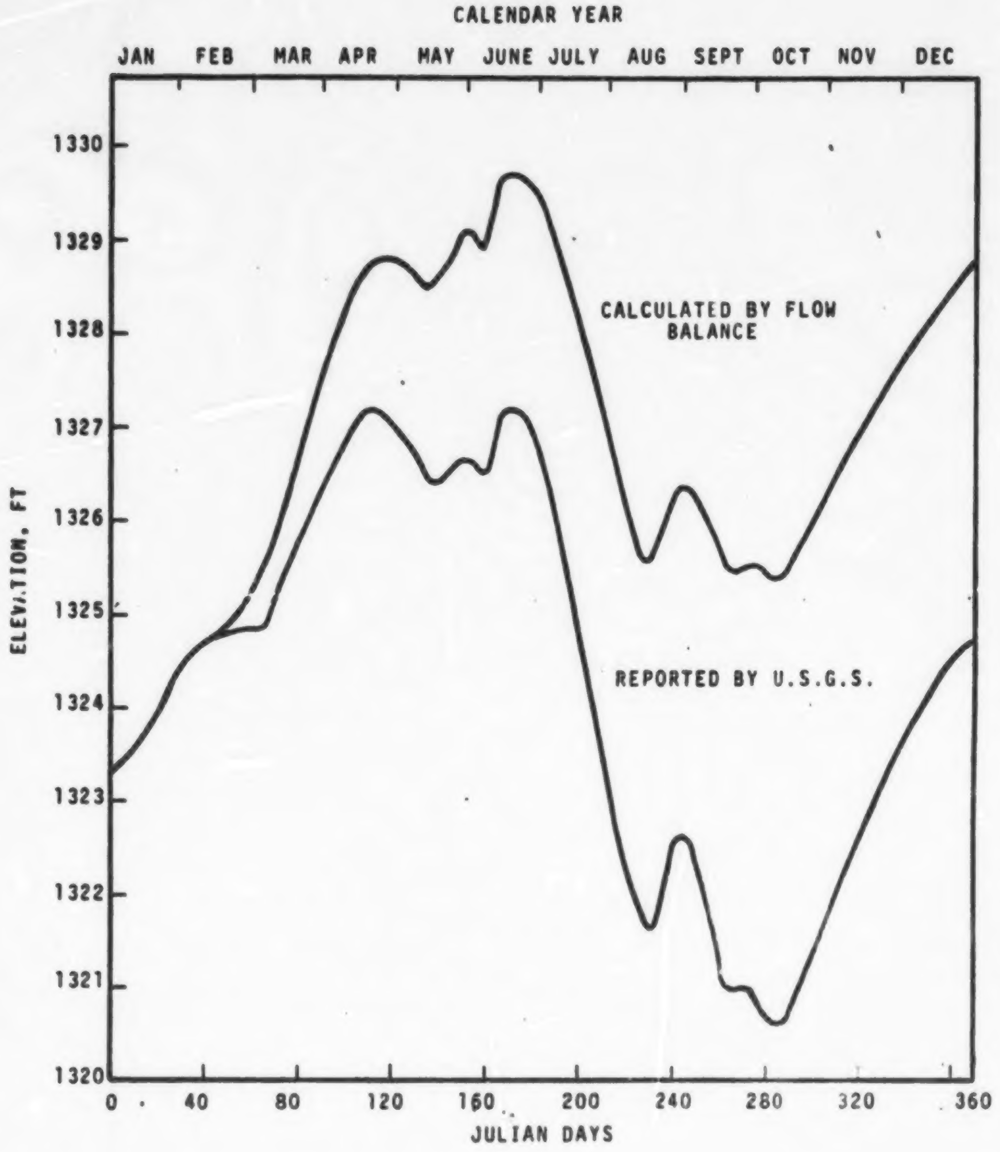

FIGURE 19. Surface Elevation Versus Time, Observed and Calculated

Given these data, the assumption was made that during the simulation period until July 20, all flow up to 10,000 cfs (283.2 m^3/sec) was assigned to the gates at the base of the dam and any flow in excess of 10,000 cfs (283.2 m^3/sec) was assigned as flow over the spillway. The elevation of the spillway was assumed to be 4350.0 ft MSL (1328.88 m MSL) while the elevation of the orifice outlets at the dam base was given as 4300.0 ft MSL (1310.64 m MSL).

Influent water quality and temperature data were obtained from Bushnell.[36] The flow and concentrations of the various parameters in each tributary are shown in Figures A-1 through A-28 in the Appendix for the study period during 1968.

Reservoir water quality was measured in some detail during the summer (May-September) of 1968. Bushnell[36] reported water quality data including measurements of temperature, dissolved oxygen, ammonia, nitrate, and orthphosphate at biweekly intervals at seven stations within the reservoir. Measurements were normally made at 5 foot depth intervals for temperature and oxygen and at surface, mid-depth and bottom for the other parameters. These data are shown in Section VII along with calculated results.

SECTION VII

MODEL APPLICATION AND RESULTS

The hydrothermal water quality model was applied to American Falls Reservoir using data described in the previous section. The hydrothermal model was first applied and found to give very good temperature simulations. The water quality model was then applied using output information from the hydrothermal model for transport of the constituents. Good simulations of water quality data were also obtained.

APPLICATION OF THE HYDROTHERMAL MODEL

The hydrothermal model was applied to the American Falls Reservoir for the period from May 8 (Julian day 128) to December 31, 1968 (Julian day 365). The meteorologic, hydrologic and temperature data described in Section VI were input as required. The results for each of the segments are shown in Figures 20 through 30. Figures 20, 21 and 22 depict the observed and predicted surface temperatures throughout the simulation period. The calculated surface temperatures show very good agreement with the observed values.

Figures 23 through 30 show observed and calculated temperature profiles on specified days for each of the segments. The calculated and prototype data are in good agreement on most days.

The ice cover addition to the model indicated that ice cover first formed at about day 350 and reached a thickness of around 35 cm by the end of the simulation period. There are no data available to check the accuracy of these predictions. However, they seem to be at least reasonable.

APPLICATIONS OF THE WATER QUALITY MODEL

The water quality model was applied to American Falls Reservoir for the same time period as the hydrothermal model

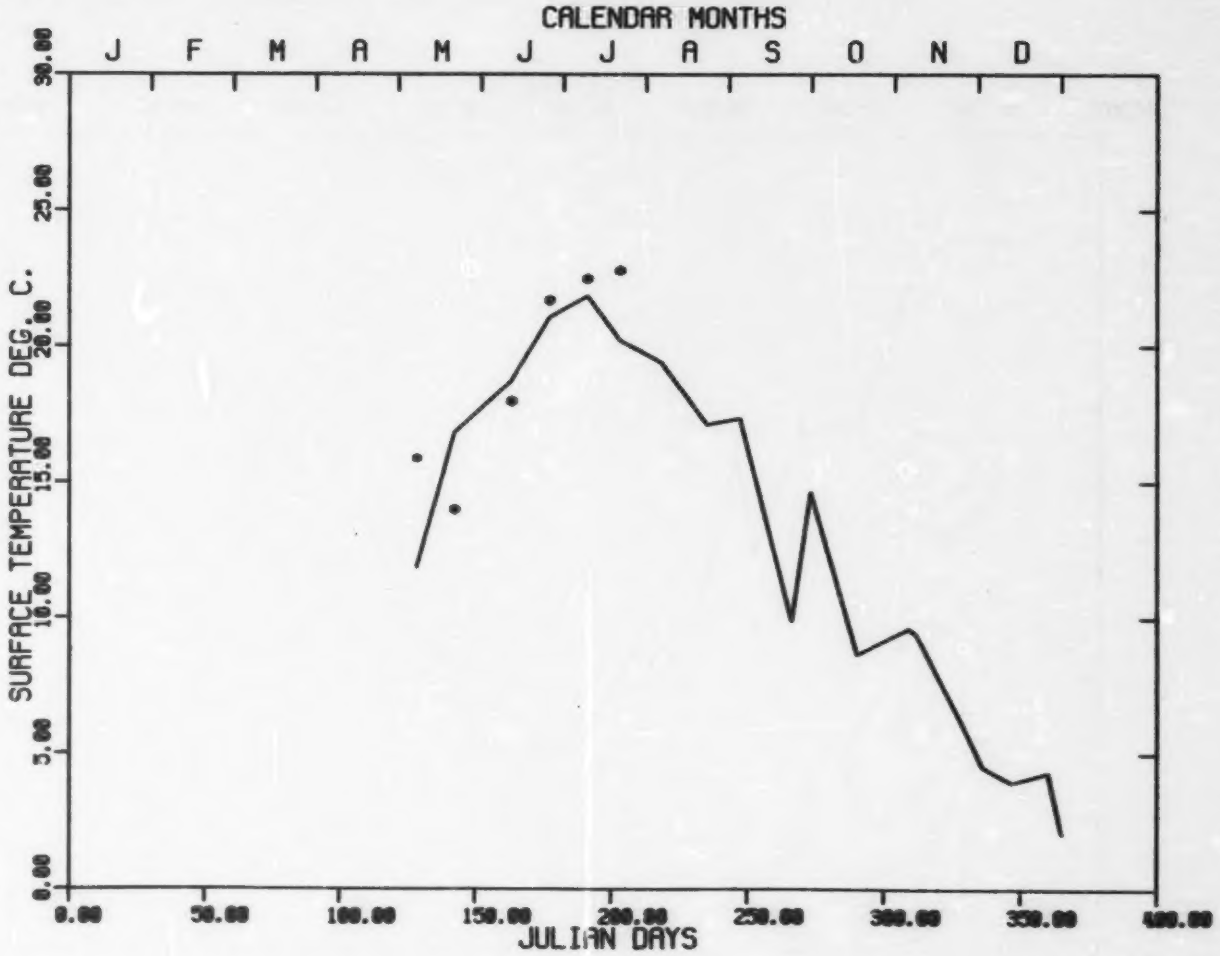

FIGURE 20. Segment 1-Surface Temperature Versus Time

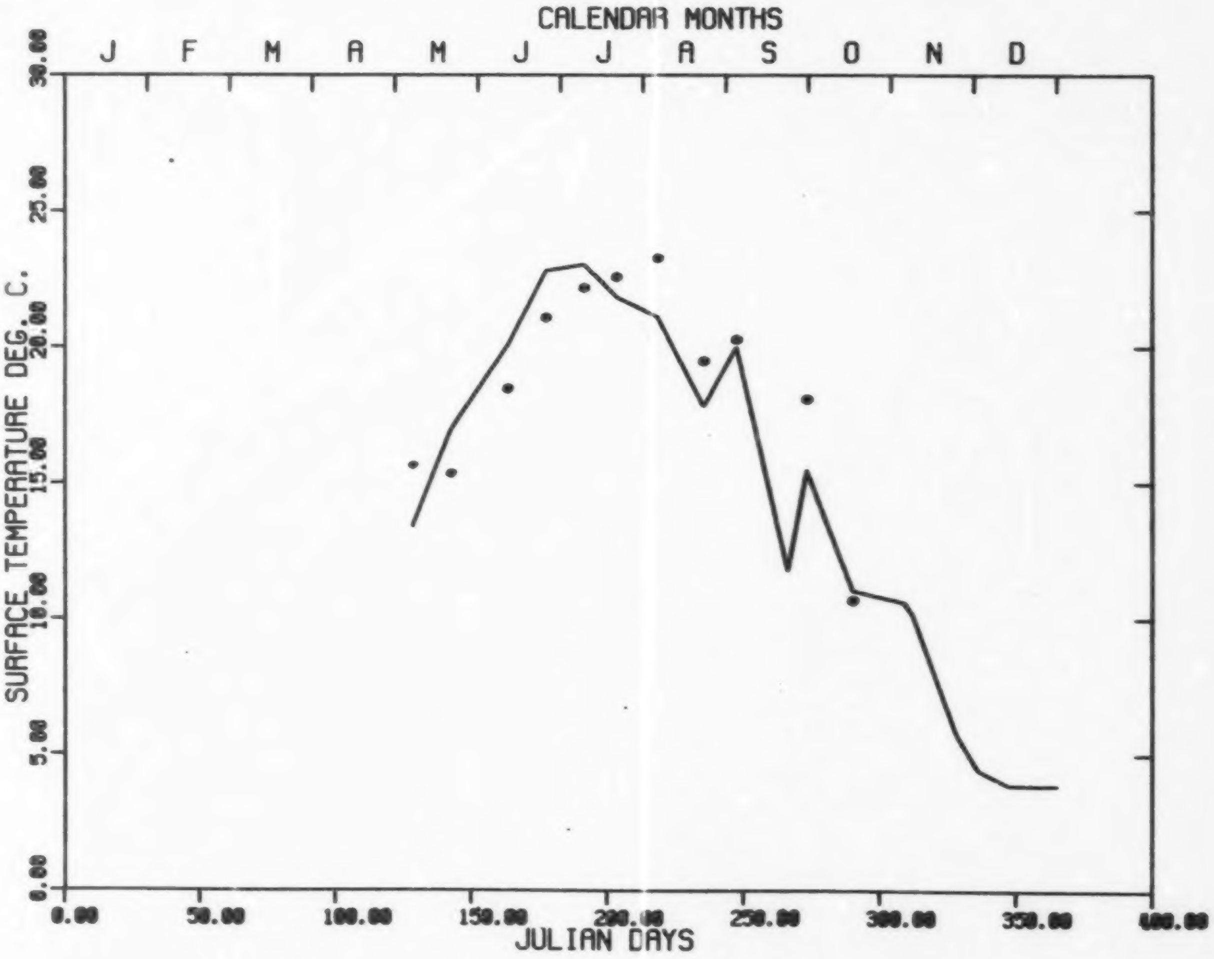

FIGURE 21. Segment 2-Surface Temperature Versus Time

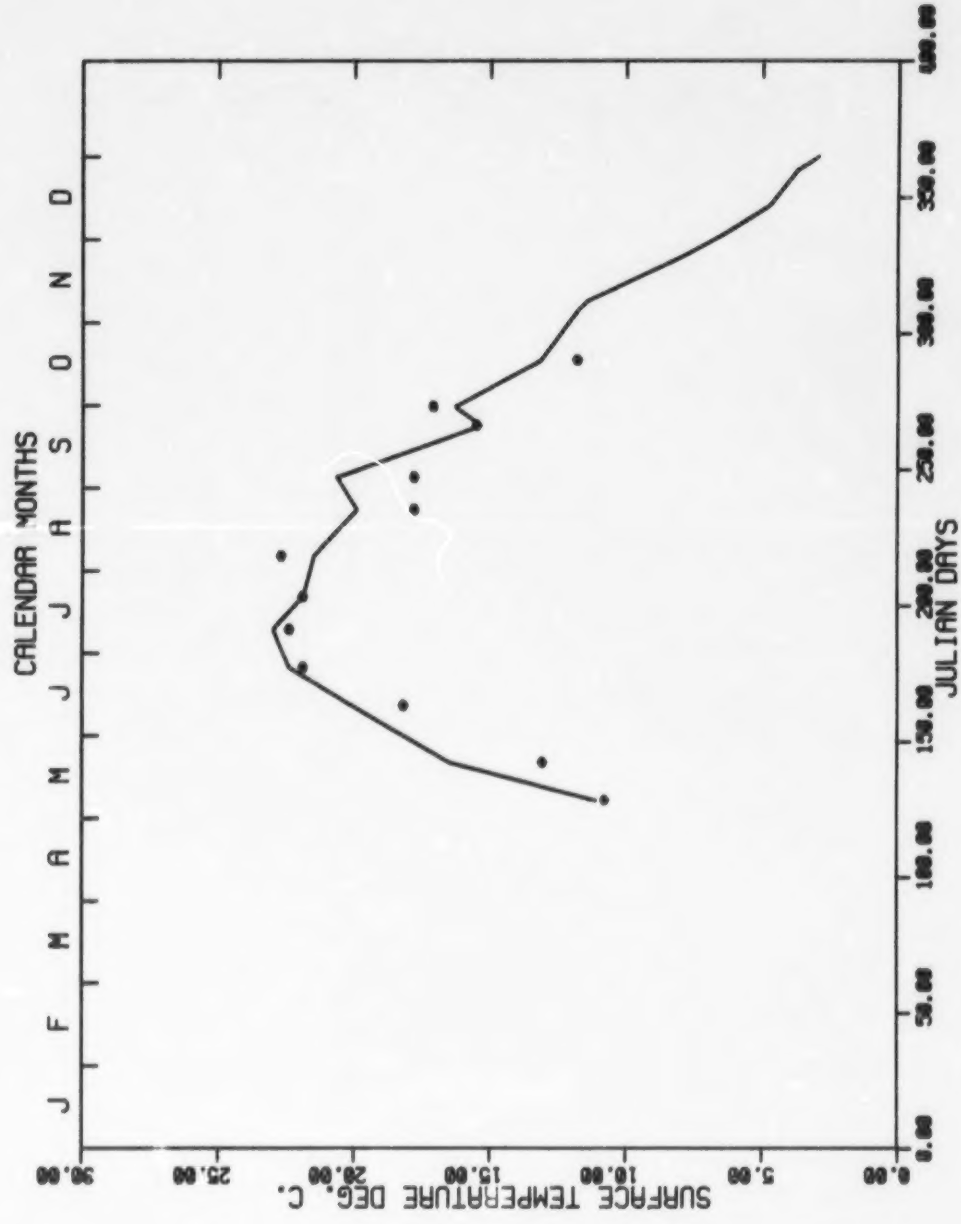

FIGURE 22. Segment 3-Surface Temperature Versus Time

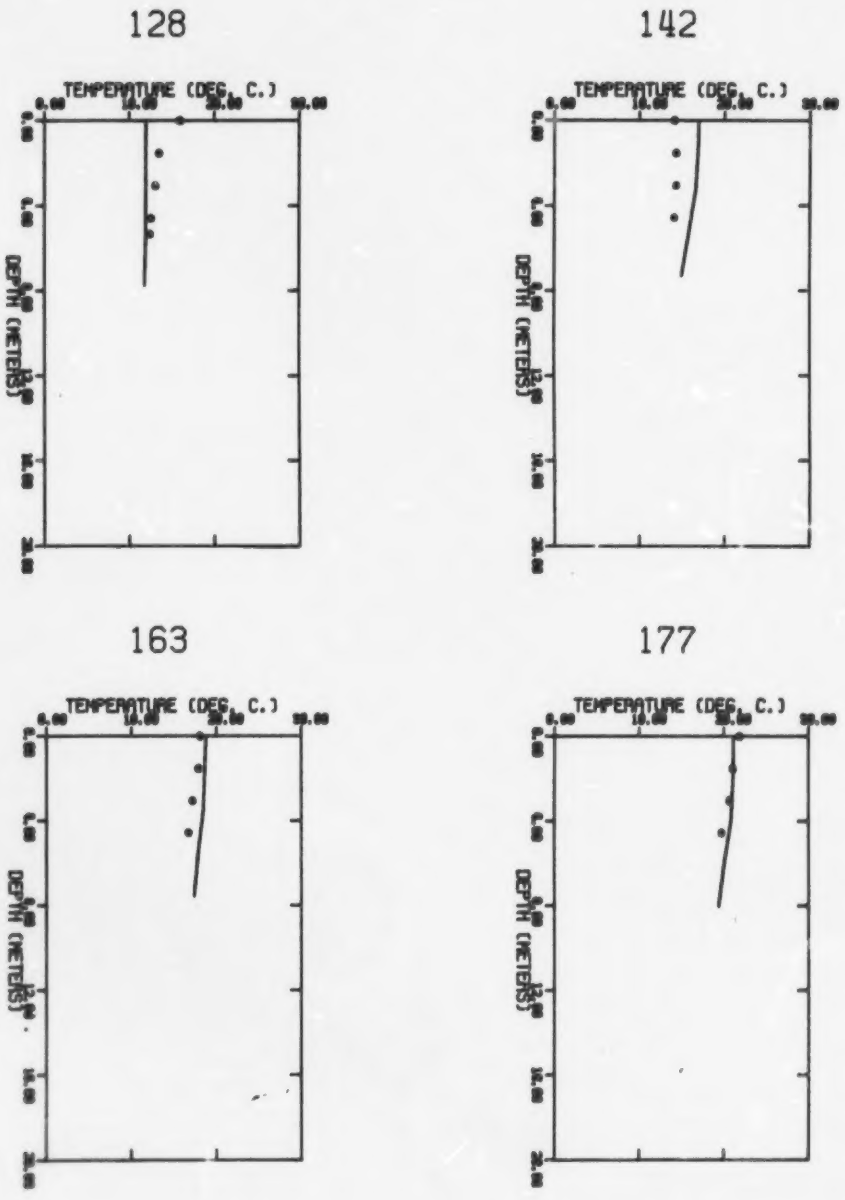

128

142

163

177

FIGURE 23. Segment 1-Temperature Profiles for Given Julian Day

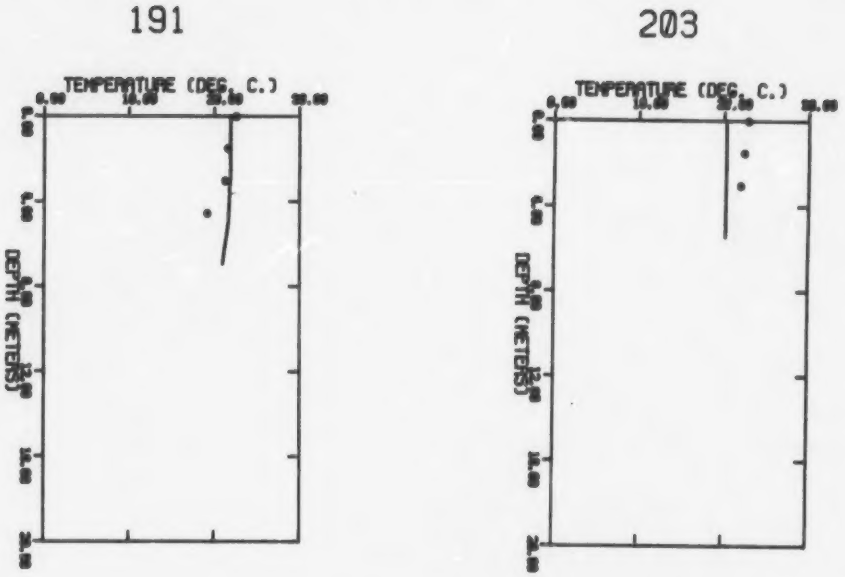

FIGURE 24. Segment 1-Temperature Profiles for Given Julian Day

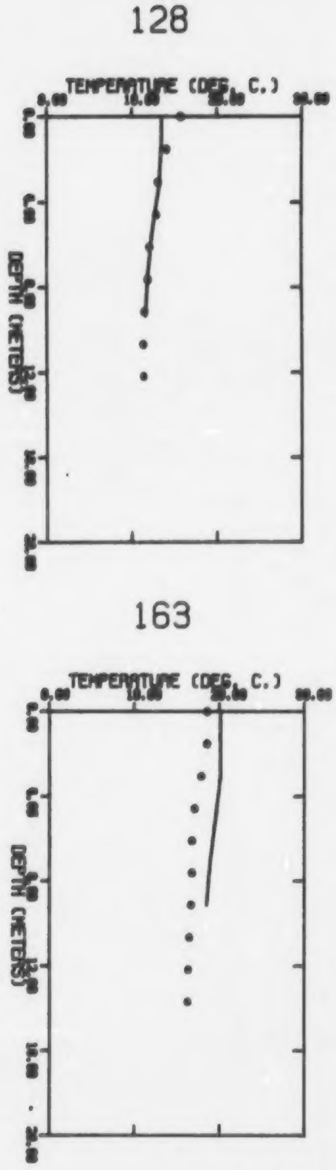

FIGURE 25. Segment 2-Temperature Profiles for Given Julian Day

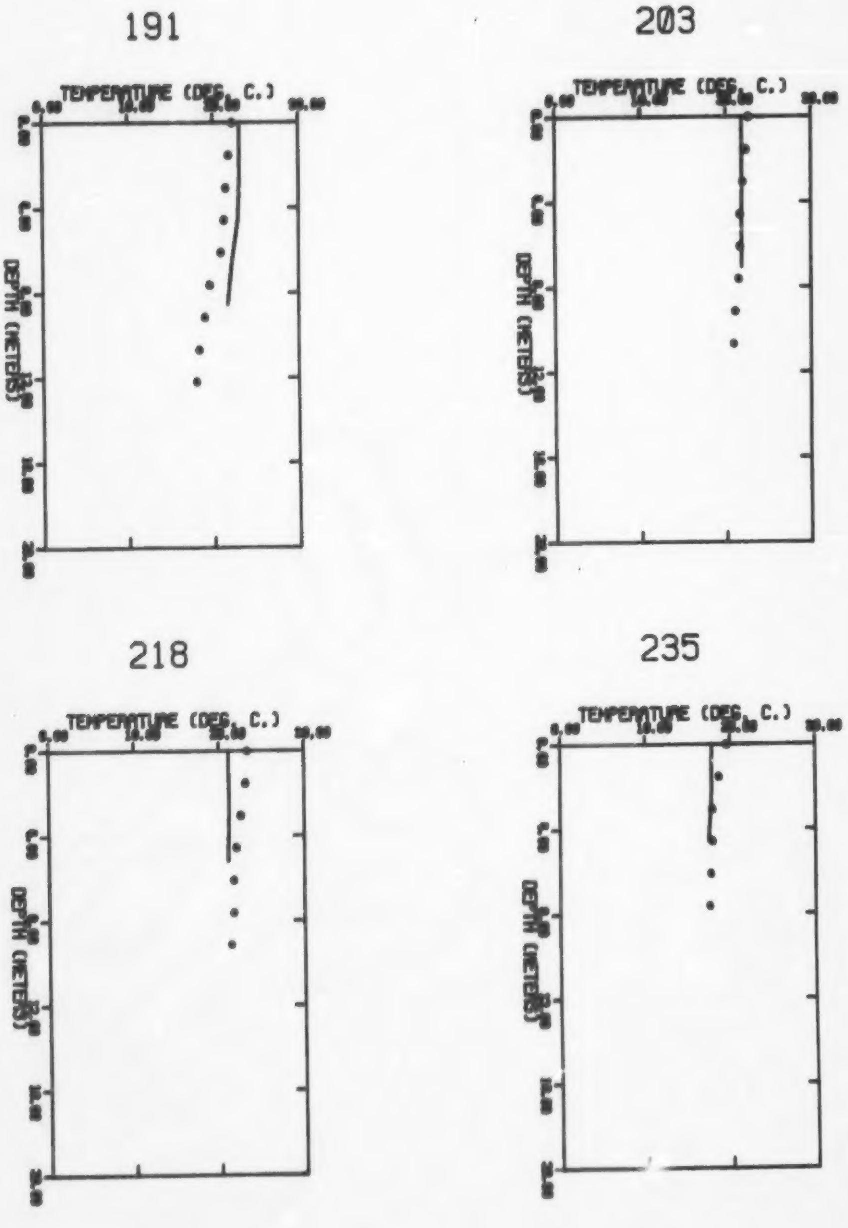

FIGURE 26. Segment 2-Temperature Profiles for Given Julian Day

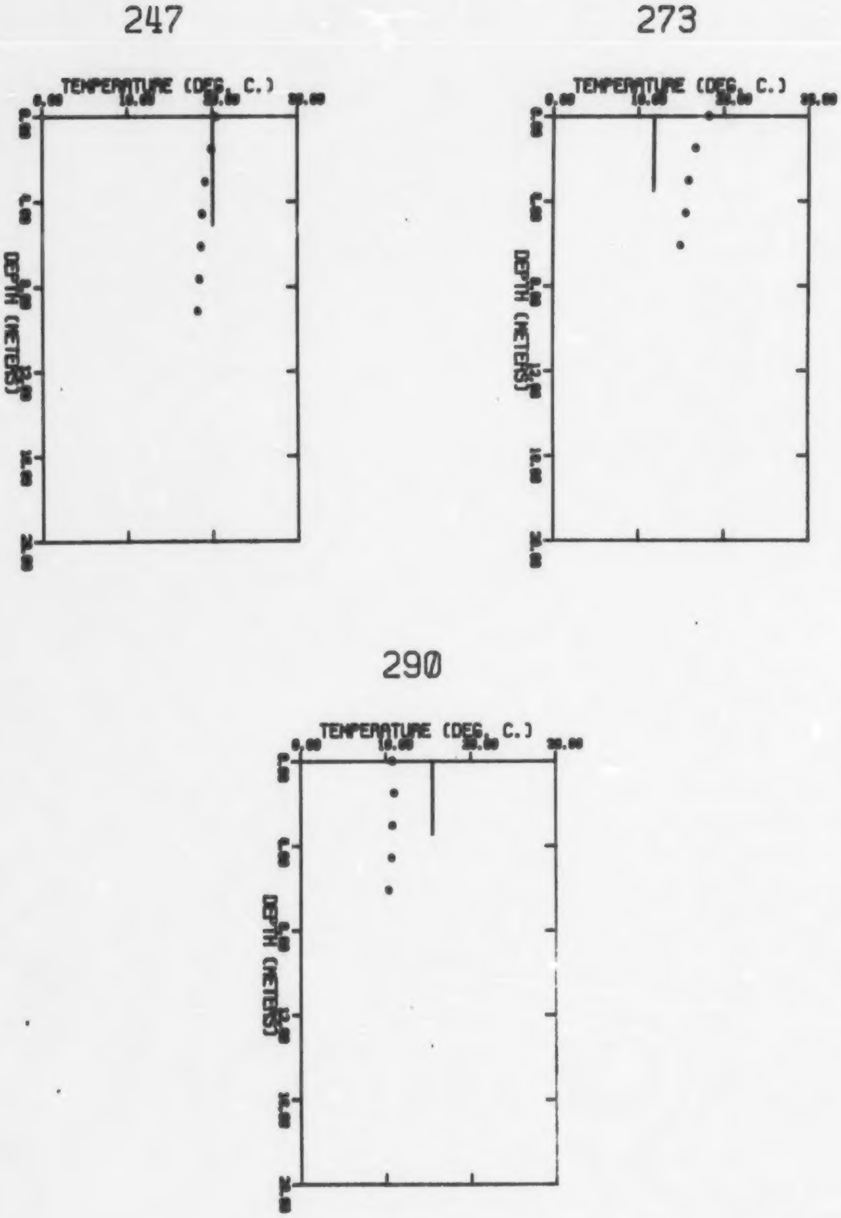

FIGURE 27. Segment 2-Temperature Profiles for Given Julian Day

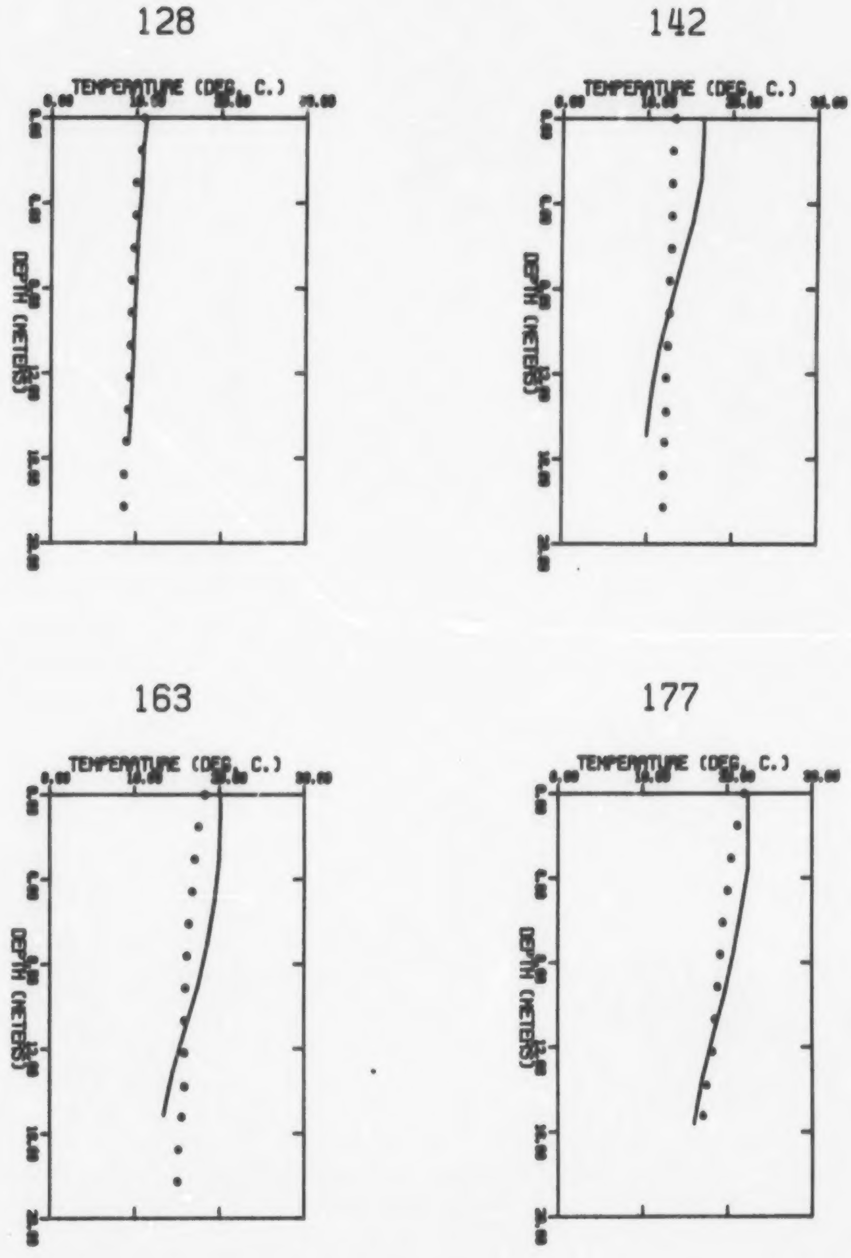

FIGURE 28. Segment 3-Temperature Profiles for Given Julian Day

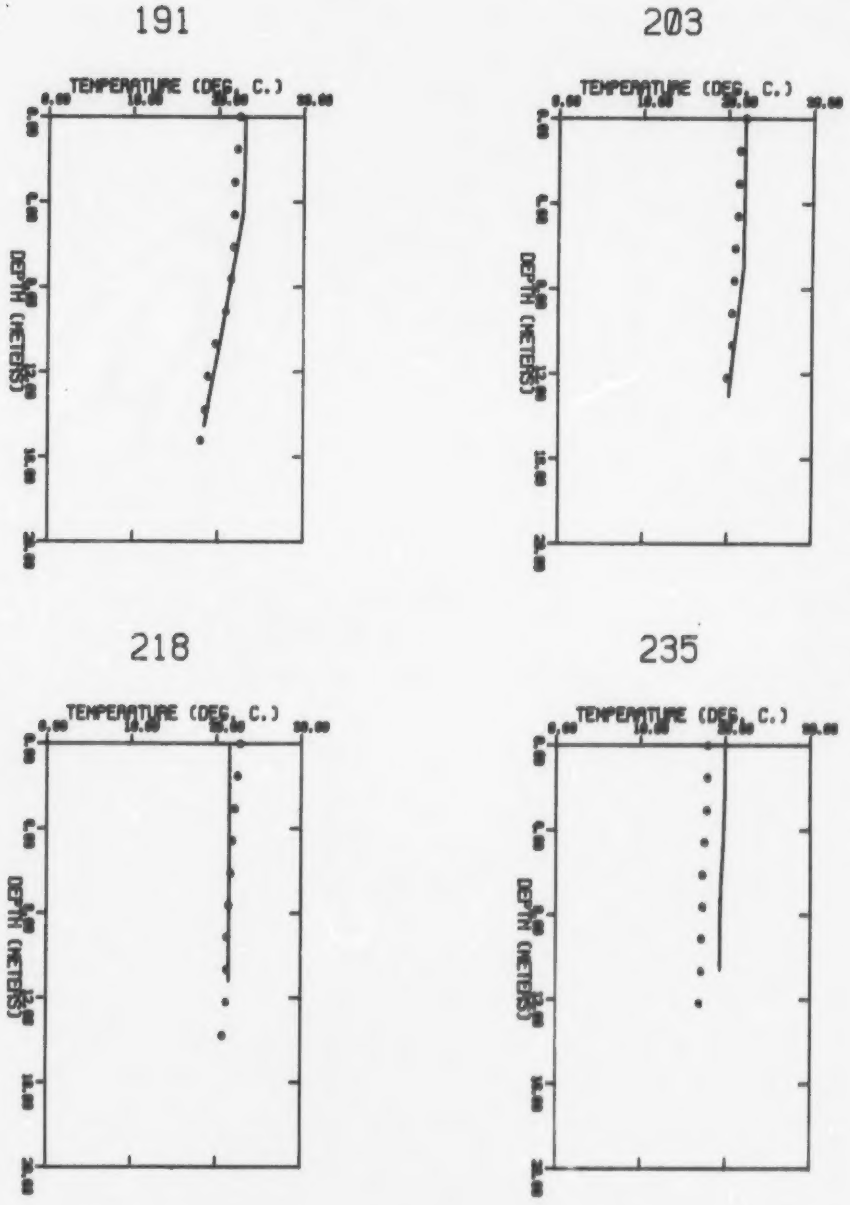

FIGURE 29. Segment 3-Temperature Profiles for Given Julian Day

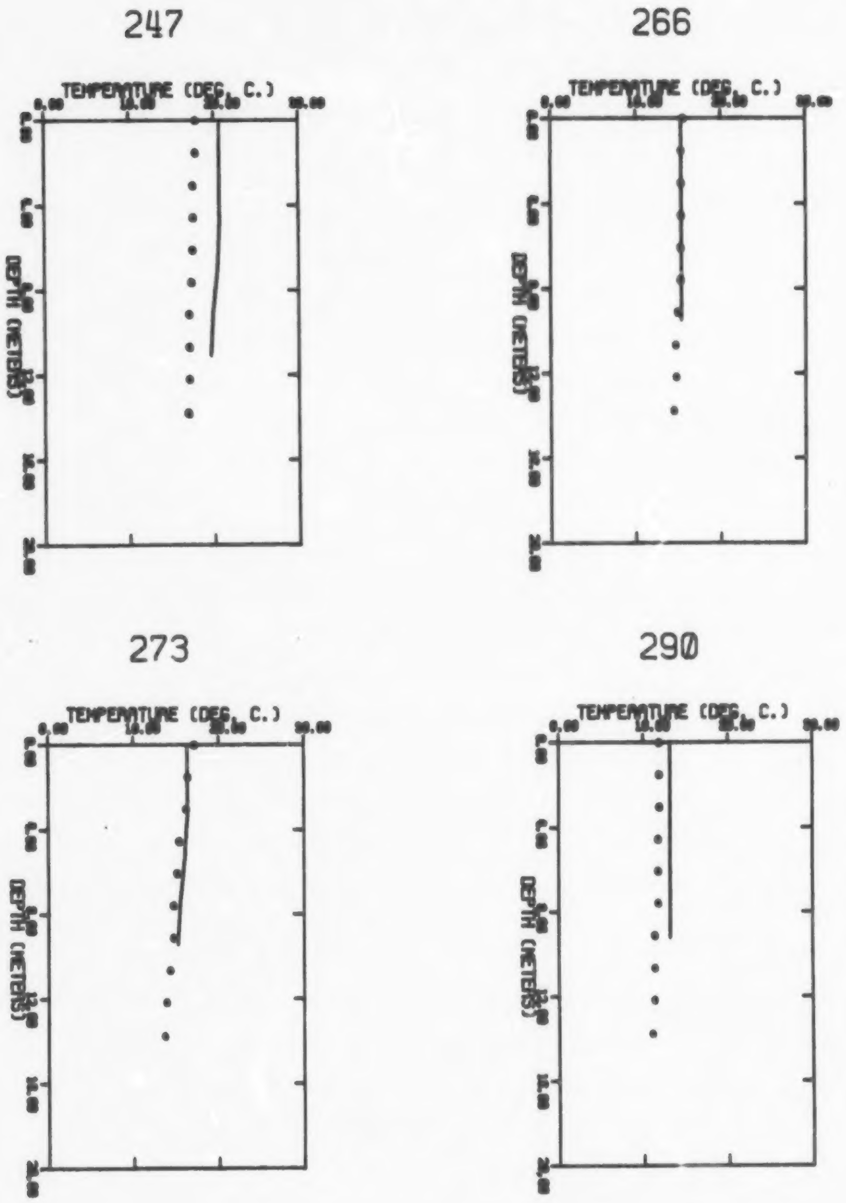

FIGURE 30. Segment 3-Temperature Profiles for Given Julian Day

(May 18, 1968 - December 31, 1968). Tributary quality data used are summarized in Section VI.

The simulation results for the calibrated model are shown in Figures 31 through 40. Data collected by Bushnell[36] are also shown on these figures for comparison.

DISCUSSION OF RESULTS

Temperature

The results of the thermal simulations show remarkable agreement with the observed data in both time and space. These results reflect the models general capability to accurately describe the thermal energy distribution within the reservoir and its response to atmospheric heating and cooling. The tracking of seasonal temperature patterns, see Figure 20 through 22, in the surface zone is excellent for all three segments. The few instances where model results disagree with observed data is attributed to the meteorologic data base which is not fully characteristic of the site. The meteorologic data used in the simulations were obtained for Pocatello and Boise. In addition, Bushnell reports occurrences of "unusually intense storms" in early and late August which produced distinct but short term perturbations of the thermal regime.

Dissolved Oxygen

By and large, very good agreement was achieved between the predicted distribution of dissolved oxygen and the conditions observed by Bushnell. The model predicts well the seasonal DO trends in the surface zone for all three segments. It is noted that DO levels in the surface zone are generally close to saturation values. It can be seen in Figure 31 that three data points for segment 2 deviate markedly from the predicted curve and the natural trend of other data points as well.

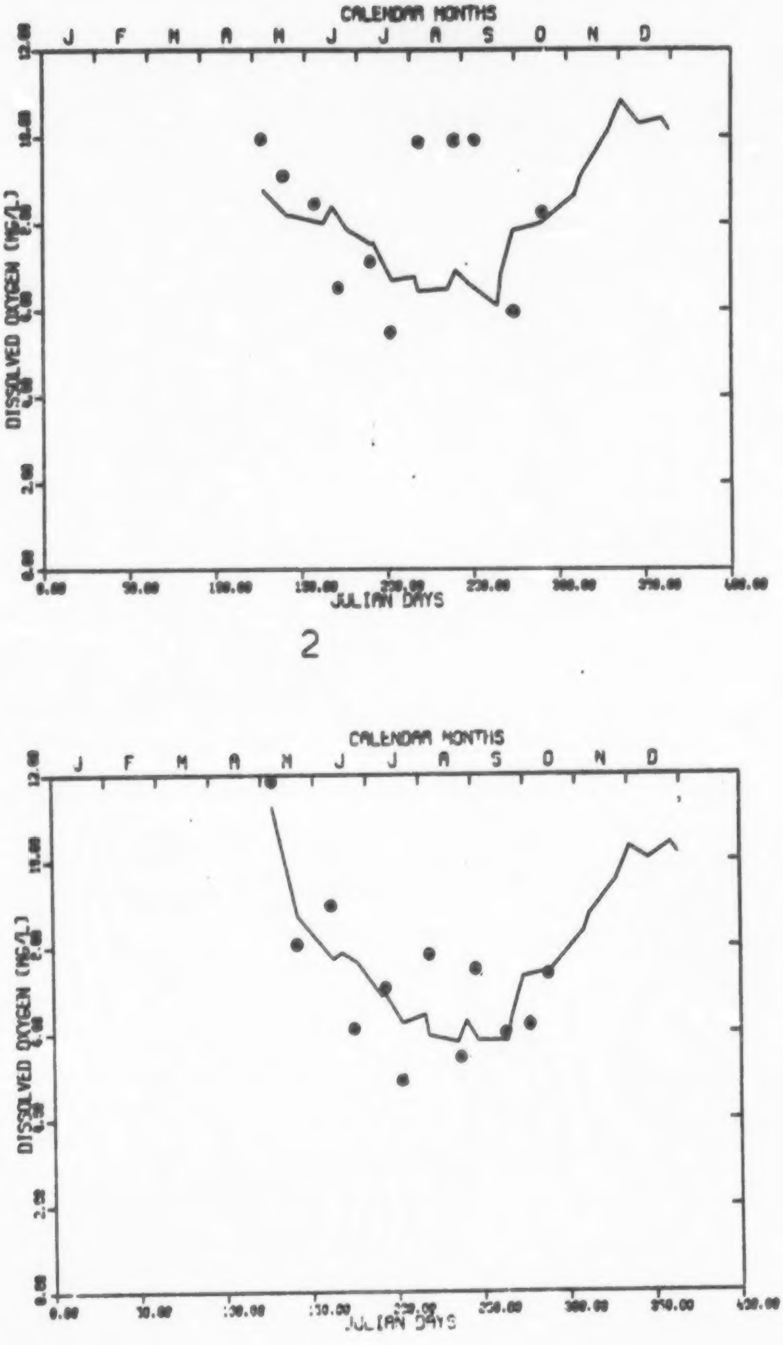

2

3

FIGURE 31. Segments 2 and 3 Dissolved Oxygen Surface Concentrations History

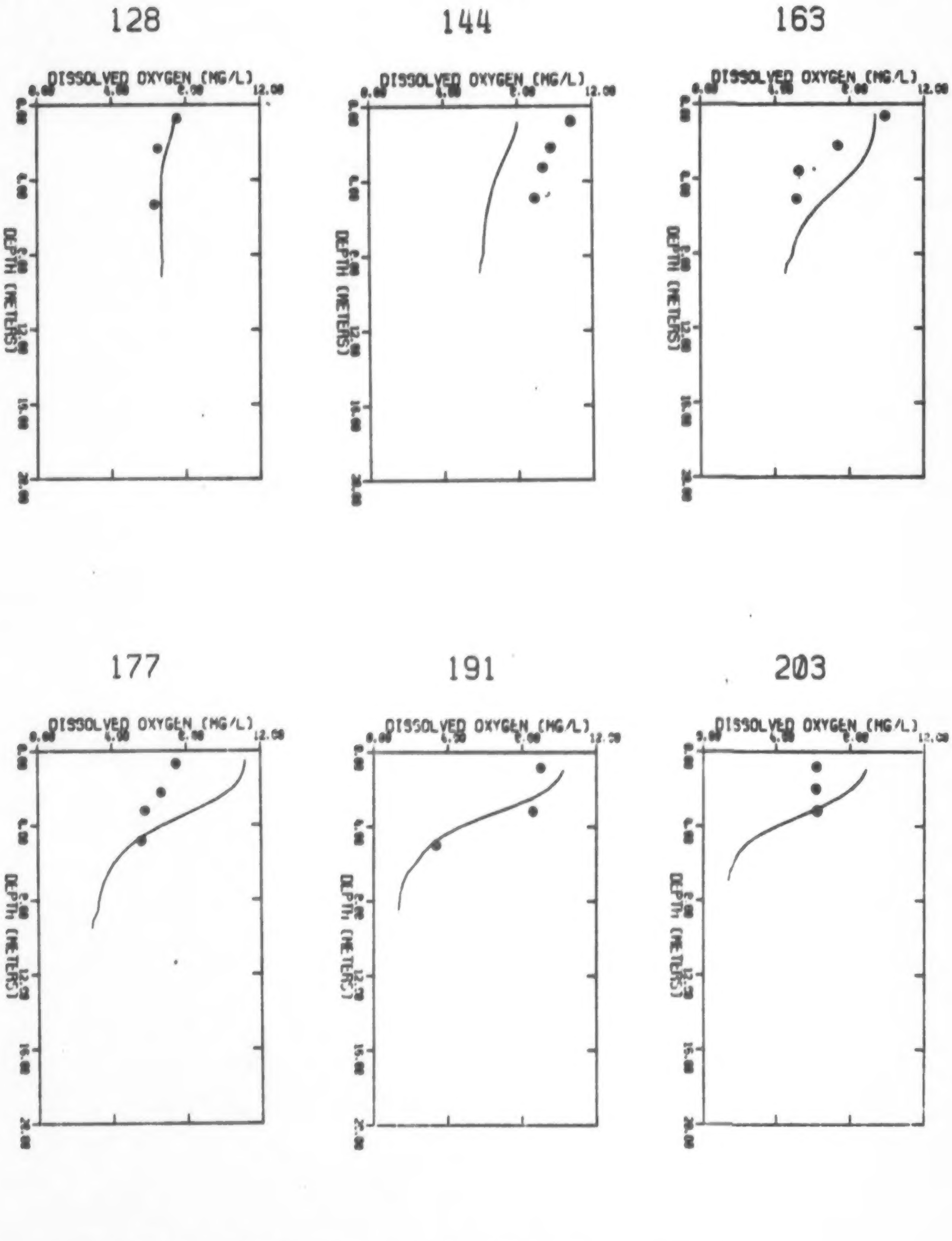

FIGURE 32. Dissolved Oxygen Profiles - Segment 1

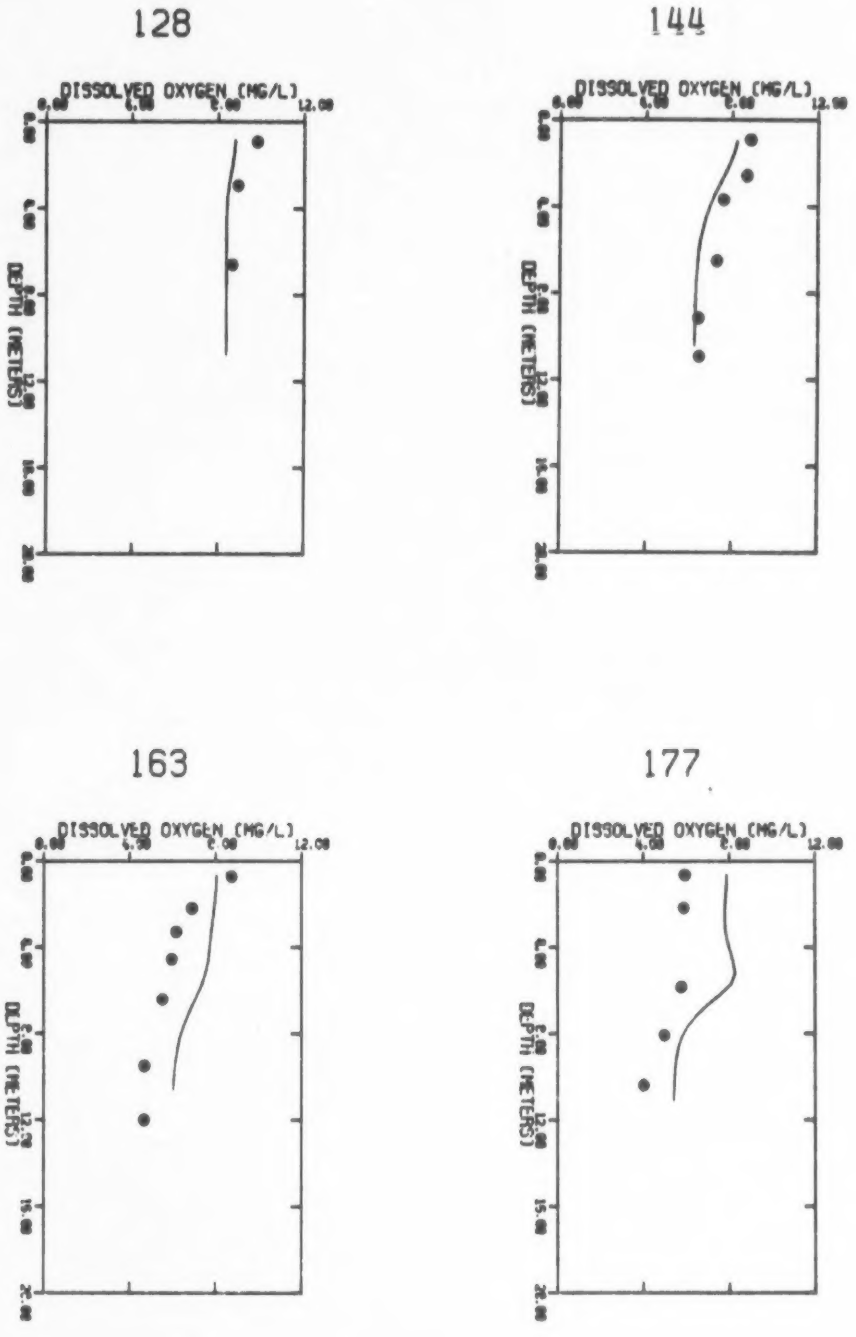

FIGURE 33. Dissolved Oxygen Profiles - Segment 2

247

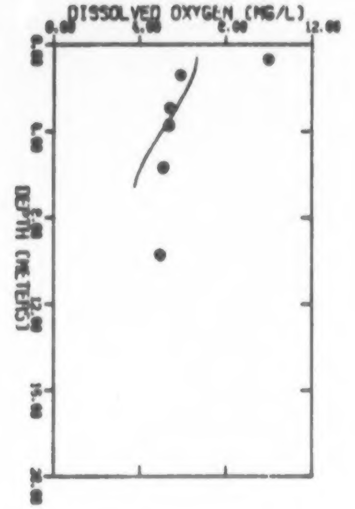

266

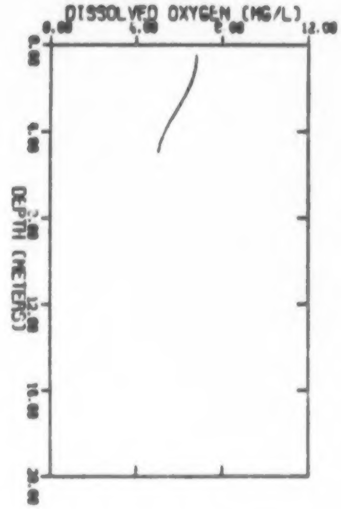

273

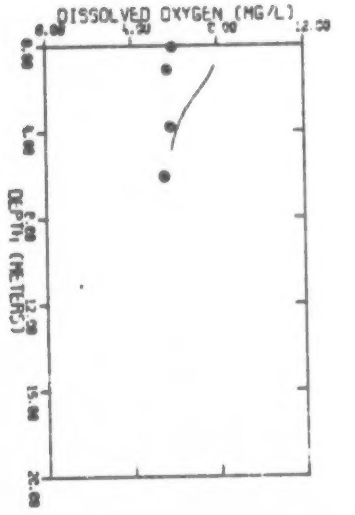

290

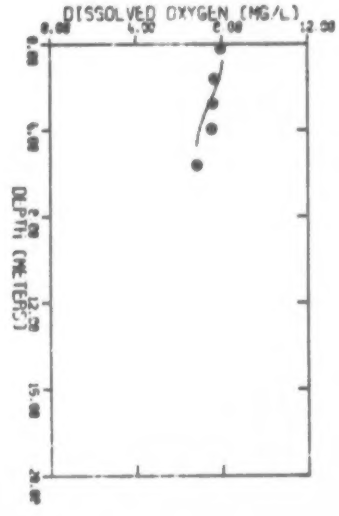

FIGURE 33. (continued)

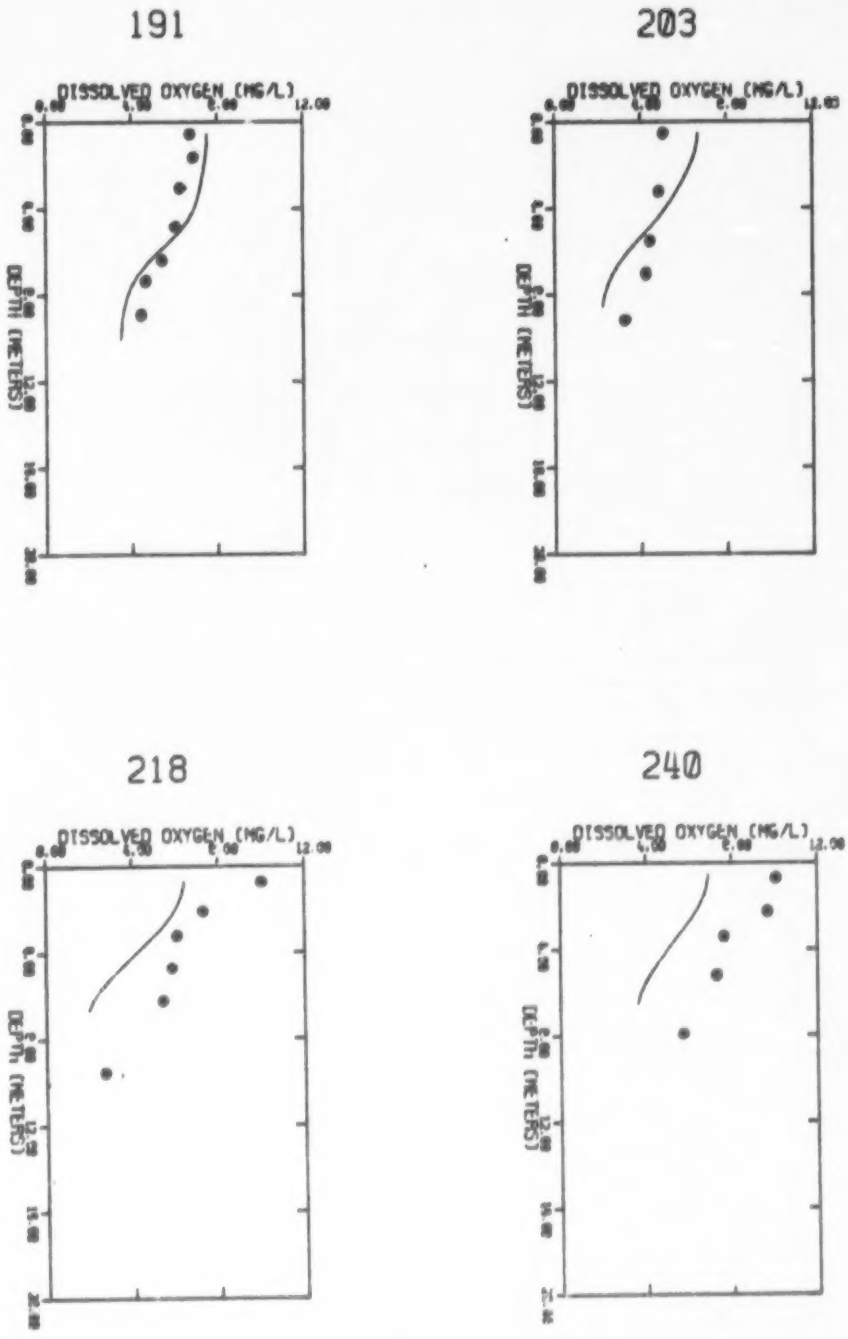

FIGURE 33. (continued)

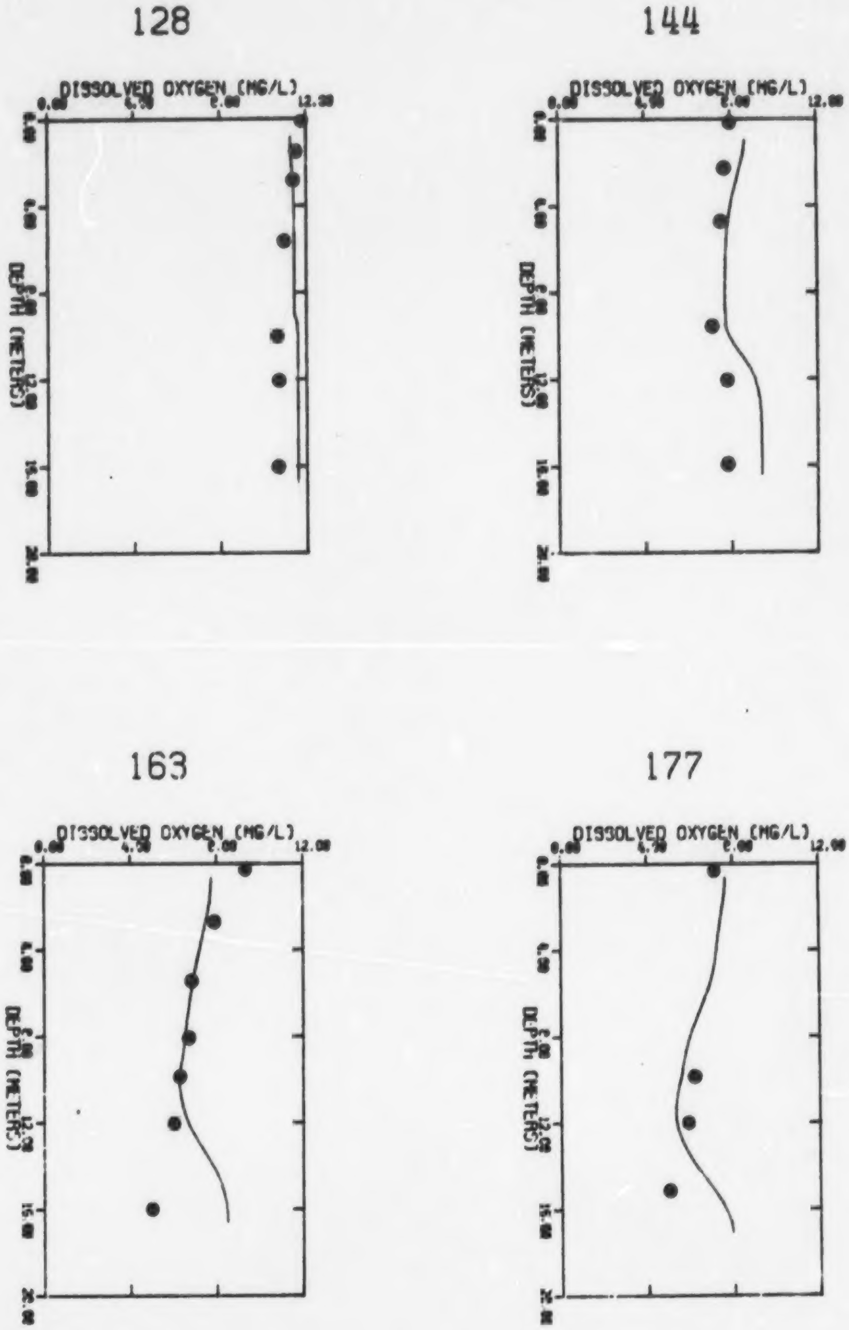

FIGURE 34. Dissolved Oxygen Profiles - Segment 3

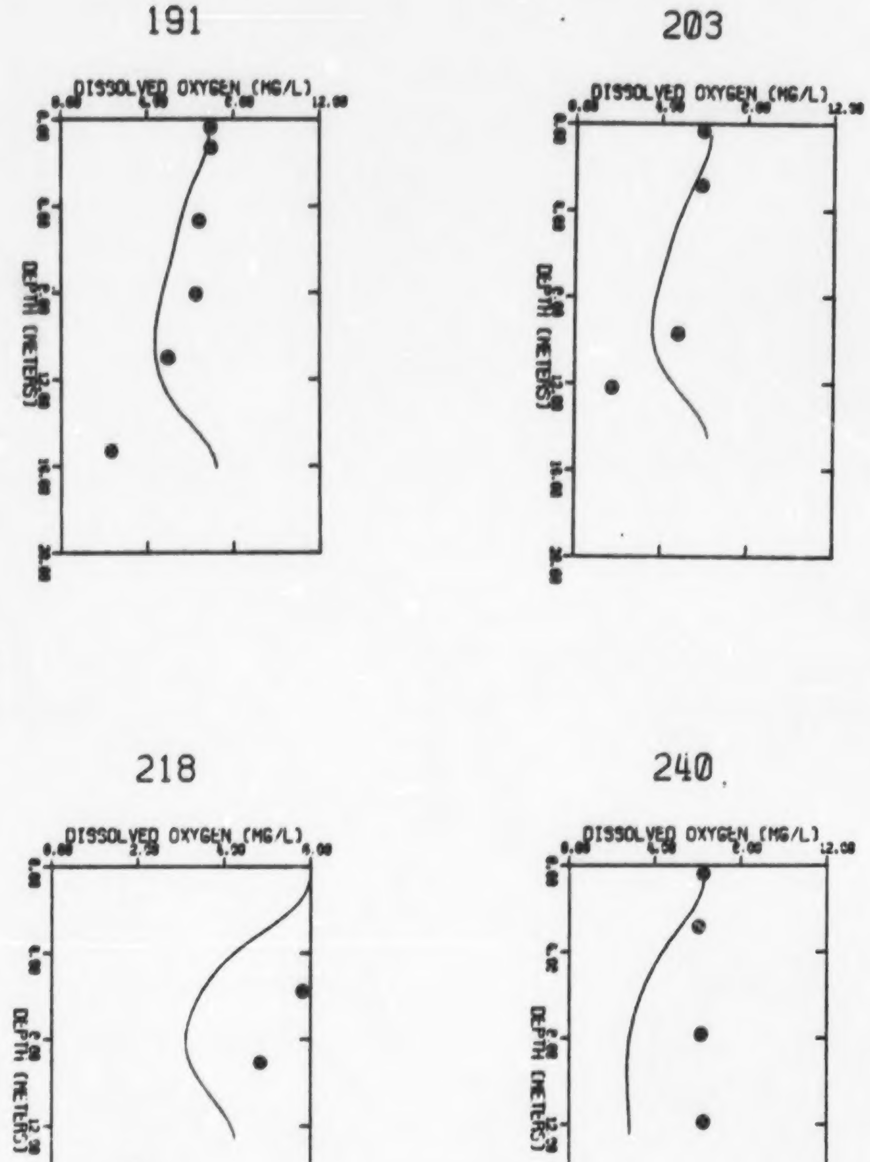

FIGURE 34. (continued)

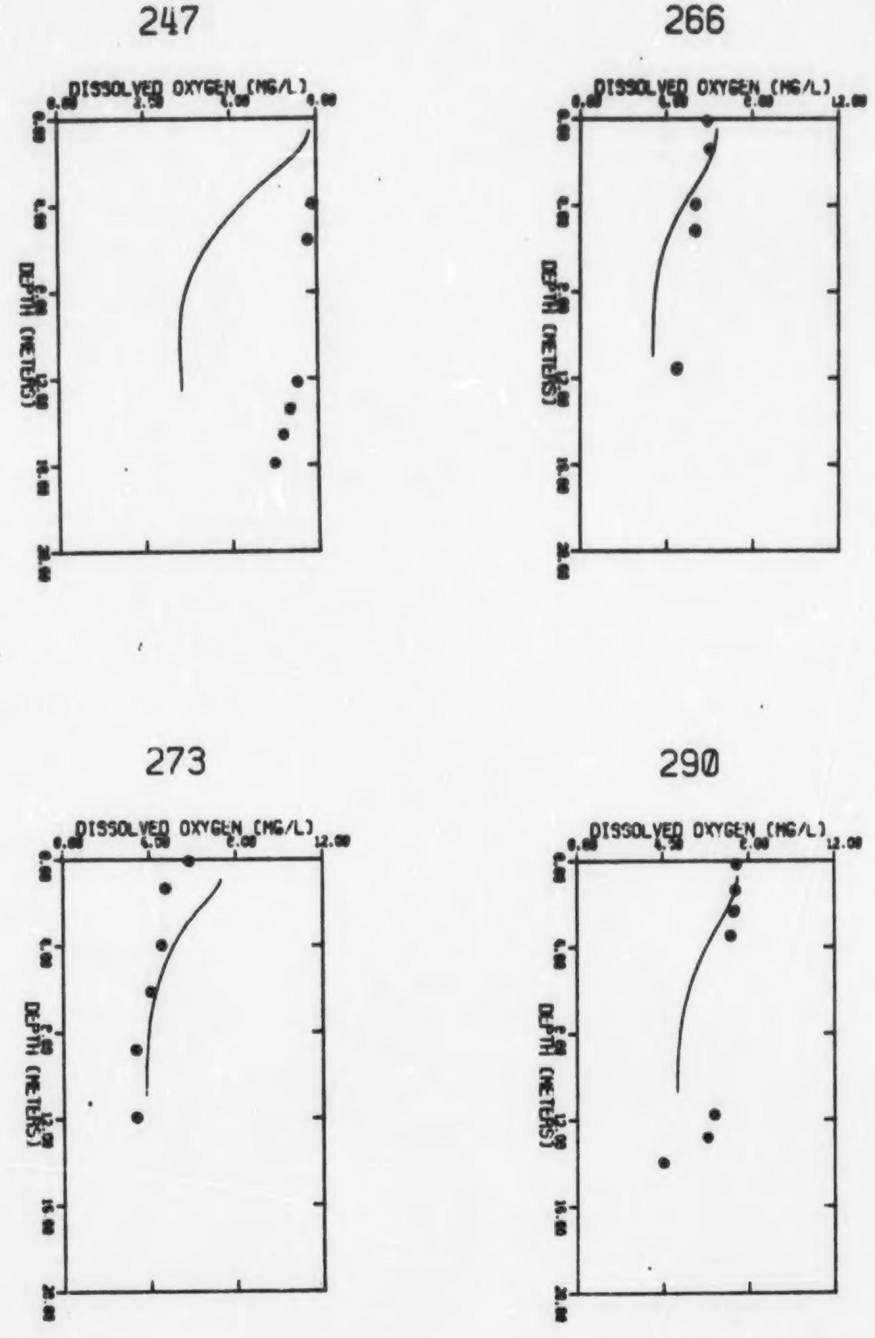

FIGURE 34. (continued)

This disparity is attributed to the unusual effects of the intense storms observed in August by Bushnell.[36] It is likely that the incoming tributary waters were highly aerated (supersaturated) causing a sudden perturbation in the surface DO. In segment 3, DO concentrations predicted for the bottom layers were consistently higher than observed levels. No attempt was made to model a benthic uptake in segment 3 principally because of the lack of data on chemical makeup of the sediments. Bushnell[36] had suspected the existence of bottom sludges which exert strong oxygen demand and release nutrients.

Phosphorus

Only limited data on soluble phosphorus was available for comparative purposes. In this case the complete lack of data on algal distributions prevented the development of a working knowledge of phosphorus cycling within the reservoir. Consequently, no major attempt was made to calibrate the phosphorus model. As illustrated in Figure 35 the model predicted higher concentrations of soluble phosphorus in the surface zone than was observed by Bushnell. The vertical profiles shown in Figure 36 indicate that the sediment uptake rate of phosphorus used in the model is too high. Better results should be easy to attain by proper adjustment of the phosphorus rate constants. From gross nutrient budgets, Bushnell[36] determined that a large fraction of the incoming phosphorus was retained in the reservoir; this would suggest that much of phosphorus is tied up by algae and ultimately accumulated in the sediments.

Nitrogen

The cycling of nitrogen in the reservoir is not clear mainly because of the lack of algae data. In general, determining the fate of nitrogen is a difficult task because of its unusual versatility to assume so many forms. In the case of American Falls Reservoir, two things complicate the

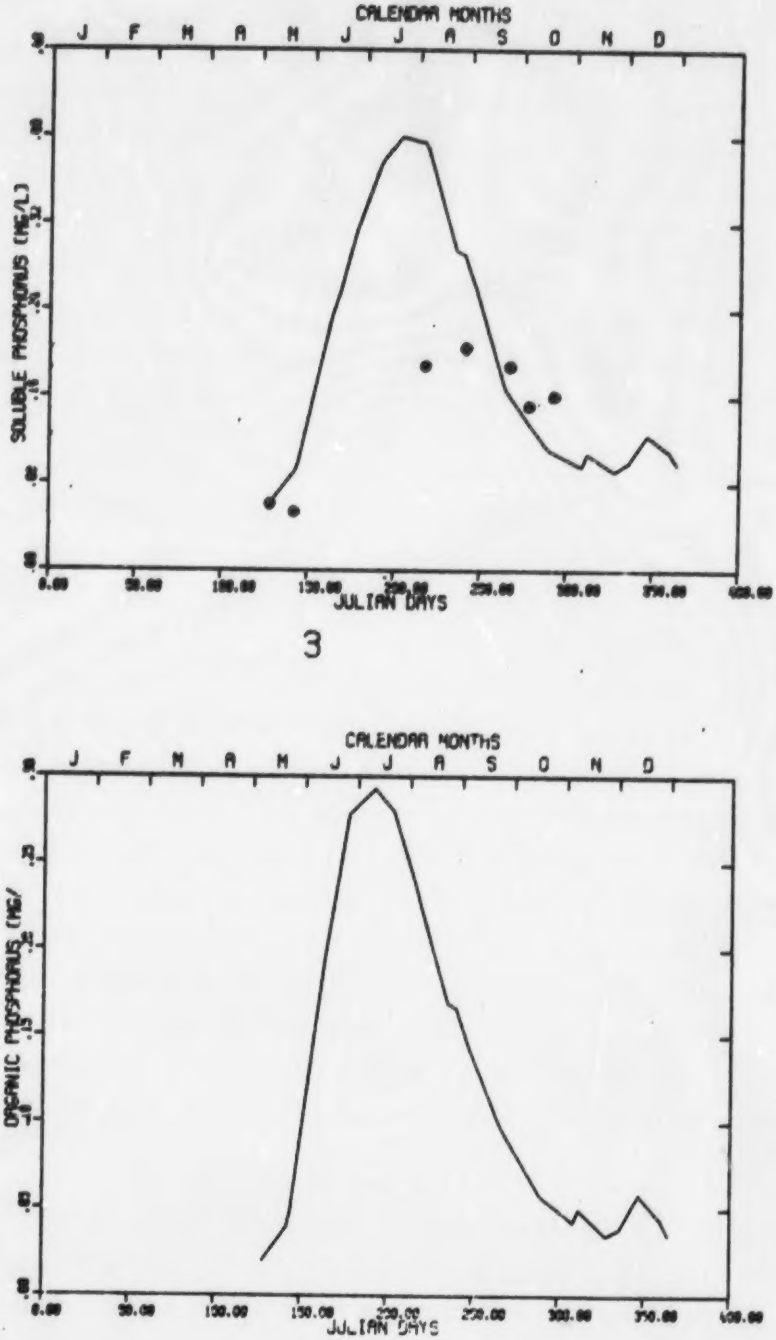

3

3

FIGURE 35. Phosphorus Concentration Histories for Surface Layer - Segment 3

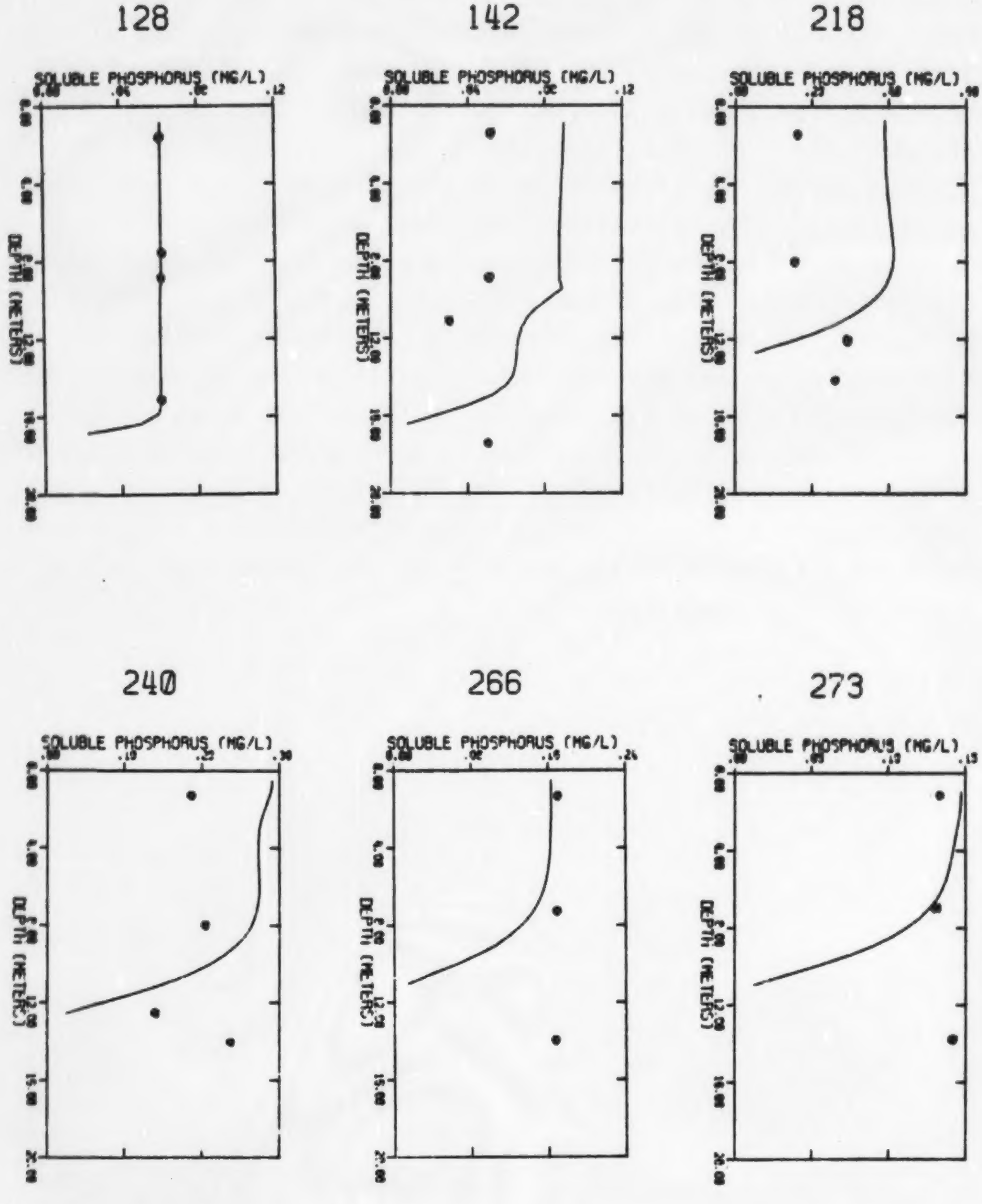

FIGURE 36. Phosphorus Profiles - Segment 3

modeling of nitrogen cycling: (1) nitrogen fixation by blue-green algae, and (2) nitrate inputs from unmeasured springs. Bushnell's estimates of the nitrogen budget indicated that the reservoir was gaining nitrogen faster than it was losing it. Bushnell observed that this gain of nitrogen coincided with the appearance of algal blooms. More interestingly, he noted that sharp losses of total nitrogen occurred during prolonged periods of cloud cover. Bushnell also reports that "unmeasured" springs seem to be major contributors of organic and inorganic nitrogens, attributing these to deep percolation losses from irrigated lands and septic tank effluents. Thus without more complete data, it is not possible to adequately describe nitrogen cycling in the reservoir. Some model results are presented in Figures 37 and 38 for illustrative purposes. These results do not represent the predictions of a fully calibrated nitrogen model, however, in most cases the results appear at least reasonable.

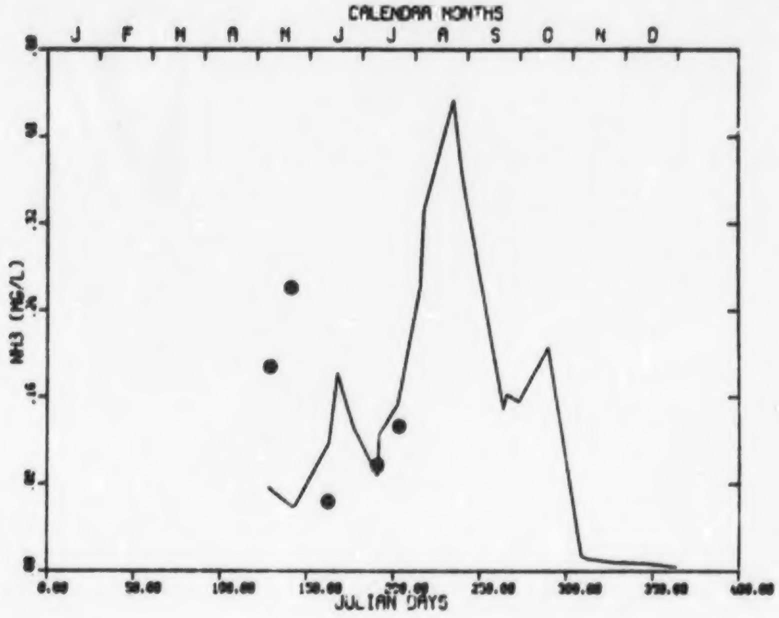

1

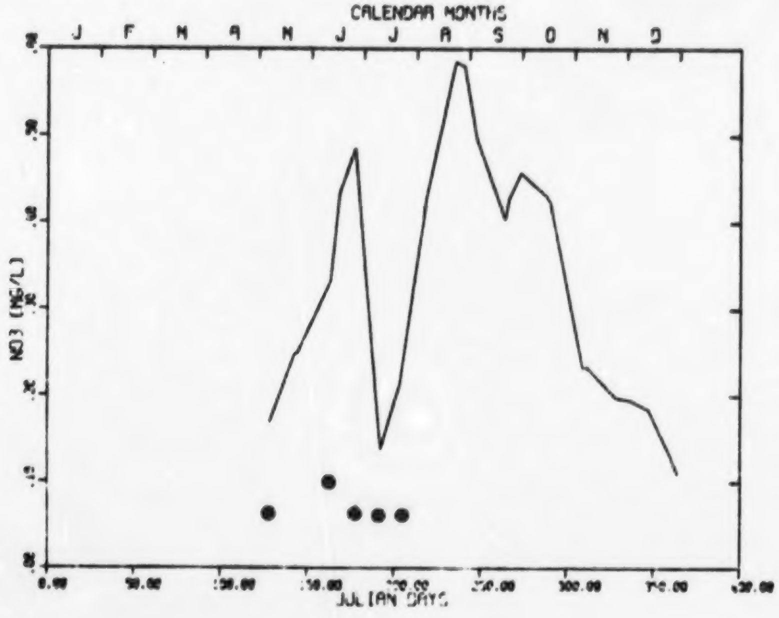

1

FIGURE 37. Nitrogen History for Surface Layer - Segment 1

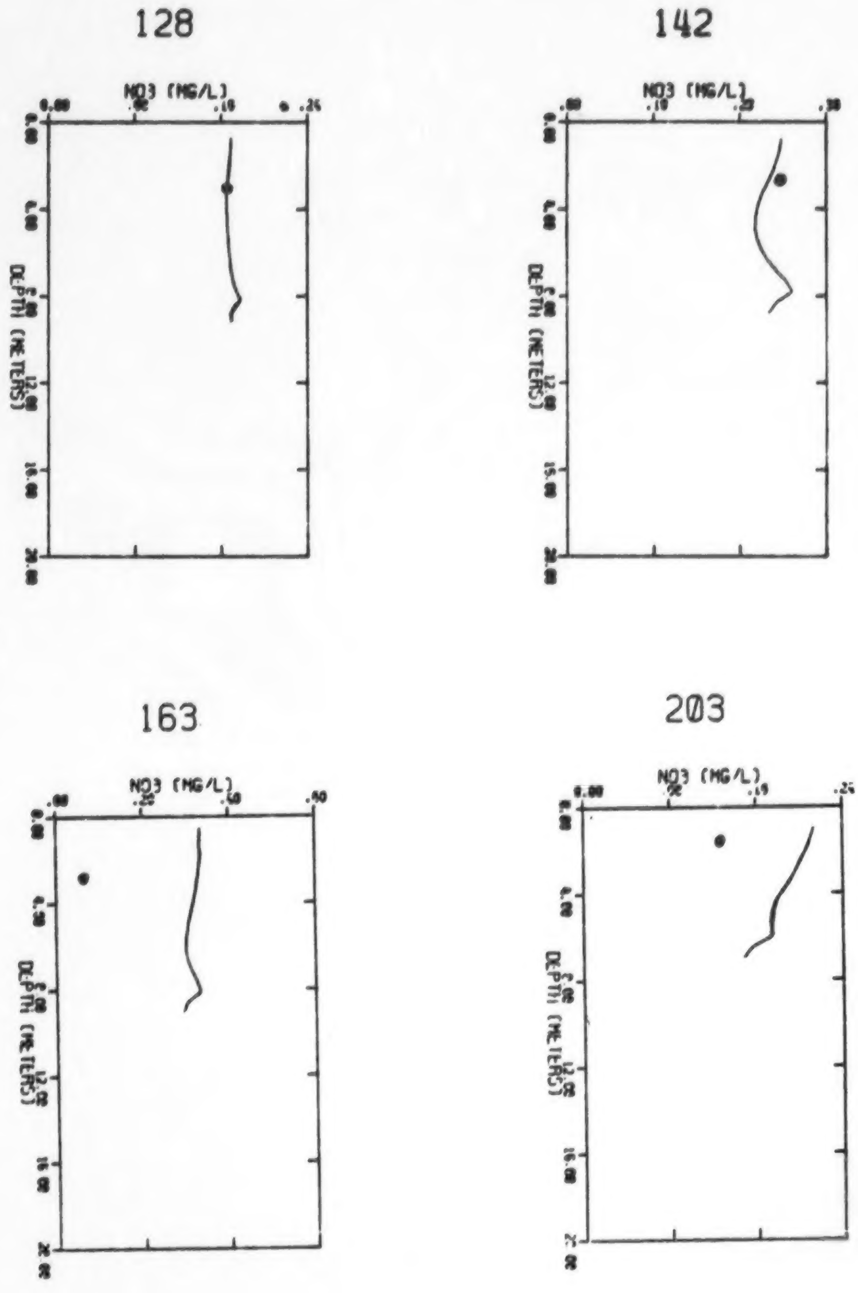

FIGURE 38. Nitrate Profiles - Segment 1

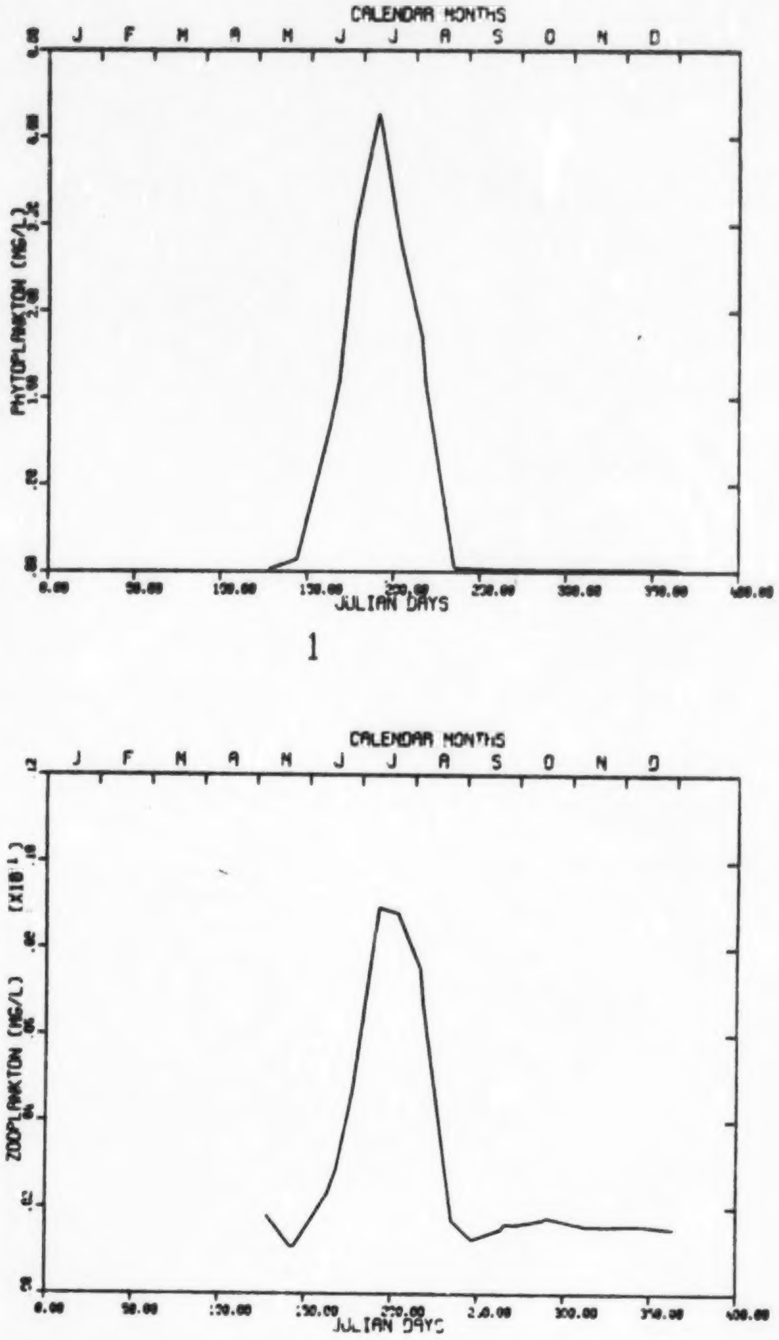

FIGURE 39. Phytoplankton and Zooplankton Histories for Surface Layer - Segment 1

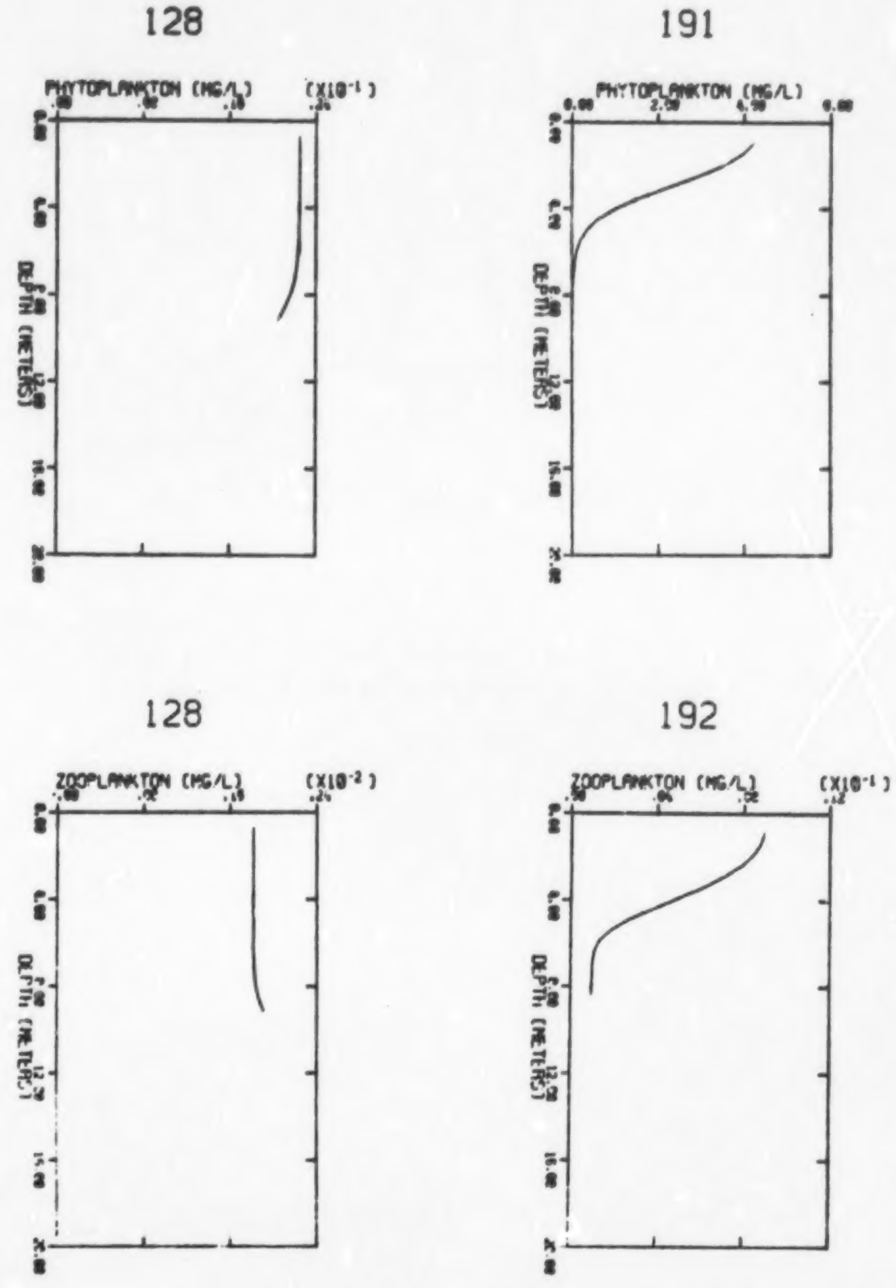

FIGURE 40. Phytoplankton and Zooplankton Profiles - Segment 1

SECTION VIII

SENSITIVITY ANALYSIS

Evaluating the effects of component changes on complex systems is a difficult and complicated task. Interest is often centered on the results of changing input parameters. However, the sensitivity of a model to the formulations and rate constants from which it is constructed is also an important problem. It is desirable to know the sensitivity of results to values which are often only estimates. The user must keep in mind that model results are only as good as the underlying assumptions and model formulations. It is always possible to achieve correct simulations for the wrong reasons.

Any sensitivity analysis is inherently limited, because all of the infinite number of possible variations cannot be tried. The sensitivity of model results to variations in one parameter may vary depending on the values of other parameters which are held constant. In view of these problems, some intuition and specific working knowledge of the model and system behavior were used to evaluate what were considered the most significant parameters. Model predictions were felt to be more sensitive to certain types of parameters than others. For this analysis the effects of transport parameters, rate constants, and changes in input data were evaluated.

Because each computer run for the simulation of 1968 data results in approximately 200,000 numbers, a summary method of presenting results had to be decided on. The following summary presents quantitative results where possible and a discussion of the importance of the variables analyzed.

HYDROTHERMAL MODEL

The refinements developed for the hydrothermal model during the project removed a great deal of the subjectivity in parameter selection. The minimum and maximum allowable thermal gradients and separate diffusion coefficients for the hypoliminon and epilimnion are no longer needed. Diffusion coefficients are now calculated as a function of wind speed, water depth and thermocline depth.

Diffusion Constants

A sensitivity analysis of the choice of parameters for the diffusion coefficients is shown in Figures 41 and 42. The unnumbered line resulted from the calibrated model calculations. The line marked with a "1" resulted from diffusion coefficients 10 times larger than the calibrated values, while the line marked "2" is for diffusion coefficients 10 times smaller. Table 3 lists the parameter choices. As shown in Figure 41 all choices produce reasonable results for the surface temperature calculations. Alternative 1 produces unsatisfactory results for the temperature profiles, Figure 42. The higher diffusion coefficients, Alternative 1, transfer the surface heat too rapidly to the lower elements, resulting in lower surface

TABLE 3. Diffusion Coefficients for Equation 12

Alternative	a_1, m^2/sec	a_2, m
Calibration	1.0E-5	1.0E-4
1	1.0E-4	1.0E-3
2	1.0E-6	1.0E-5

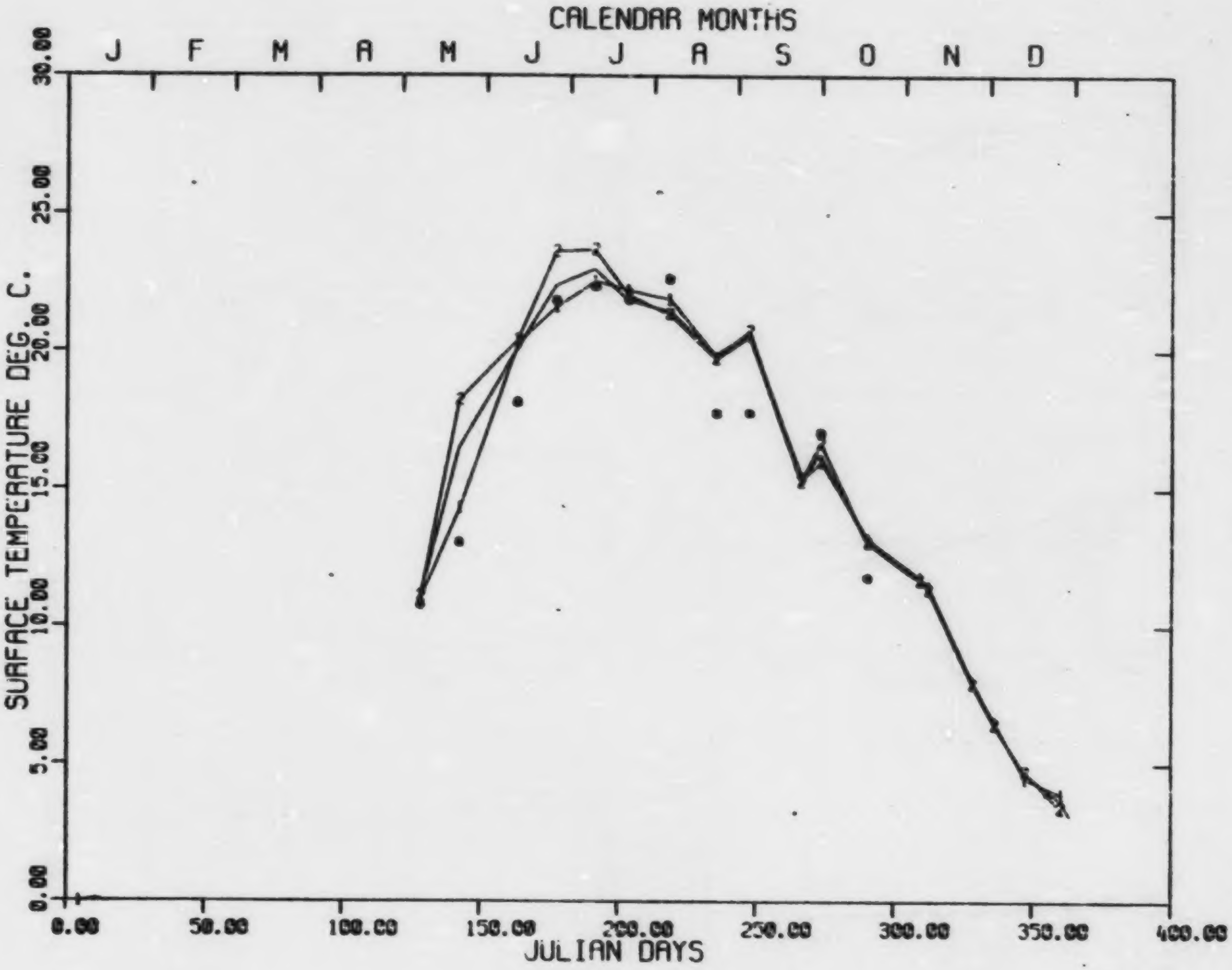

FIGURE 41. Segment 3-Diffusion Coefficient Variation Surface Temperature Versus Time

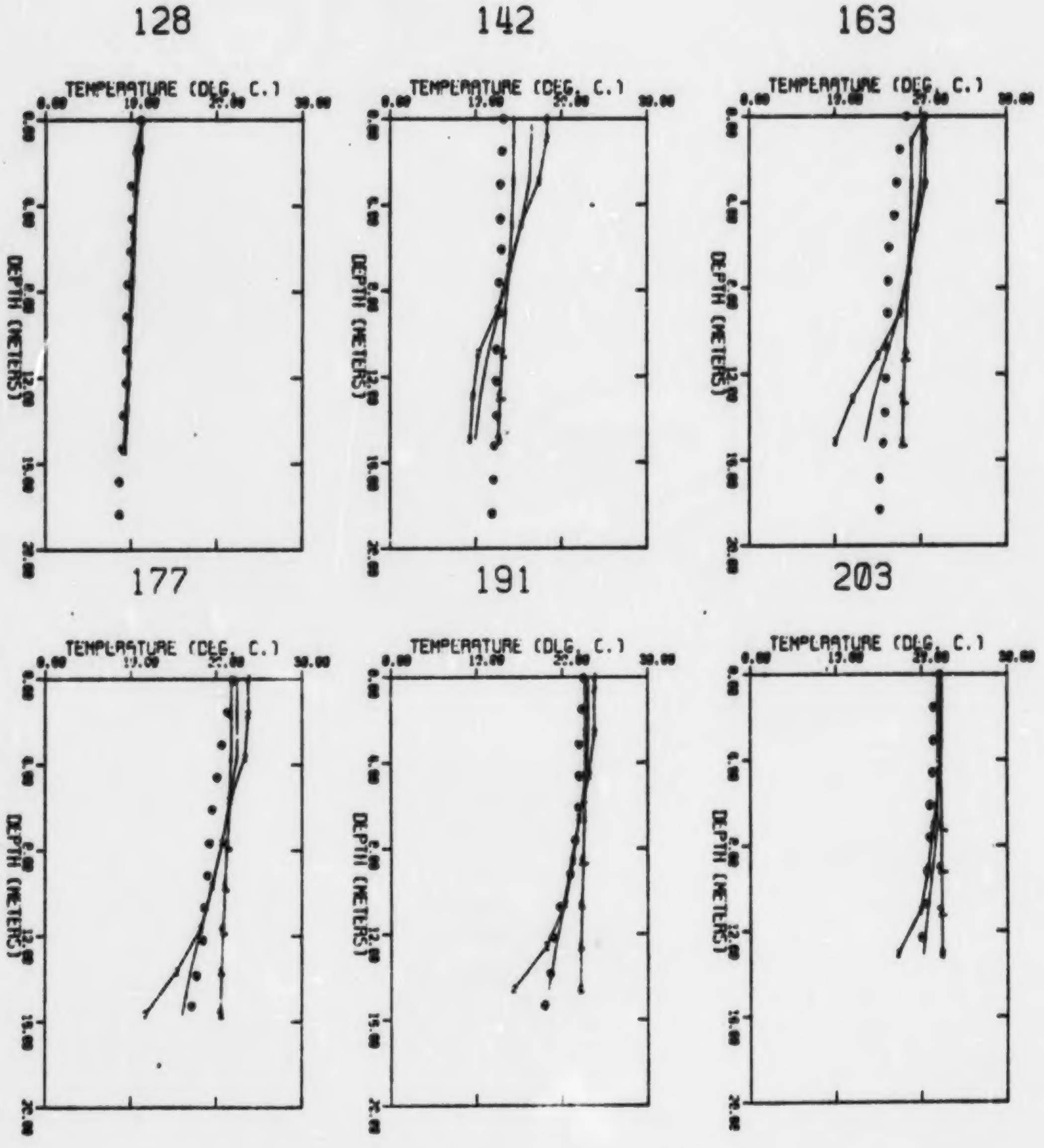

FIGURE 42. Temperature Versus Depth on Indicated Julian Day for Three Different Diffusion Coefficients

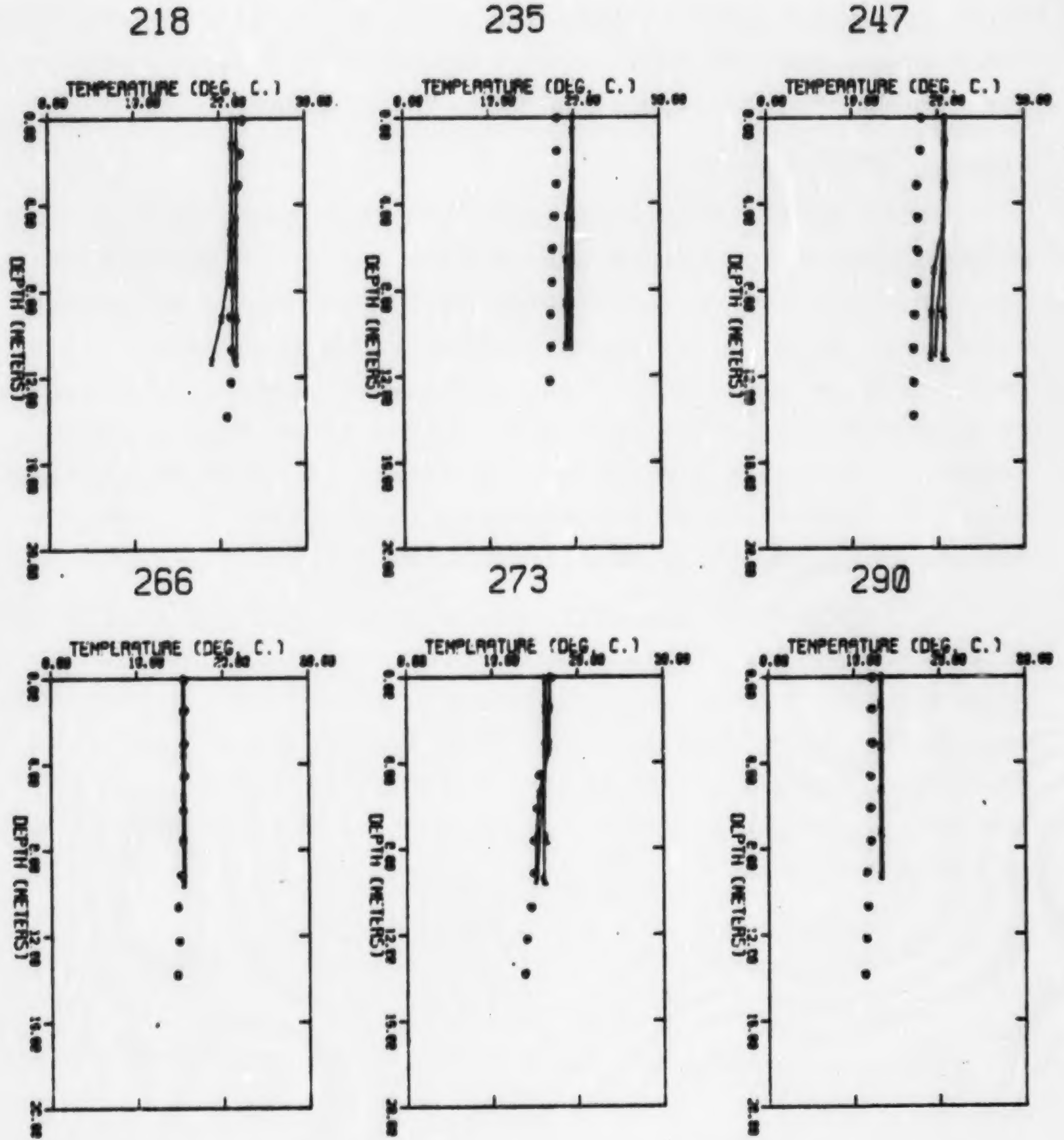

FIGURE 42. (continued)

temperatures and essentially an isothermal structure. Alternative 2 with its lower diffusion coefficients produces higher surface temperatures because the heat is not transferred from the surface fast enough. This results in too large a temperature gradient with respect to the measured data.

Element Thickness

Other sensitivity runs indicated that there were only very minor differences between the results for a 0.5 meter element thickness and a 0.25 meter thickness. The choice of element thickness has an upper bound in that there must be at least four elements remaining in the shallowest segment at the point of lowest water elevation. Hence, if a segment in a lake reaches a depth of 1 meter at low water, it would be necessary to use a meter element thickness no larger than 0.25 meters for the solution algorithm to function.

In conclusion, the hydrothermal model is very easily calibrated since most of the subjectivity has been removed. A precise and accurate water balance is essential. A digitized representation of the lake bed from topographical maps would greatly enhance the water balance effort in that it would accurately establish the volume-elevation relationship of each of the segments.

WATER QUALITY MODEL

Time Step .

Extensive analysis of the effects of using different time steps yielded the conclusion that average daily or even weekly values for input data were adequate. However, the key limitation was found to be in the number of iterations performed in the solution of the transport equations for biotic constituents.

It was found that the time period per iteration must be less than the time required for a constituent to be transported a distance equal to one element thickness. Knowing the diffusion, this time can be estimated from the relation[37]

$$t = \frac{\Delta z^2}{\varepsilon} \qquad (95)$$

where

Δz = element thickness

ε = diffusion coefficient

With diffusion coefficients[38,39] of about 10^{-5} m/sec and 0.5 meter elements, the time step should be less than 7 hours. However, if diffusion coefficients are on the order of 10^{-4} m/sec, the time step needed is less than 1 hour. These limitations occur only when settling rates are relatively large (4 m/day).

Algal Growth and Death Rates

Variations in the specific growth rate produce the most interesting effects on the patterns of algal growth and nutrient cycling. The results presented in Figures 39 and 40 were obtained using a specific growth rate of 0.05/day-°C which is a mid-range value. Increasing the specific growth rate to 0.10/day-°C produces an earlier bloom, late March, but a lower maximum phytoplankton concentration, 2.8 mg-C/l. In addition it is noted that the growth curve becomes increasingly responsive to rate limiting factors, principally light and temperature, and to their fluctuations during the bloom period. In addition, a greater uptake of soluble phosphorus, ammonium and nitrate is observed in the euphotic zone with attendent increases in the organic forms in the bottom layers. Dissolved oxygen levels in the surface zone are greatly affected by photosynthetic production resulting in supersaturated conditions of about 150%. In contrast, a specific growth rate of 0.025/day-°C completely damps out the effects of biomass limiting factors, i.e. nutrient inputs, resulting in no bloom at all. Similarly, changing the endogenous respiration rate from 0.007/day-°C to 0.014/day-°C results in phytoplankton concentrations below bloom levels.

Sinking Velocities

For constituents such as algae, with sinking velocities,[38,39] the transport due to sinking or floating may require a shorter time step. For example, a particle with a sinking velocity of 3 meters per day would require a time step size of about 4 hours. The current model is programmed to iterate 8 times per day in the algae transport equations. The computer time could be reduced significantly if thicker elements and longer time steps were used. However, at American Falls the element thickness had to be less than 1 meter in order to maintain at least four elements at low water.

Diffusion Coefficients

Diffusion coefficients are calculated in TERMA on the basis of wind speed and depth. The parameter values used to calculate the diffusion coefficients are determined by calibrating the temperature model. It is assumed that the dispersion of mass occurs in a manner similar to the dispersion of heat, thus diffusion coefficient is the same. However, there is some "mathematical" mixing from one segment to the next in order to conserve mass and a reduction in diffusion coefficients for the AQUA-II model may not be unreasonable. There is a definite need for a detailed field investigation of mixing and diffusion[40] in reservoirs.

Limited evaluations were performed with varying rate constants because it is felt that the processes considered were more important than the actual values of the rate constants. However, the reaeration, denitrification, and benthic BOD rates were analyzed.

Reaeration

The rate of reaeration in the calibrated model is given by

$$K_r = \left(0.5 + 2.5 \times 10^{-6} v_w\right) \theta^{(T-20)} \qquad (96)$$

where

$$\frac{dDO}{dt} = K_r(DO_s - DO) \qquad (97)$$

v_w = wind speed, m/day

Using a value of 5.0 for K_r was found to produce excessive oxygen concentrations, essentially at equilibrium with the atmosphere at all times.

Denitrification

Denitrification was not originally included in the model but was added due to apparent large nitrogen losses from the system. A model rate constant was approximated as a linear function of oxygen concentration:

$$J_3 = 1.0 - DO/DO_s \quad (\text{for } DO < DO_s) \qquad (98)$$

This rate of denitrification reduced nitrate concentrations from maximum values of about 1.6 mg/l with $J_3 = 0$ to about 0.3 mg/l.

Benthic BOD

Very little benthic BOD was needed to simulate the observed oxygen data. However, it should be noted that field measurement of BOD and benthic BOD will not correspond to modeled values because the model separately accounts for ammonium oxidation and algal decay, values which would be included in a BOD measurement. When a benthic BOD of 1 g/m^2/day was added, oxygen concentrations were reduced to zero in the bottom layers.

Phosphorus Loss to Sediment

Both organic and soluble phosphorus are lost to the sediments from the bottom element. The calibrated model used a rate constant of 2.0/day. Lower rates resulted in excessive phosphorus concentrations in the overlying waters.

SECTION IX

FINAL REMARKS

Accelerating eutrophication of the nation's lakes and reservoirs is a sizable and challenging problem. The scope of the problem[41] is remarkably diverse and complex requiring the use of our current scientific knowledge[42,43] and best available technology.[44,45] Versatile and reliable tools are needed to test various management strategies for restoration and enhancement of water quality. It is hoped that the simulation models presented in this report will provide such a tool allowing analysts to study and assess the processes of eutrophication.

We believe the simulation models represent a considerable advancement to the art and science of water quality modeling. Nevertheless, a great deal is yet to be learned about the models' capability to handle more challenging situations. Work is currently underway to apply these models to Lakes Washington, Mendota and Wingra (Wisconsin). The results of these studies should provide an excellent basis for a thorough and complete evaluation of the models.

REFERENCES

1. Baca, R. G., W. W. Waddel, C. R. Cole, A. Brandstetter and D. B. Cearlock. "EXPLORE-I: A River Basin Water Quality Model." Battelle Pacific Northwest Laboratories, Richland, Washington, (Contract No. 68-01-0056) August 1973.

2. "Mathematical Models for Prediction of Thermal Energy Changes in Impoundments." Prepared for the Water Quality Office, Environmental Protection Agency, by Water Resources Engineers, Inc., Walnut Creek, California, December 1969.

3. Anderson, E. R., "Energy Budget Studies." in "Water Loss Investigations--Lake Hefner Studies." Technical Report, U.S.G.S. Professional Paper 269, 1954.

4. Wunderlich, W. O., "Heat and Mass Transfer Between a Water Surface and the Atmosphere." Internal Memorandum, T.V.A. Engineering Laboratory, Norris, Tennessee, 1968.

5. Debler, W. R., "Stratified Flow into a Line Sink." Journal of the Engineering Mechanics Division, ASCE, vol. 85, no. EM3, July 1959.

6. Craya, A., "Theoretical Research on the Flow of Non-Homogeneous Fluids." La Houille Blanche, 1949.

7. Carnahan, B., H. A. Luther and J. O. Wilkes, Applied Numerical Methods. John-Wiley and Sons, Inc., New York, pp. 441-448, 1969.

8. O'Conner, D. J., "Temporal and Spatial Distribution of Dissolved Oxygen in Streams." Water Resources Research, vol. 3, no. 1, pp. 65-79, 1967.

9. Streeter, H. W. and E. B. Phelps, "A Study of the Pollution and Natural Purification of the Ohio River, III, Factors Concerned in the Phenomena of Oxidation and Reaeration." U. S. Public Health Service, Pub. Health Bulletin No. 146, 75 p., February 1925.

10. Martin, D. M. and D. R. Goff, "The Role of Nitrogen in the Aquatic Environment." ANSP-CLDP-2, Dept. of Limnology, Academy of Natural Sciences of Philadelphia, Pa., 1972.

11. Anon., "Sources of Nitrogen and Phosphorus in Water Supplies." A report of Task Group 2610P--Nutrient Associated Problems in Water Quality and Treatment, Journal of American Waterworks Association, vol. 59, p. 344-366, 1967.

References (Continued)

12. Stewart, W. D. P., "Nitrogen Fixing Plants." Science, vol. 158, pp. 1426-1432, 1967.

13. Carnahan, J. E. and J. E. Castle, "Nitrogen Fixation." Annual Review of Plant Physiology, vol. 14, pp. 125-136, 1963.

14. Bartsch, A. F., "Role of Phosphorus in Eutrophication." EPA-R3-72-001, National Environmental Research Center, U.S. Environmental Protection Agency, Corvallis, Oregon, August 1972.

15. Stumm, W. and J. O. Leckie, "Phosphate Exchange with Sediments: Its Role in Productivity of Surface Waters." Proceedings of the 5th International Water Pollution Research Conference, pp. III-26/1-26/16, July 1970.

16. Patten, B. C., "Mathematical Models of Plankton Production." Int. Rev. der Gesampten Hydrobiologie, No. 53, pp. 357-408, 1968.

17. Middlebrooks, E. J., D. H. Falkenborg, and T. E. Maloney, (Editors), "Modeling the Eutrophication Process." Workshop Proceedings, Utah State University, Logan, Utah, November 1973.

18. Thomann, R. V., D. J. O'Connor and D. M. DiToro, "Modeling of the Nitrogen and Algal Cycles in Estuaries." Proceedings of the 5th International Water Pollution Research Conference, pp. III-9/1-9/14, July 1970.

19. Lorenzen, M. W. and R. J. Mitchell, "Theoretical Effects of Artificial Destratification on Algal Production in Impoundments." Environmental Science and Technology, vol. 7, no. 10, pp. 939-944, October 1973.

20. Vollenweider, R. A. in Primary Productivity in Aquatic Environments. C. R. Goldman, Editor, University of California Press, pp. 425-457, 1965.

21. Westlake, D. F., "Some Problems in Measurement of Radiation Underwater: A Review." Photochemistry and Photobiology, vol. 4, pp. 849-868, 1965.

22. DiToro, D. M., D. J. O'Conner and R. V. Thomann. "A Dynamic of Phytoplankton in Natural Waters." Environmental Engineering and Science Program, Manhattan College, Bronx, New York, June 1970.

References (Continued)

23. Lau, Y. L., "A Review of Conceptual Models and Prediction Equations for Reaeration in Open Channel Flow." Technical Bulletin No. 61, Inland Waters Branch, Dept. of the Environment, Ottawa, Canada, 1972.

24. Elmore, H. L. and T. W. Hayes, "Solubility of Atmospheric Oxygen in Water." Journal of the Sanitary Engineering Division, No. SA4, pp. 41-53, July 1960.

25. Kittrell, F. W. and S. A. Furfari, "Observations of Coliform Bacteria in Streams." Journal of Water Pollution Control Federation, vol. 35, pp. 1361-1385, 1963.

26. Holz, T., "Predictive Models of Coliforms in Streams, A Review of the State-of-the-Art." Water and Air Resources Division, University of Washington, Seattle, 1971.

27. Thomann, R. V., Systems Analysis and Water Quality Management. Environmental Research and Applications, Inc., New York, New York, 1971.

28. Velz, C. J., Applied Stream Sanitation. Wiley-Interscience, New York, N. Y., 1970.

29. Price, H. S., J. C. Cavendish and R. S. Varga, "Numerical Methods of Higher-Order Accuracy for Diffusion-Convection Equations." SPE Journal, pp. 293-303, September 1968.

30. Stone, H. L. and P. L. T. Brian, "Numerical Solution of Convective Transport Problems." AIChE Journal, vol. 9, no. 5, 1963.

31. Baca, R. G., "Finite Element Methods for a Class of Problems in Mass, Momentum and Energy Transport." (In Preparation) Battelle Pacific Northwest Laboratories, Richland, Washington, 1974.

32. Baca, R. G., "A Transport Model for Nitrogen Supersaturated Waters in River-Run Reservoirs." Battelle-Northwest, Richland, Washington, August 1974.

33. Varga, R. S., Matrix Iterative Analysis. Prentice-Hall, Englewood Cliffs, New Jersery, pp. 262-270, 1962.

34. Lapidus, L. and J. H. Seinfeld, Numerical Solution of Ordinary Differential Equations. Academic Press, New York, 1971.

35. "Water Quality Status of Upper Snake River Basin." Final Draft, Environmental Protection Agency, Surveillance and Analysis Division, March 1, 1973.

36. Bushnell, V. C., "Eutrophication of American Falls Reservoir Minidoka Project, Idaho." Interim Report, Bureau of Reclamation, Boise, Idaho, April 1969.

37. Lorenzen, M. W., "The Role of Artificial Mixing in Eutrophication Control." Ph.D. Thesis, Division of Engineering and Applied Physics, Harvard University, Cambridge, Mass., 1972.

38. Bella, D. A., "Simulating the Effect of Sinking and Vertical Mixing on Algal Population Dynamics." Journal of the Water Pollution Control Federation, 42, pp. 140-152, 1970.

39. Eppley, R. W., R. W. Holmes and J. D. Strickland, "Sinking Rates of Marine Phytoplankton Measured with a Fluorometer." Jour. Exp. Mar. Biol. Ecol., 1, 2, 1967.

40. Wilson, J. R. and F. D. Marsh, "Field Investigation of Mixing and Dispersion in a Deep Reservoir." Tech. Rept. HYD 10-670, Hydraulic Engineering Laboratory, University of Texas at Austin, 141 p., 1967.

41. Ketelle, M. J. and P. D. Uttormark, "Problem Lakes in the United States." The University of Wisconsin, Water Resource Center, Hydraulic and Sanitary Laboratory, Madison, WI, December 1971.

42. Vollenweider, R. A., "Scientific Fundamentals of the Eutrophication of Lakes and Flowing Waters with Particular Reference to Nitrogen and Phosphorus as Factors in Eutrophication." Technical Report to O.E.C.D., Paris DAS/CSI/68, 1970.

43. Hutchinson, G. E., A Treatise on Limnology, Vol. I, John Wiley and Sons, Inc., New York, NY, 1957.

44. Anon. "Measures for the Restoration and Enhancement of Quality of Freshwater Lakes." EPA-430/9-73-005, U.S. Environmental Protection Agency, Washington, DC, 1973.

45. Eutrophication: Causes, Consequences, Correctives, National Academy of Science, Washington, D.C., 1969.

ACKNOWLEDGMENTS

The Battelle-Northwest study team wishes to express its sincere appreciation to the Environmental Protection Agency for the opportunity to conduct this research. The cooperation and help of Mr. Lee Fortier and Mr. Kenneth Feigner, project officers, are particularly appreciated. Special thanks are extended to Mr. Jack Frank and Mr. Dick Henry of the Bureau of Reclamation for providing all available data on American Falls Reservoir.

The authors extend their grateful appreciation to Leila Counts for her excellent contributions in editing the final report. Special thanks are also expressed to Jan Greenwell and Velva Harris for their patience in typing and retyping the report.

APPENDIX A

SUMMARY OF AMERICAN FALLS DATA

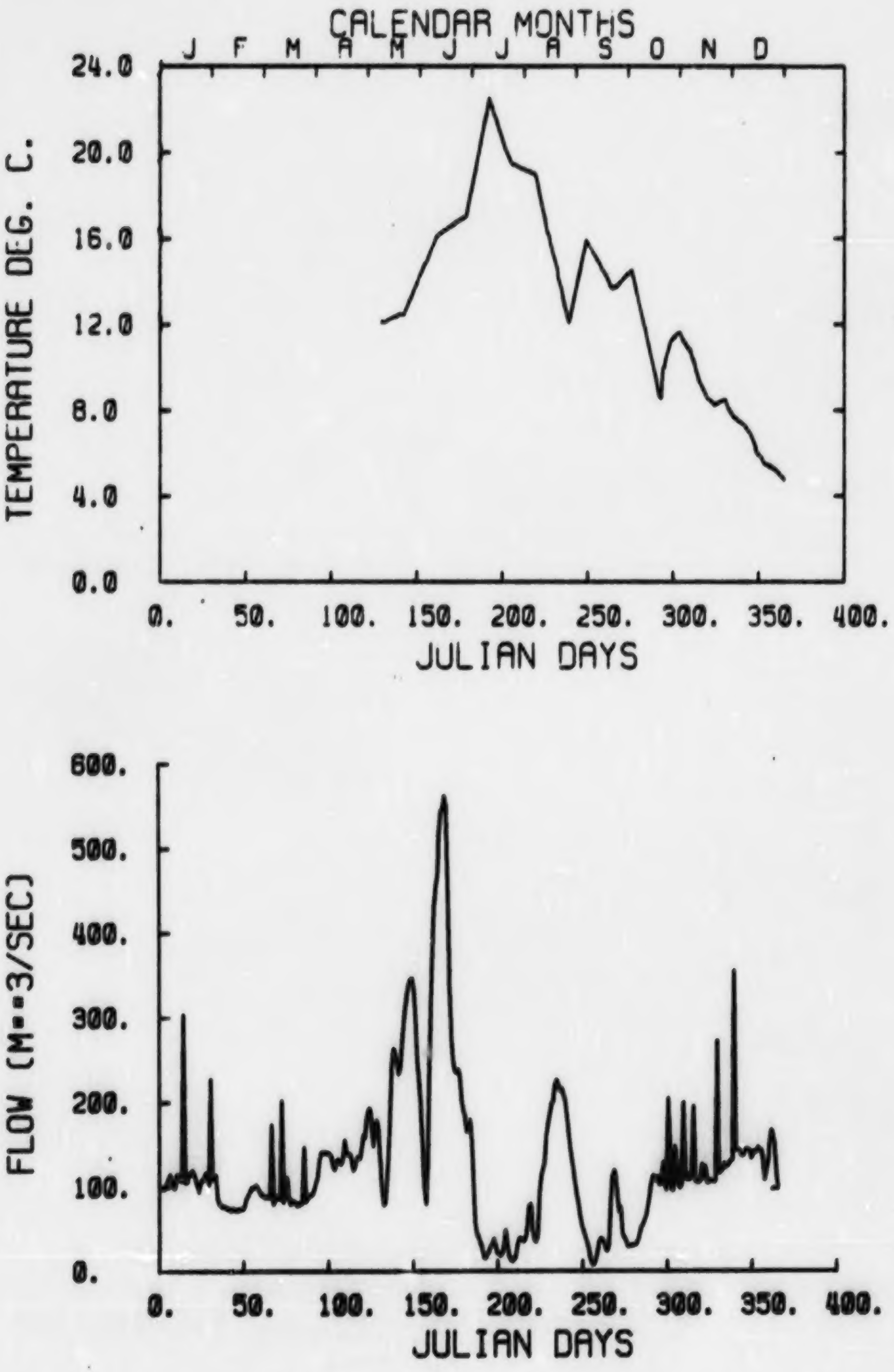

FIGURE A-1. Snake River Flow and Temperature, 1968

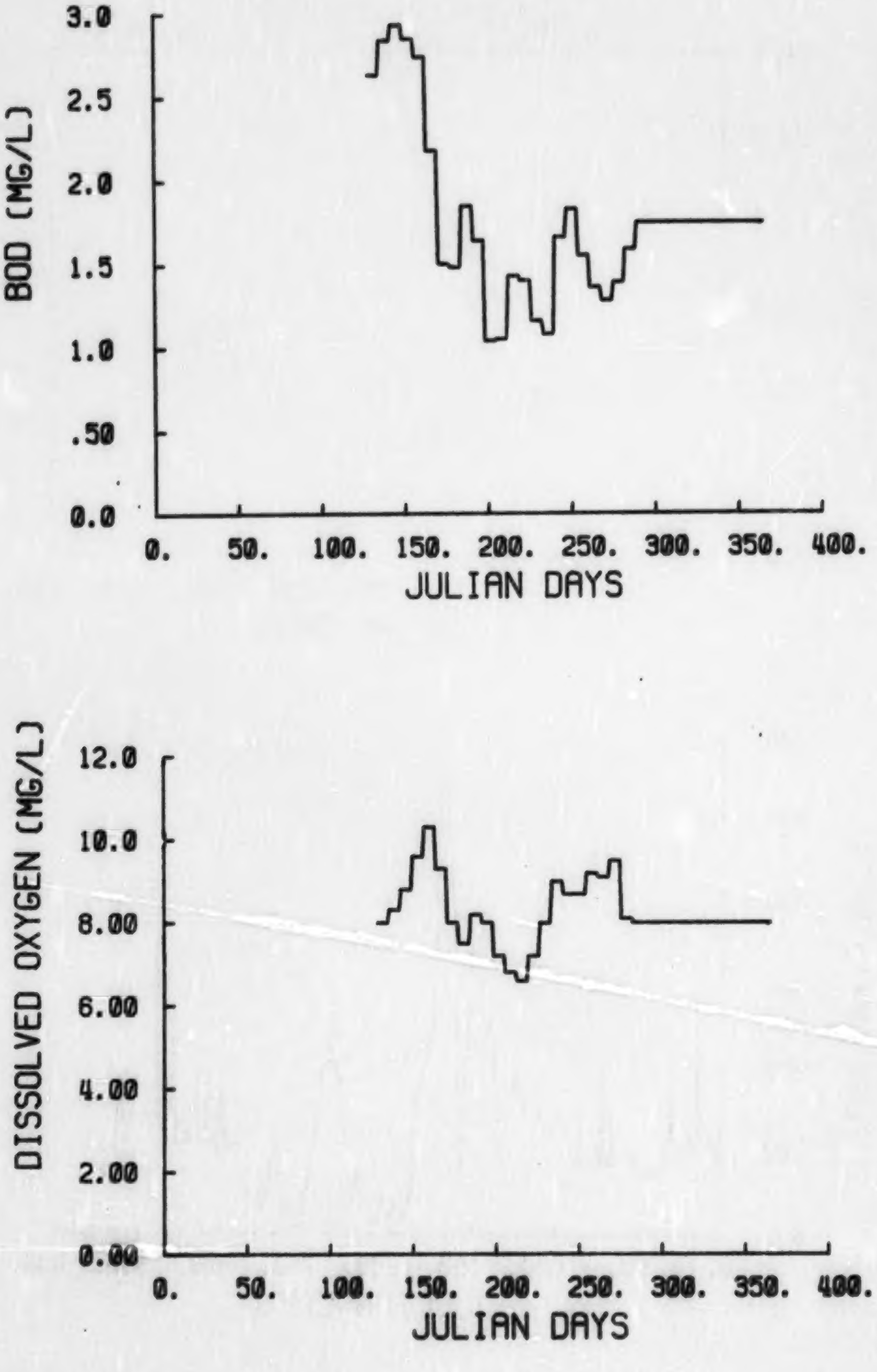

FIGURE A-2. Snake River Oxygen and BOD, 1968

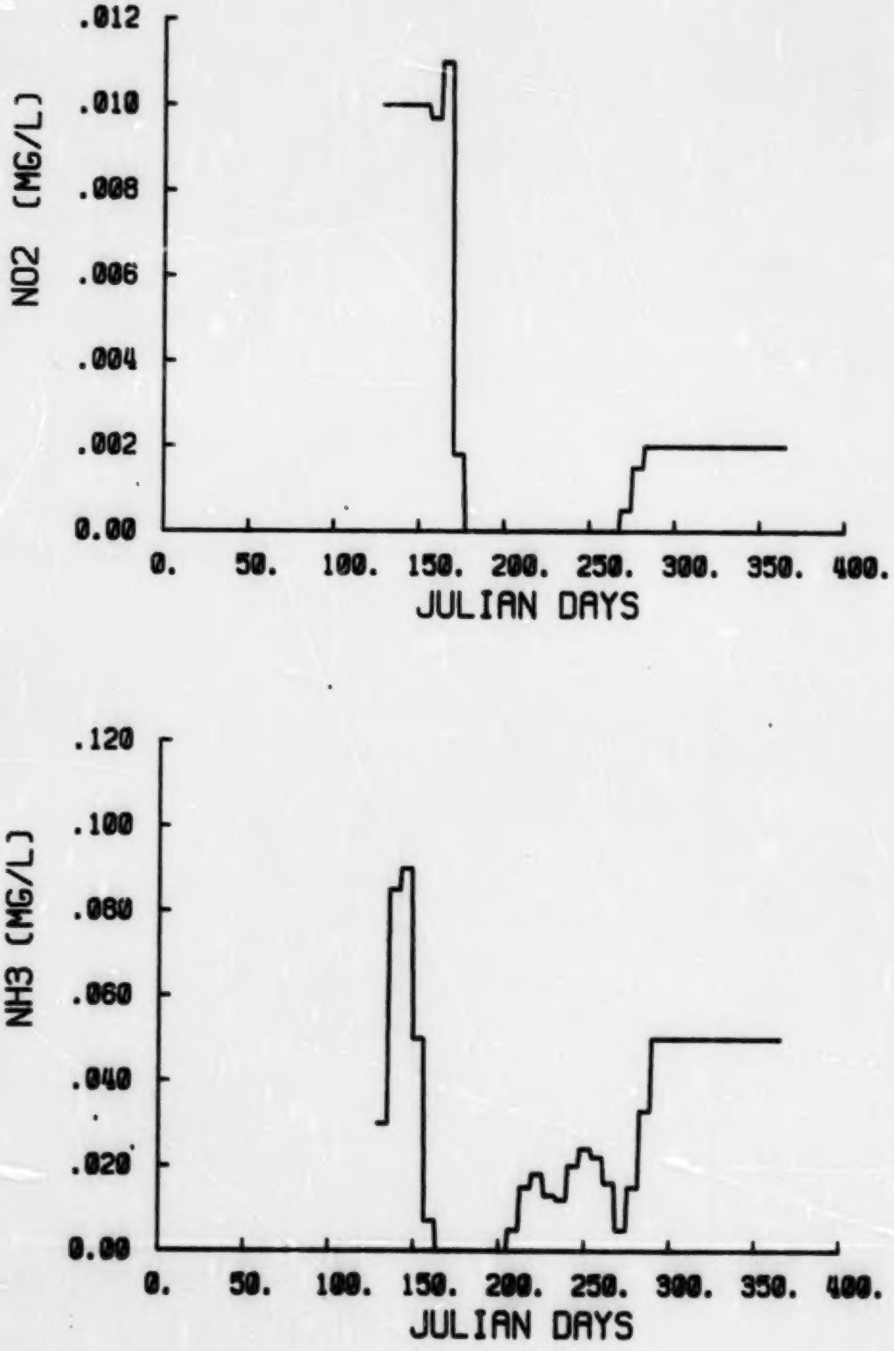

FIGURE A-3. Snake River Ammonia and Nitrite, 1968

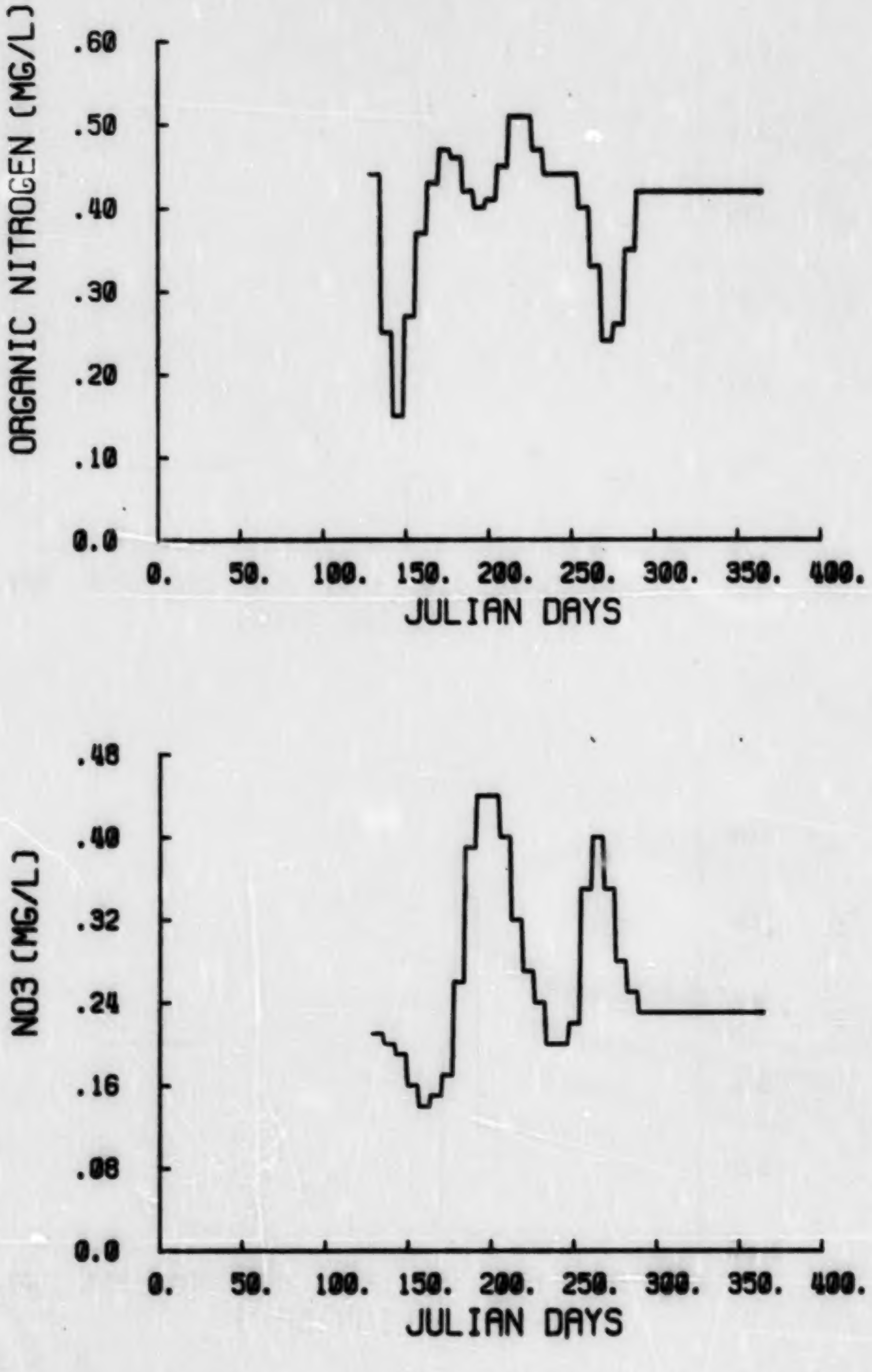

FIGURE A-4. Snake River Nitrate and Organic Nitrogen, 1968

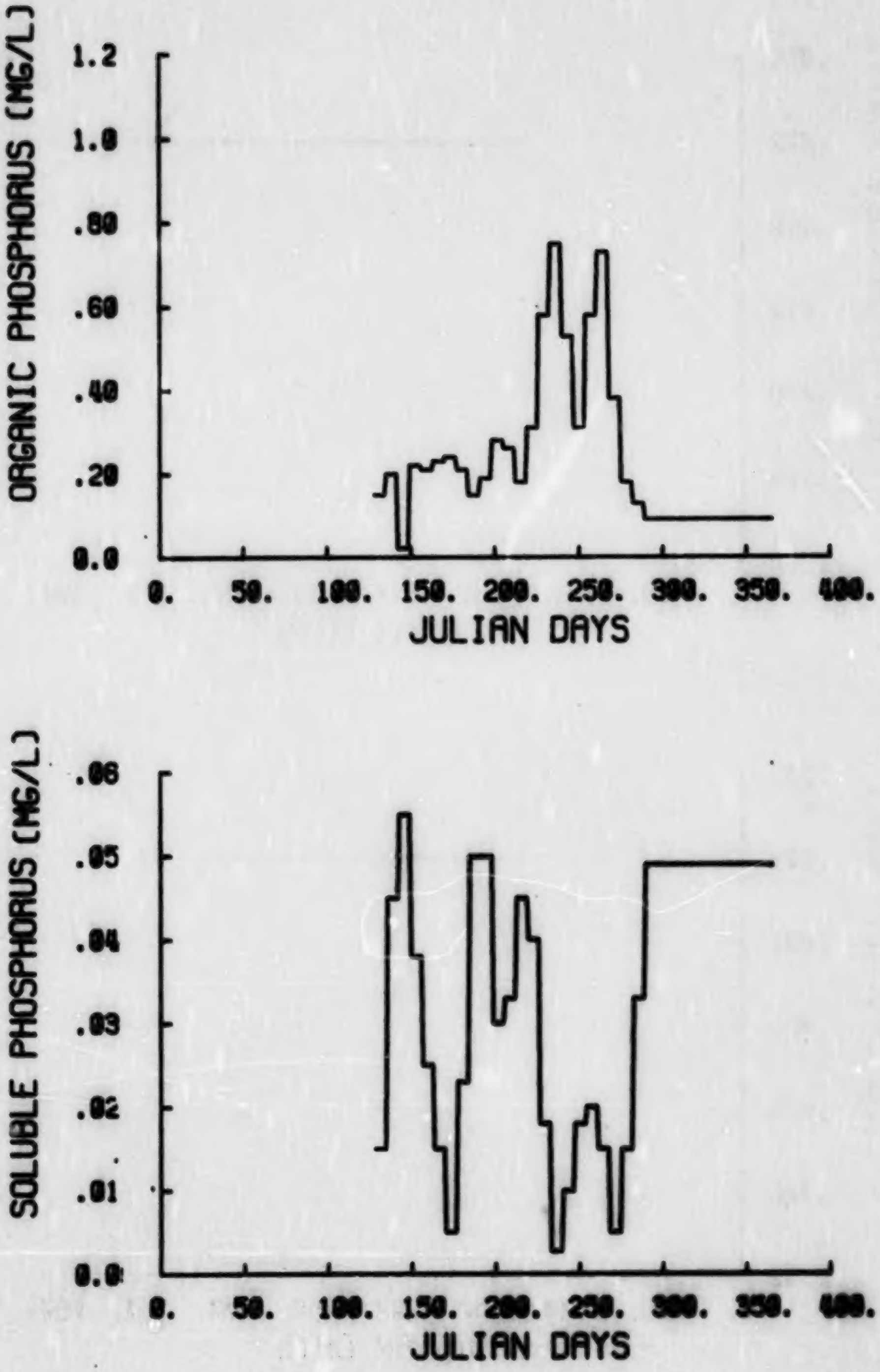

FIGURE A-5. Snake River Soluble and Organic Phosphorus, 1960

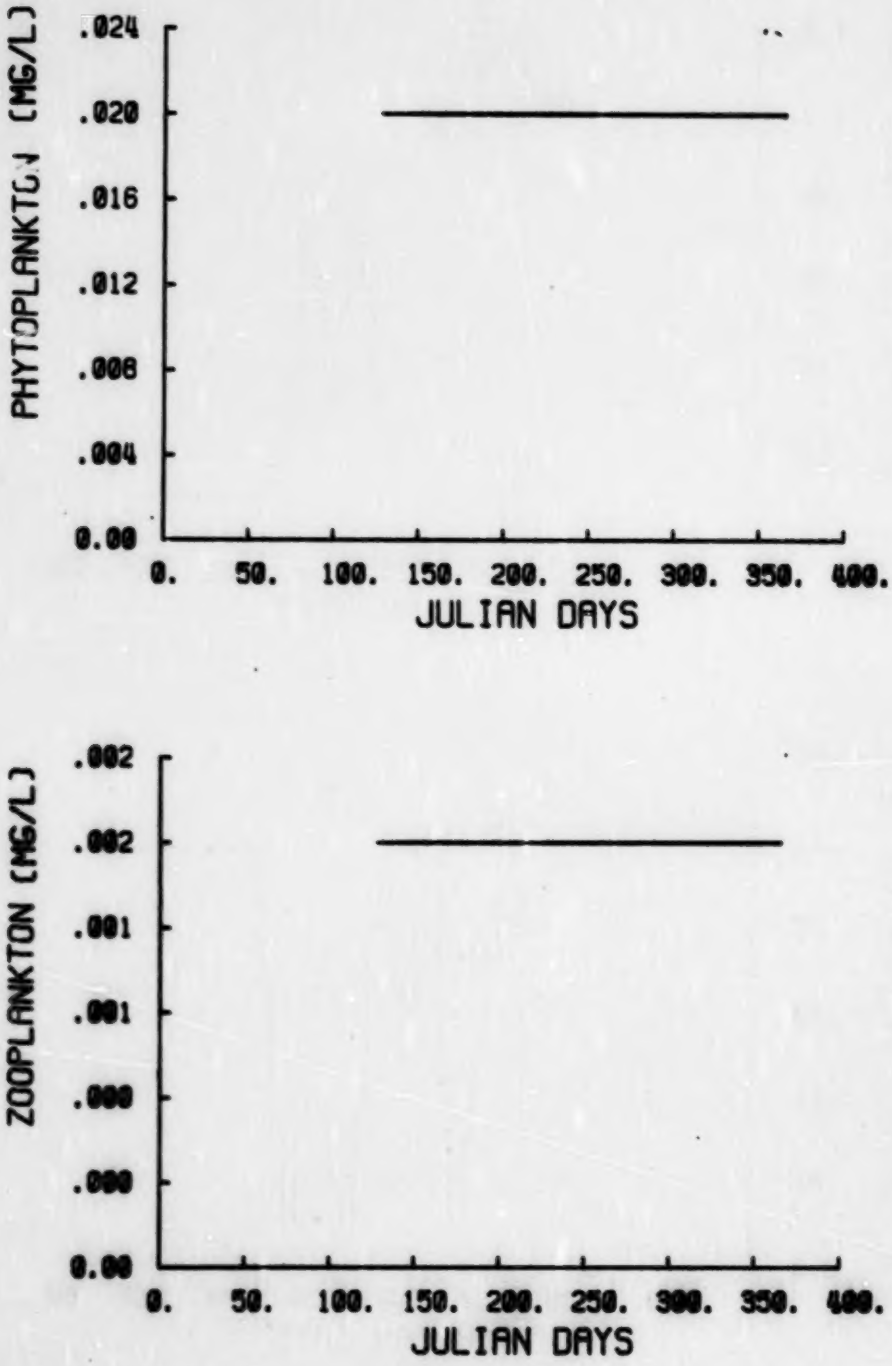

FIGURE A-6. Snake River Phytoplankton and Zooplankton, 1968 (assumed)

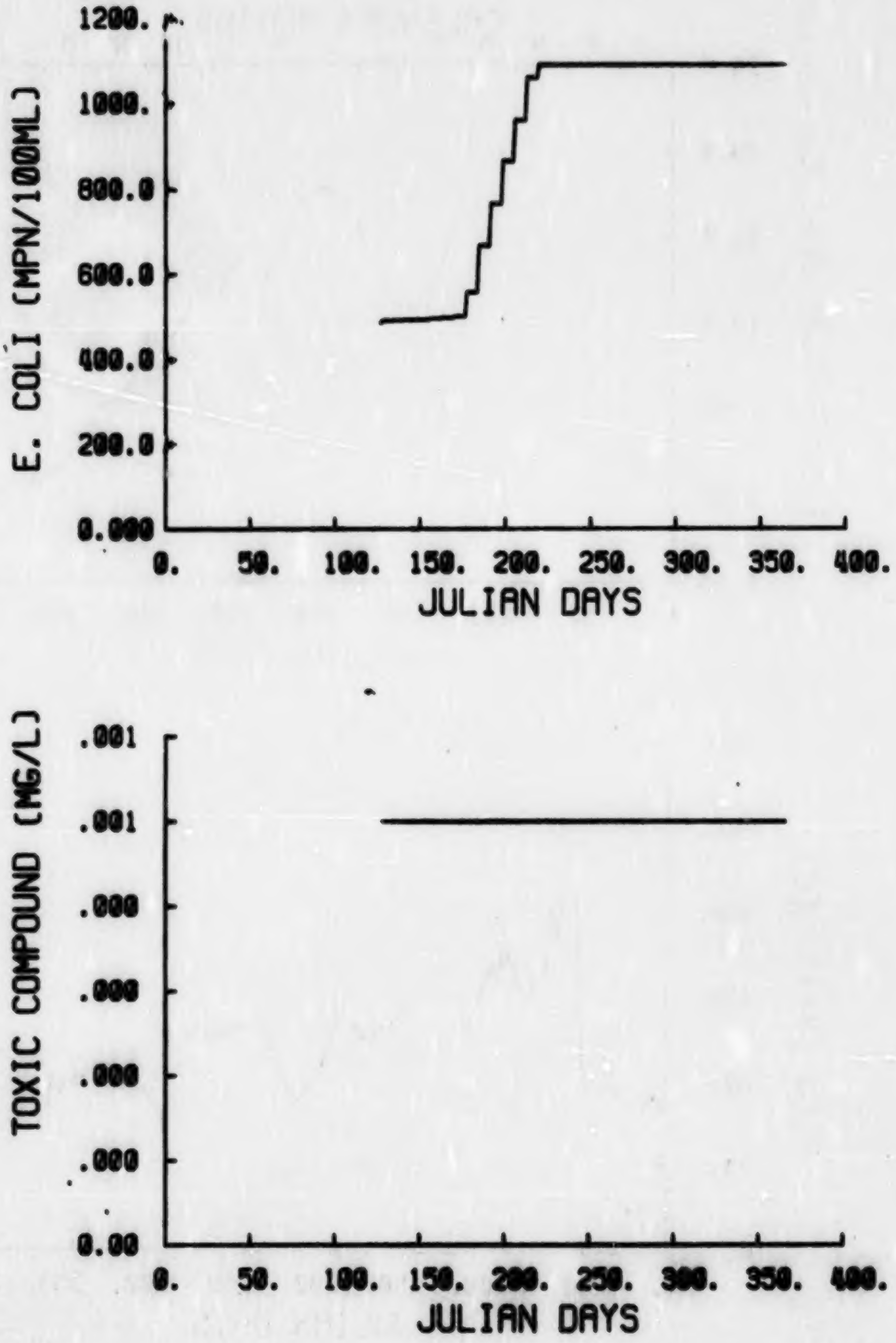

FIGURE A-7. Snake River *E. coli* and Toxic Compound, 1968

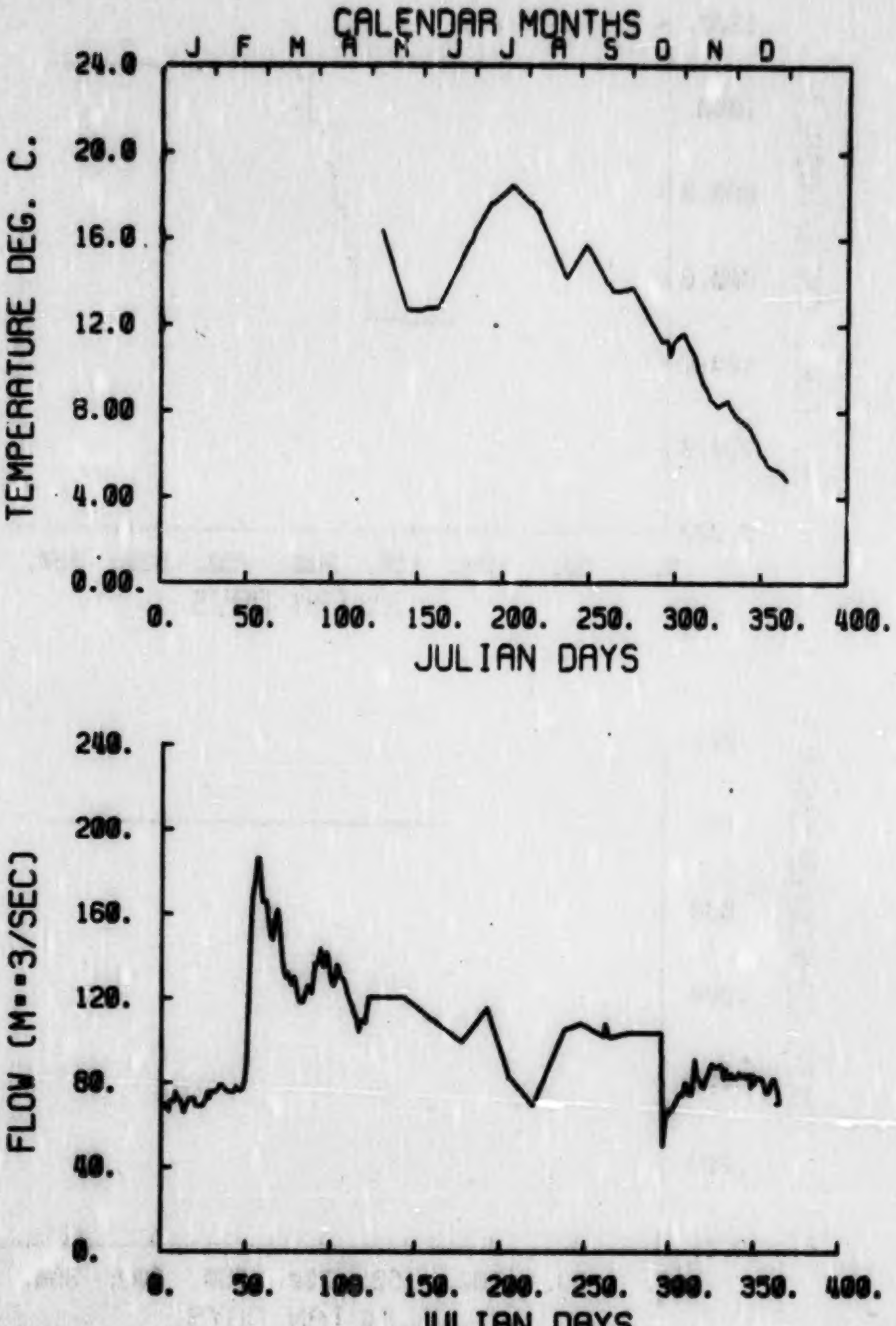

FIGURE A-8. Tributary 1-Flow and Temperature, 1968

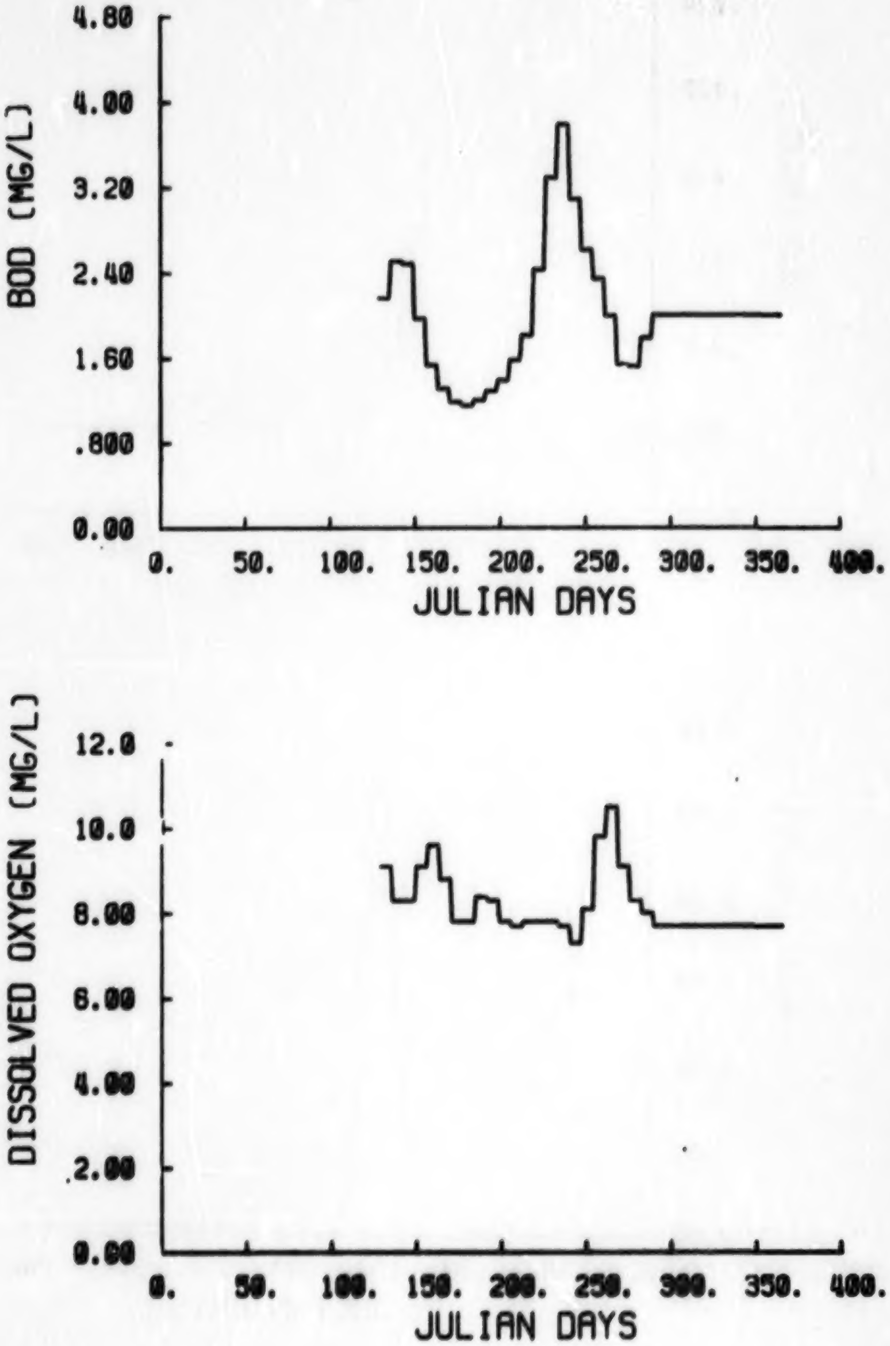

FIGURE A-9. Tributary 1-Dissolved Oxygen and BOD, 1968

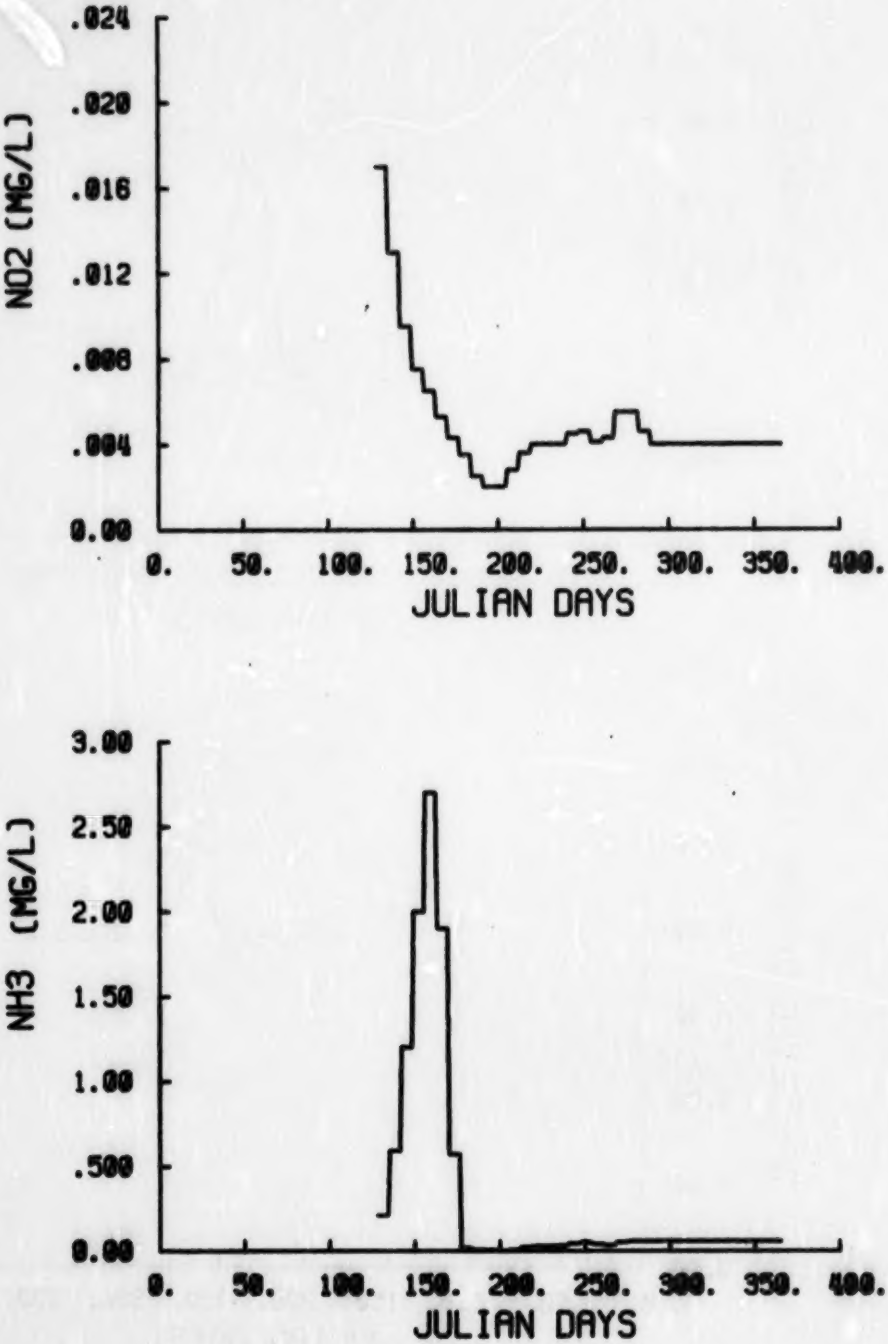

FIGURE A-10. Tributary 1-Ammonia and Nitrite, 1968

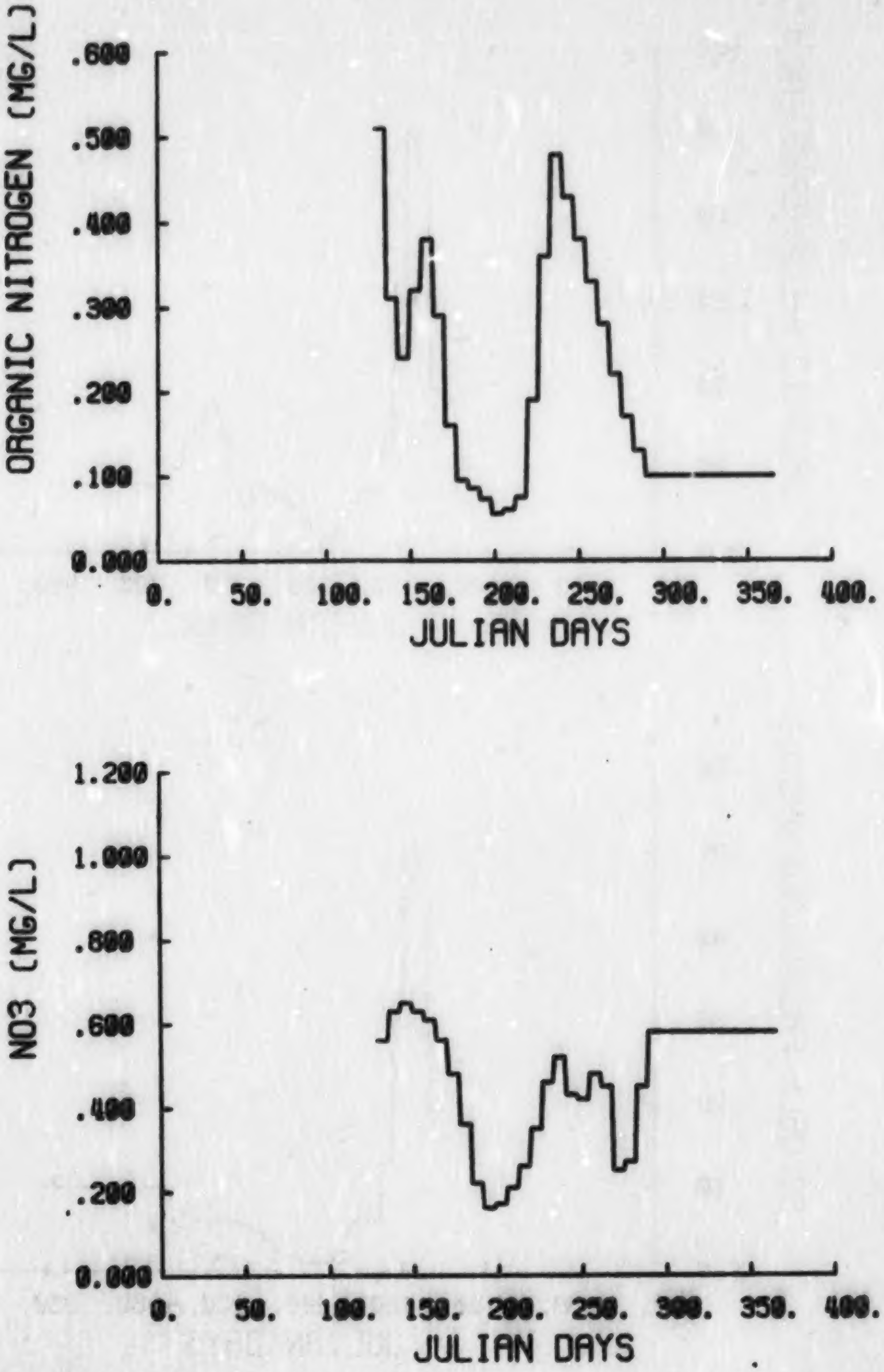

FIGURE A-11. Tributary 1-Nitrate and Organic Nitrogen, 1968

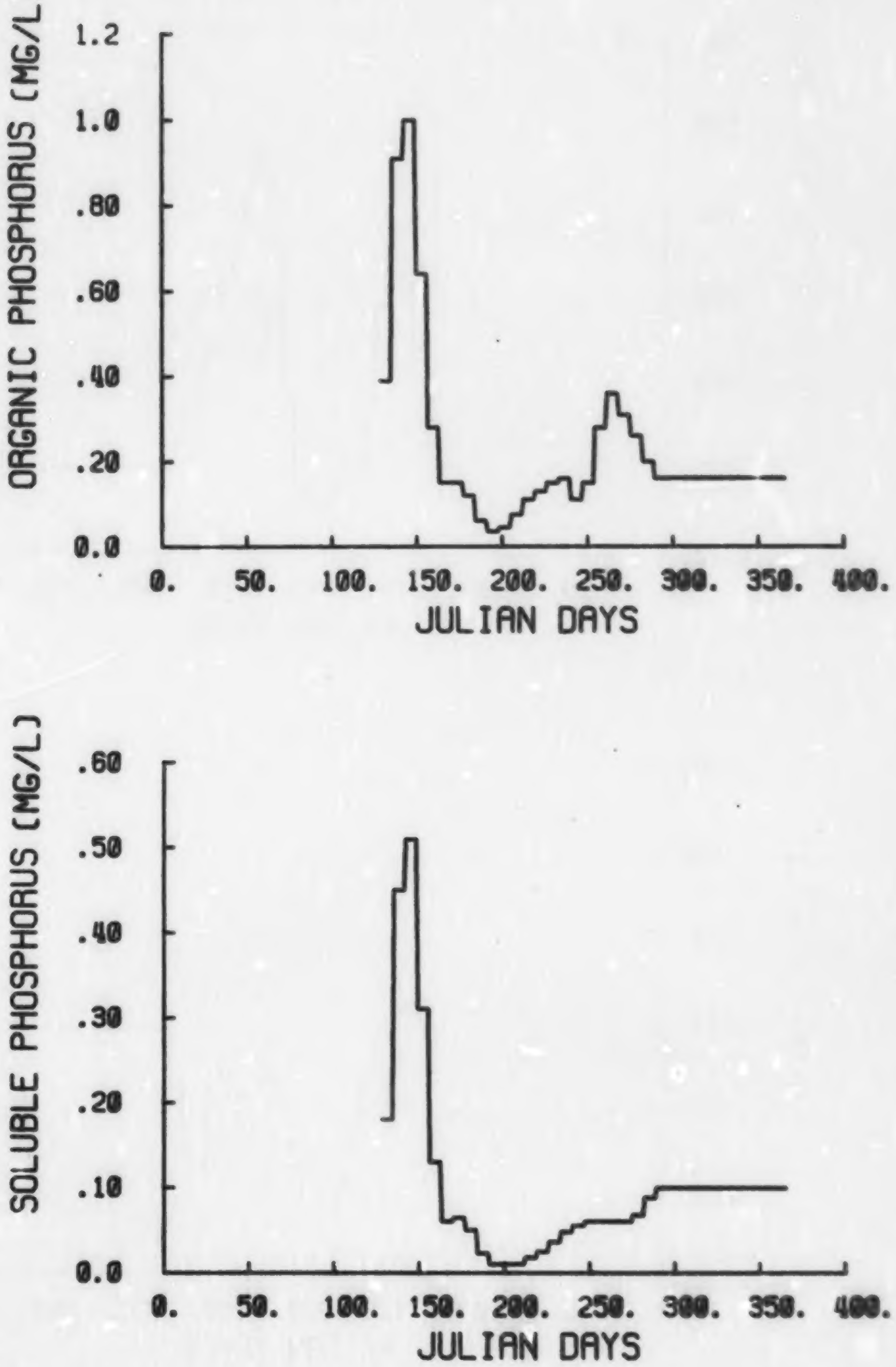

FIGURE A-12. Tributary 1-Soluble and Organic Phosphorous, 1968

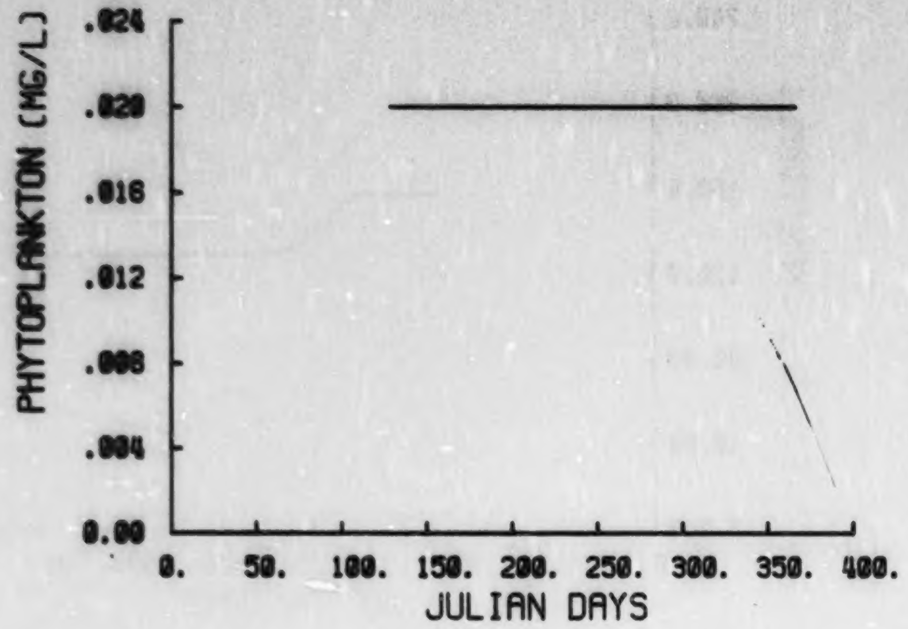

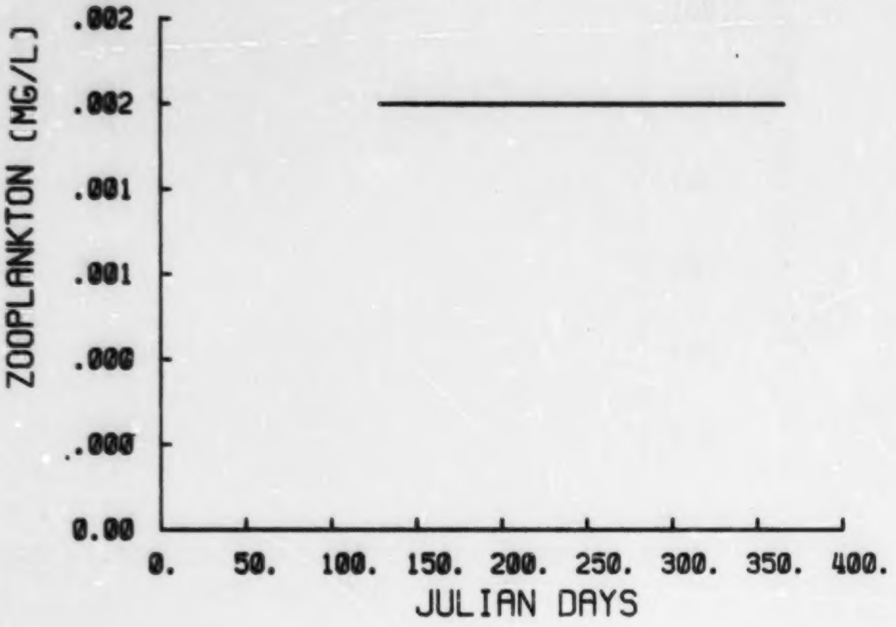

FIGURE A-13. Tributary 1-Phytoplankton and Zooplankton, 1968

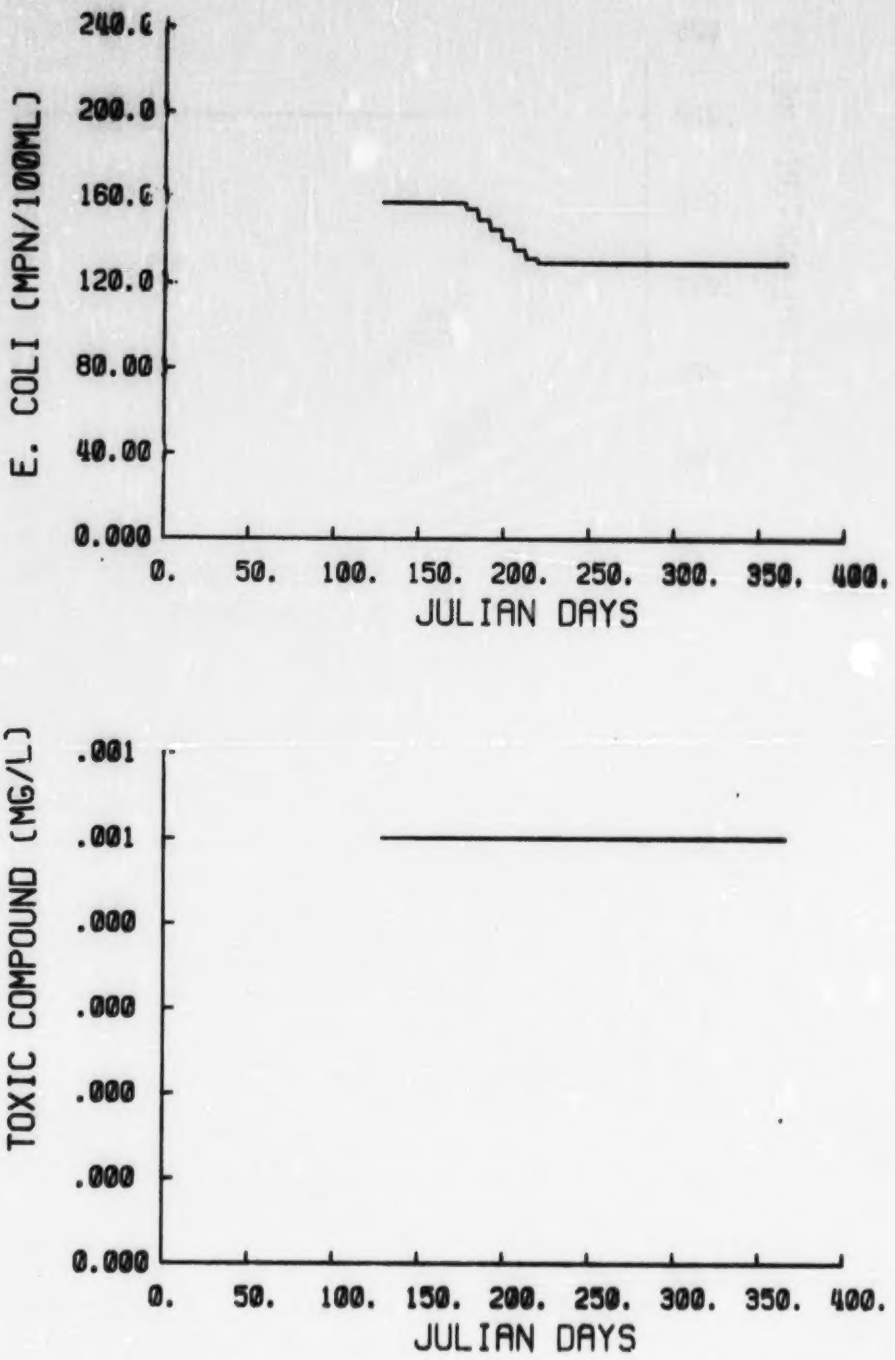

FIGURE A-14. Tributary 1-*E. coli* and Toxic Compound, 1968

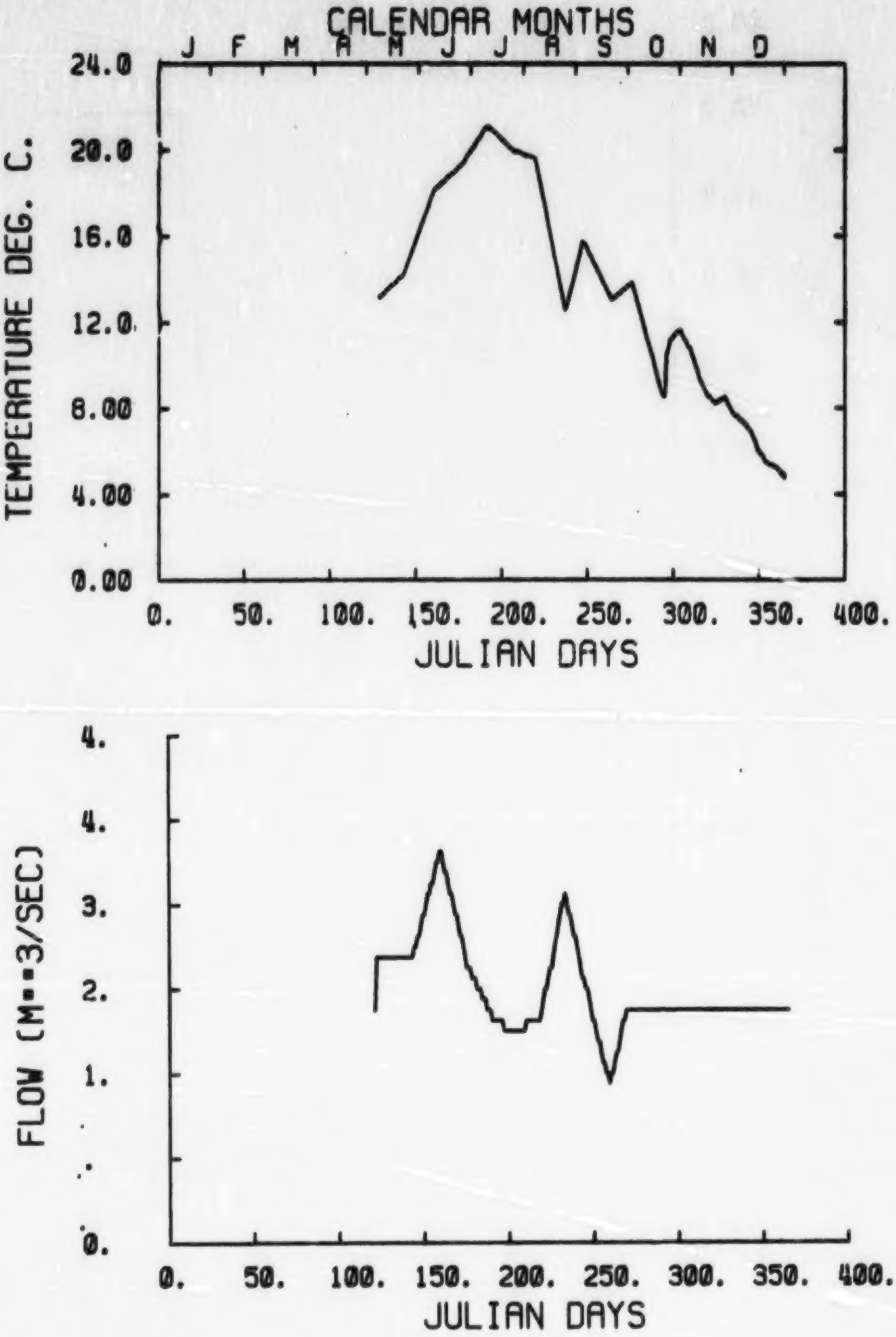

FIGURE A-15. Tributary 2-Flow and Temperature, 1968

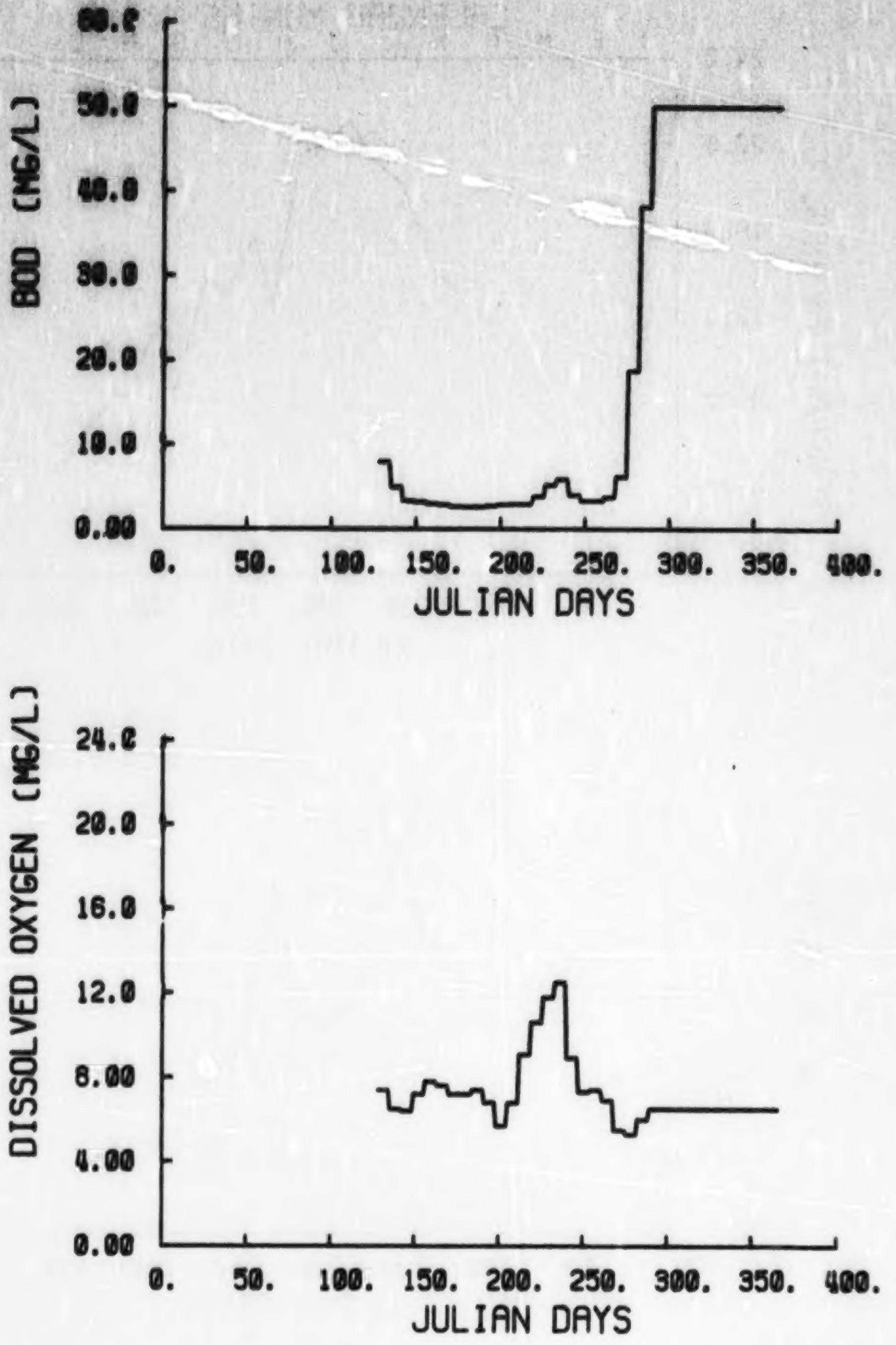

FIGURE A-16. Tributary 2-Dissolved Oxygen and BOD, 1968

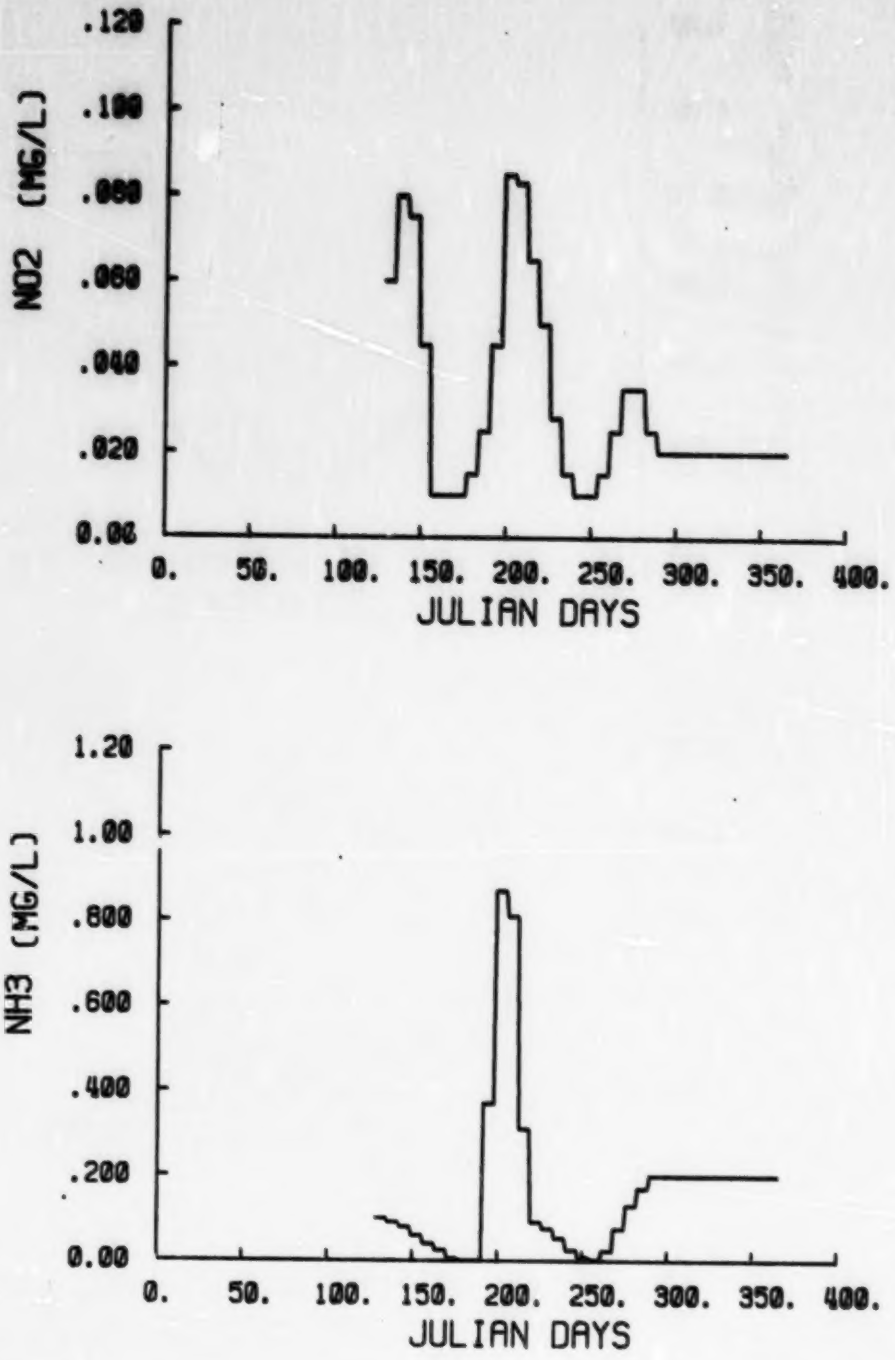

FIGURE A-17. Tributary 2-Ammonia and Nitrite, 1968

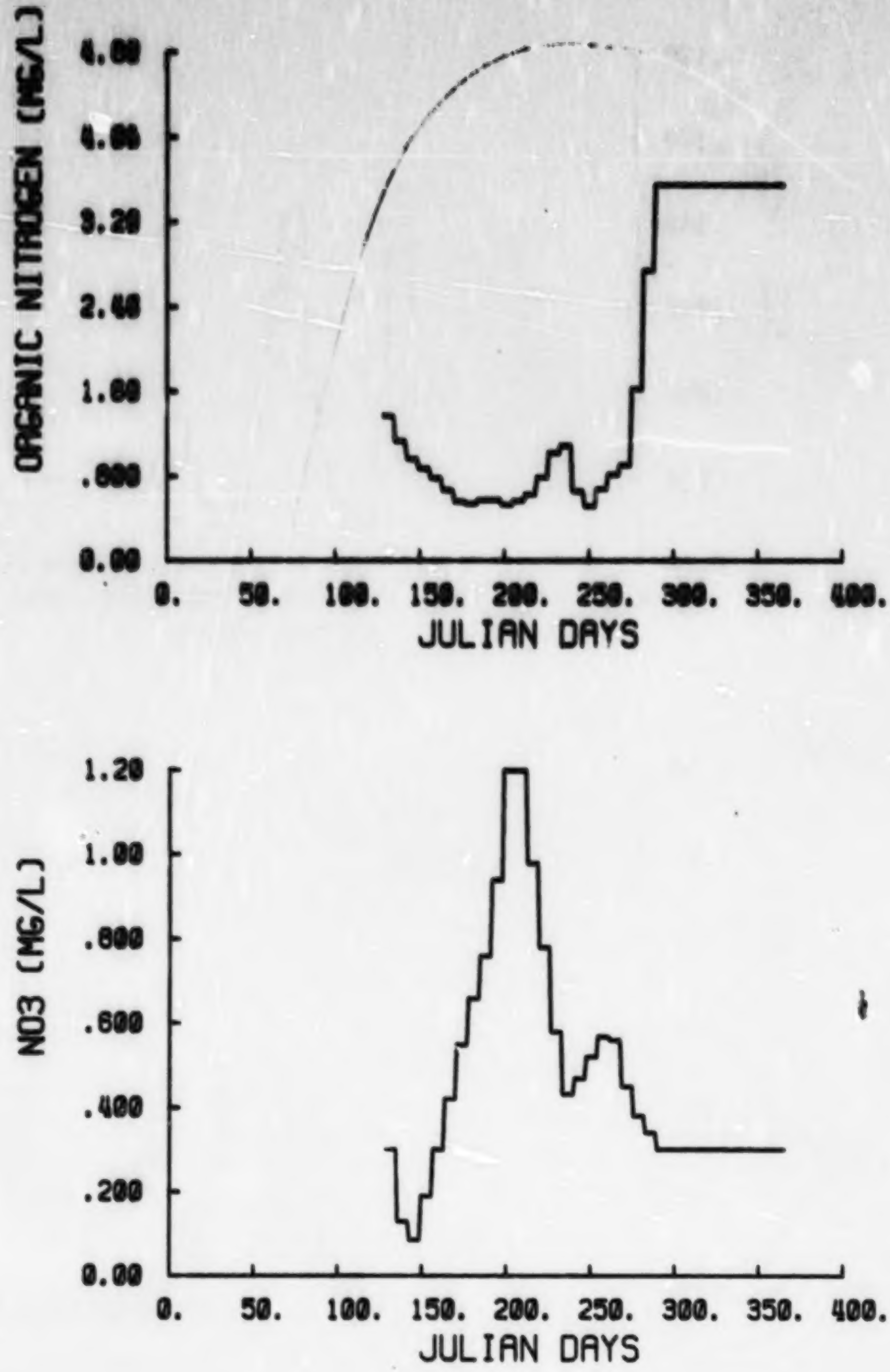

FIGURE A-18. Tributary 2-Nitrate and Organic Nitrogen, 1968

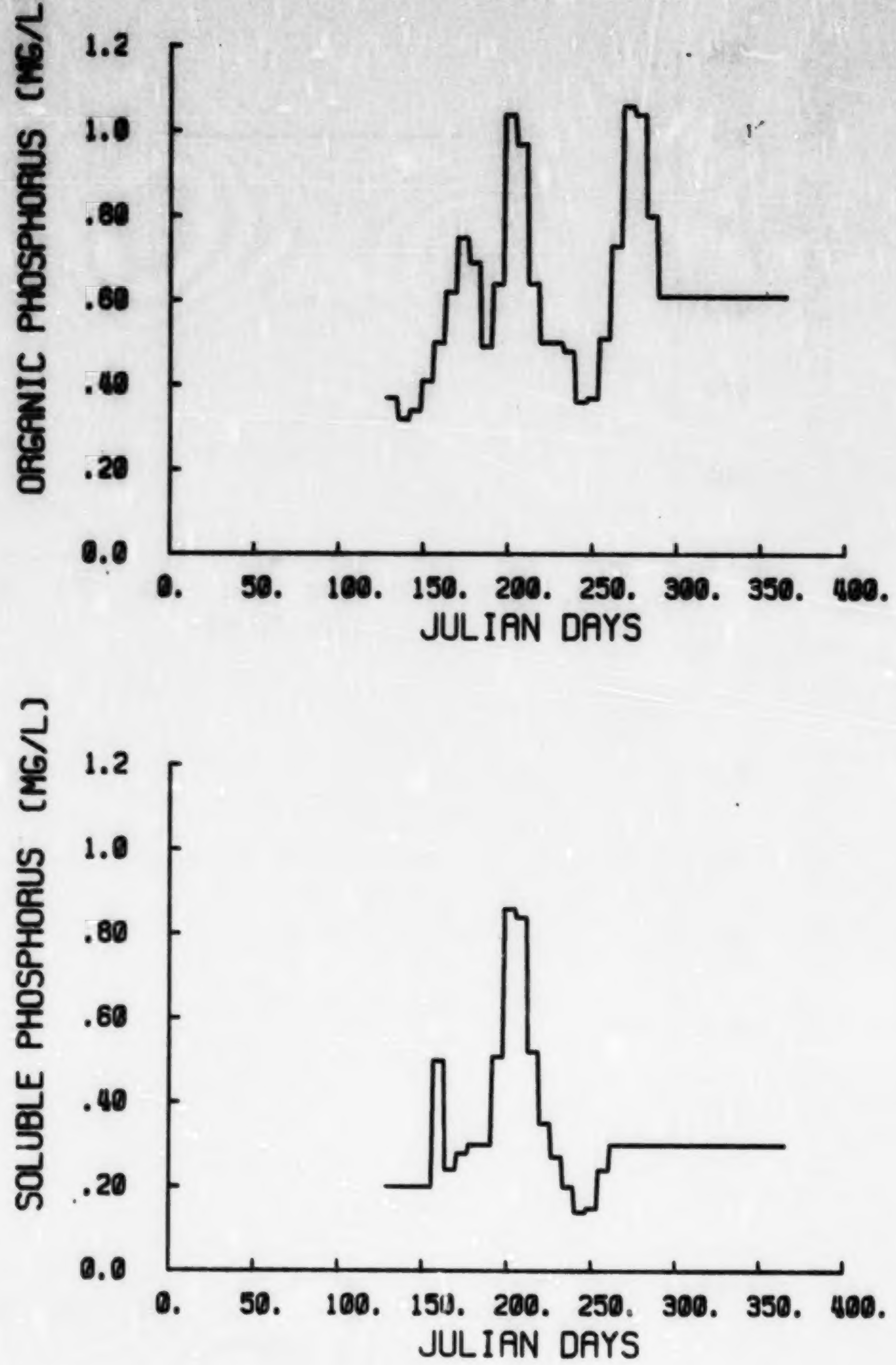

FIGURE A-19. Tributary 2-Soluble and Organic Phosphorus, 1968

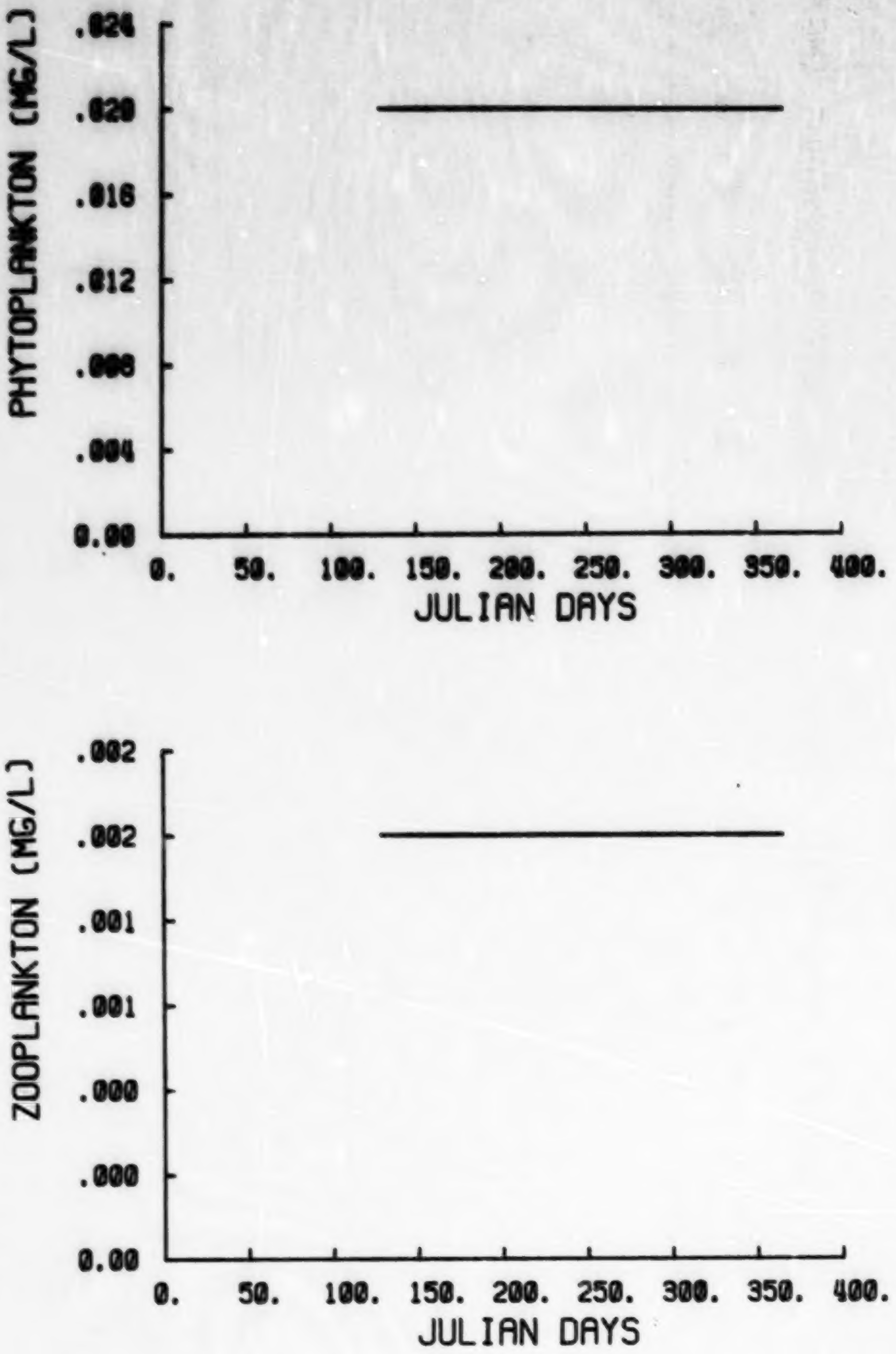

FIGURE A-20. Tributary 2-Phytoplankton and Zooplankton, 1968

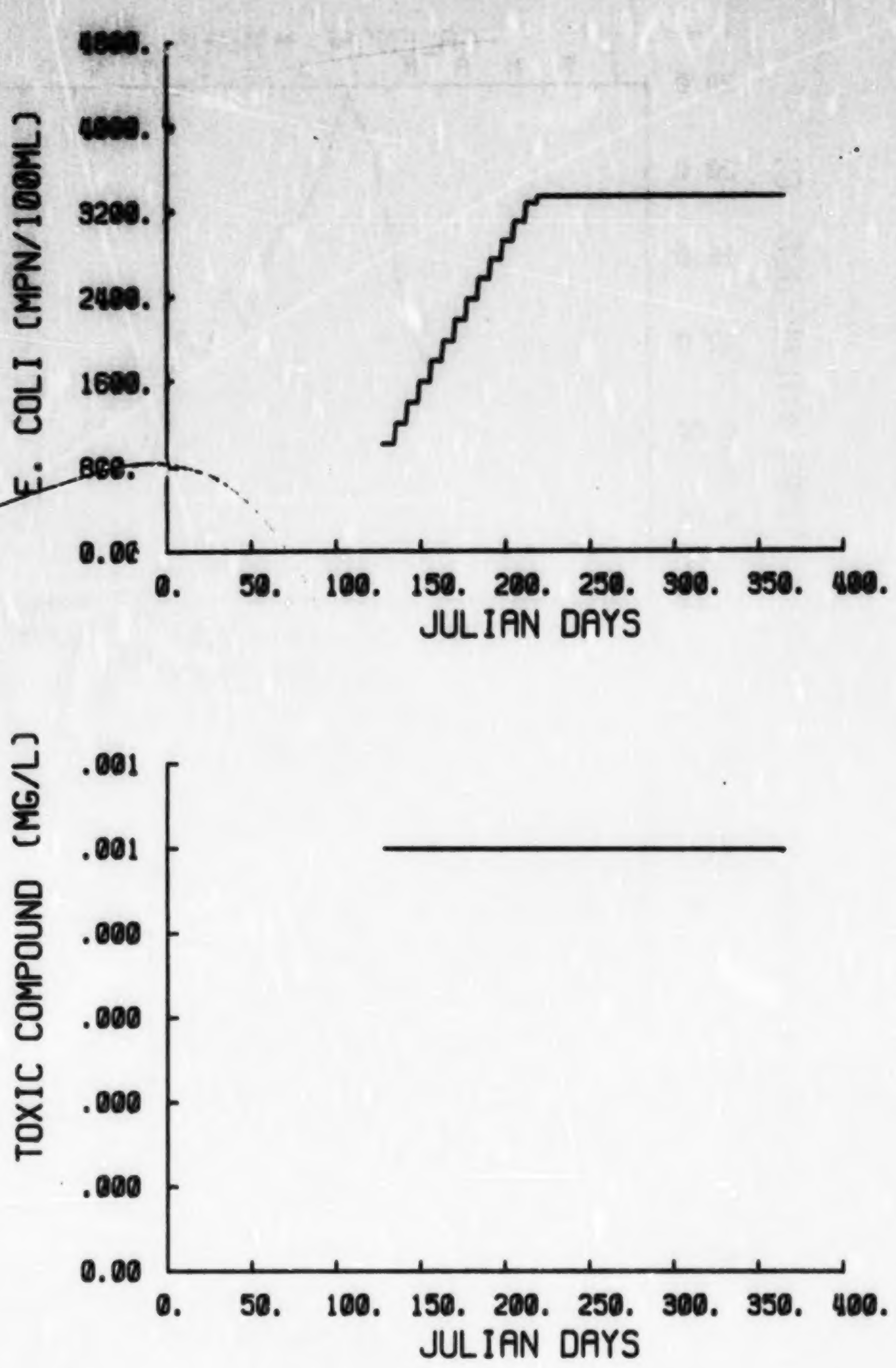

FIGURE A-21. Tributary 2-*E. coli* and Toxic Compound, 1968

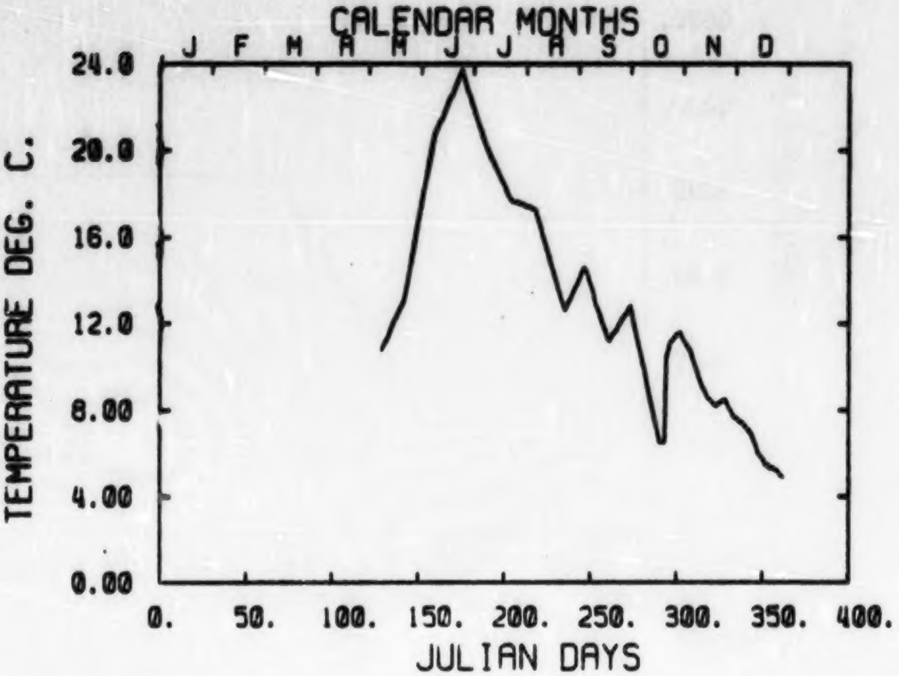

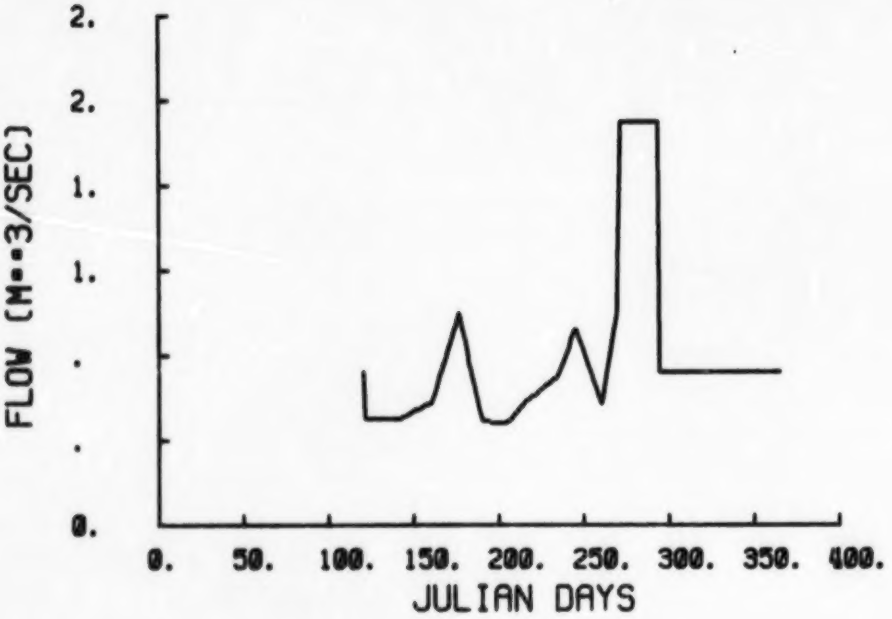

FIGURE A-22. Tributary 3-Flow and Temperature, 1968

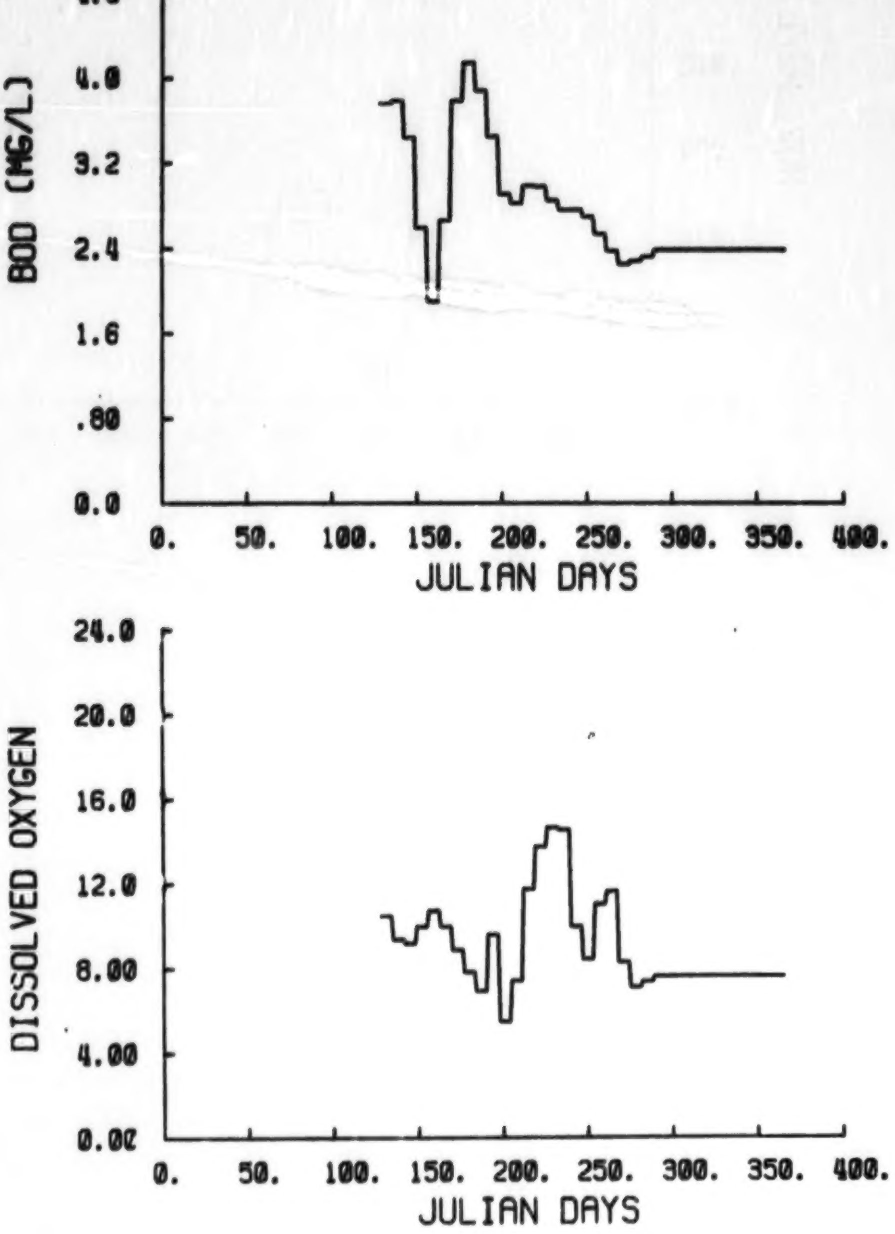

FIGURE A-23. Tributary 3-Dissolved Oxygen and BOD, 1968

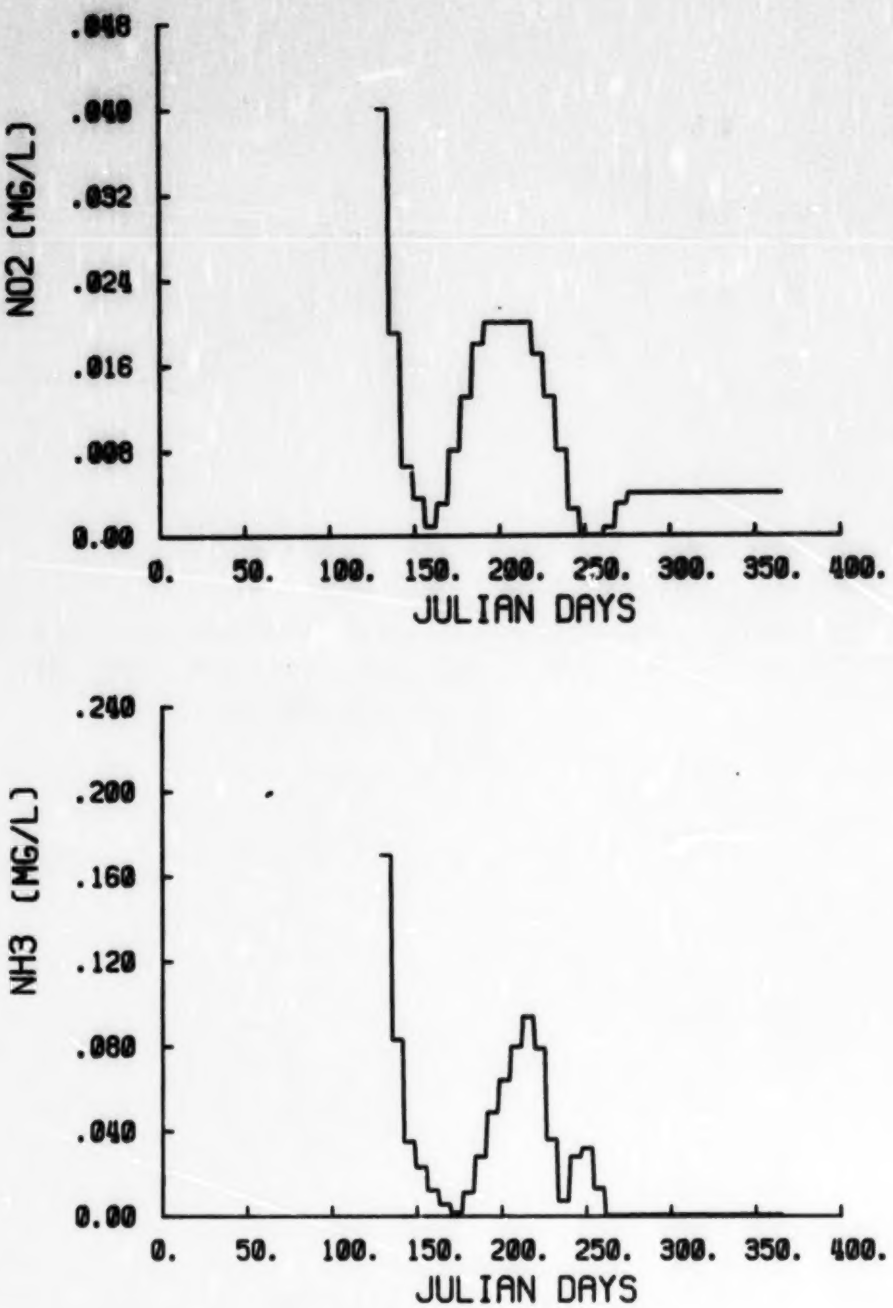

FIGURE A-24. Tributary 3-Ammonia and Nitrite, 1968

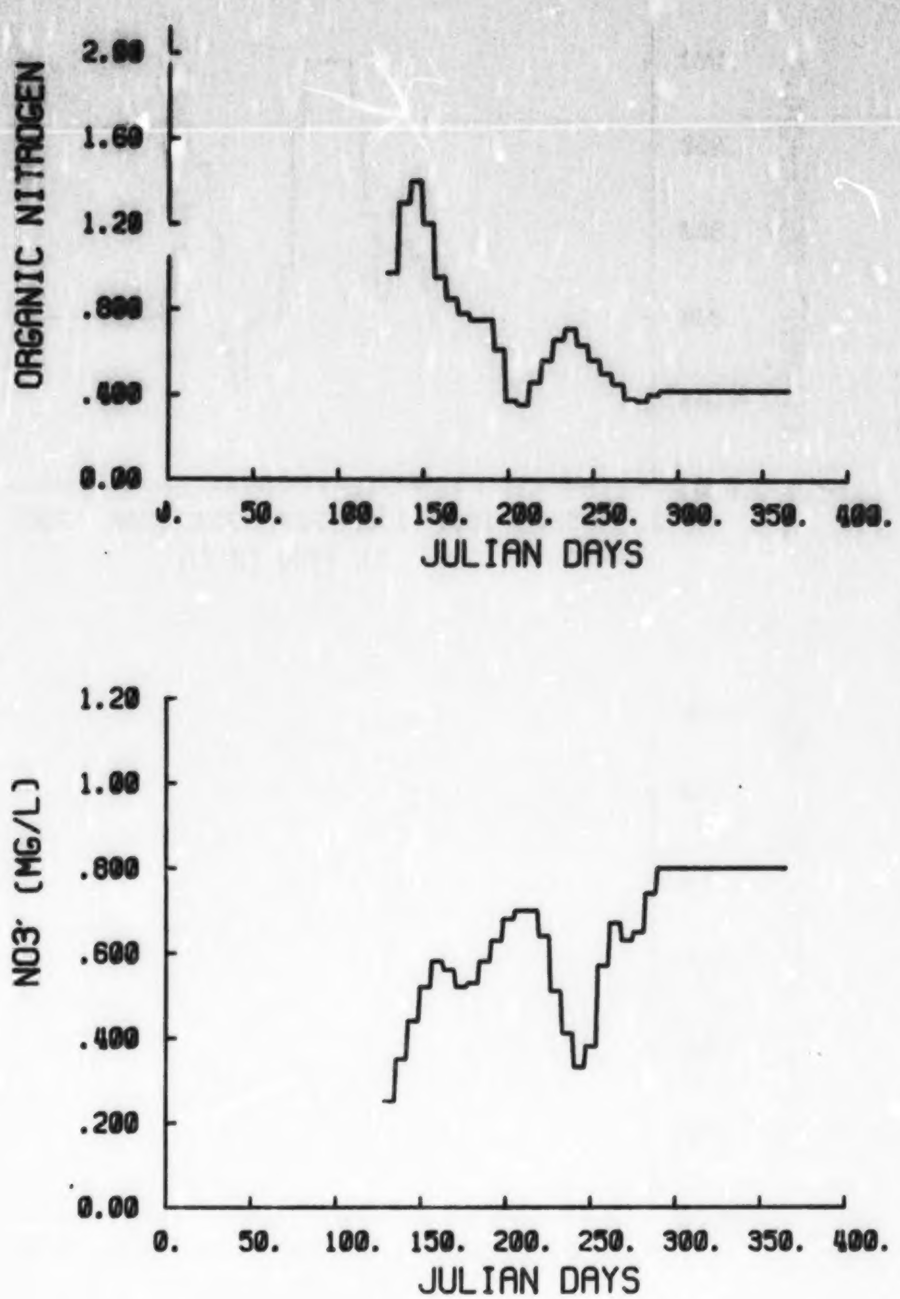

FIGURE A-25. Tributary 3-Nitrate and Organic Nitrogen, 1968

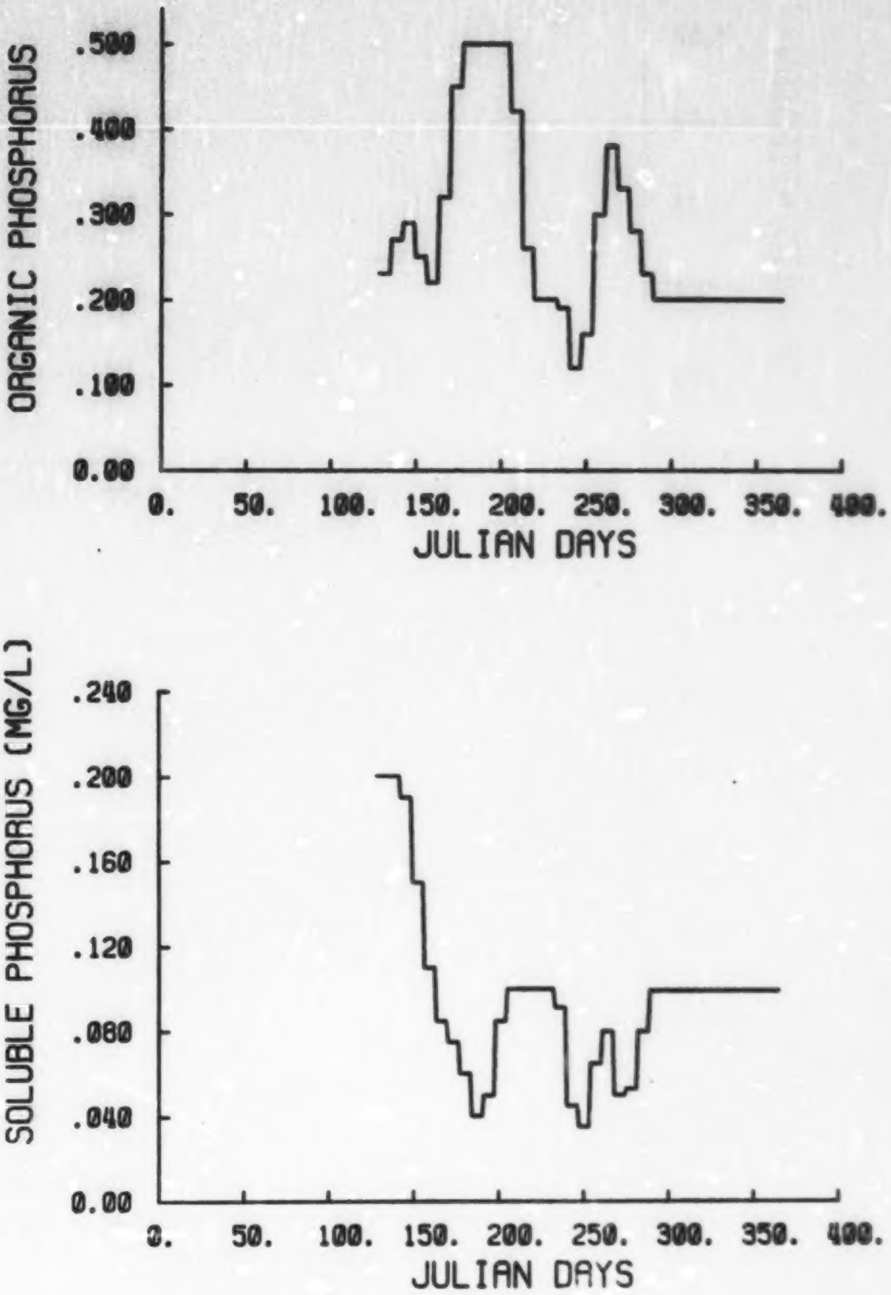

FIGURE A-26. Tributary 3-Soluble and Organic Phosphorus, 1968

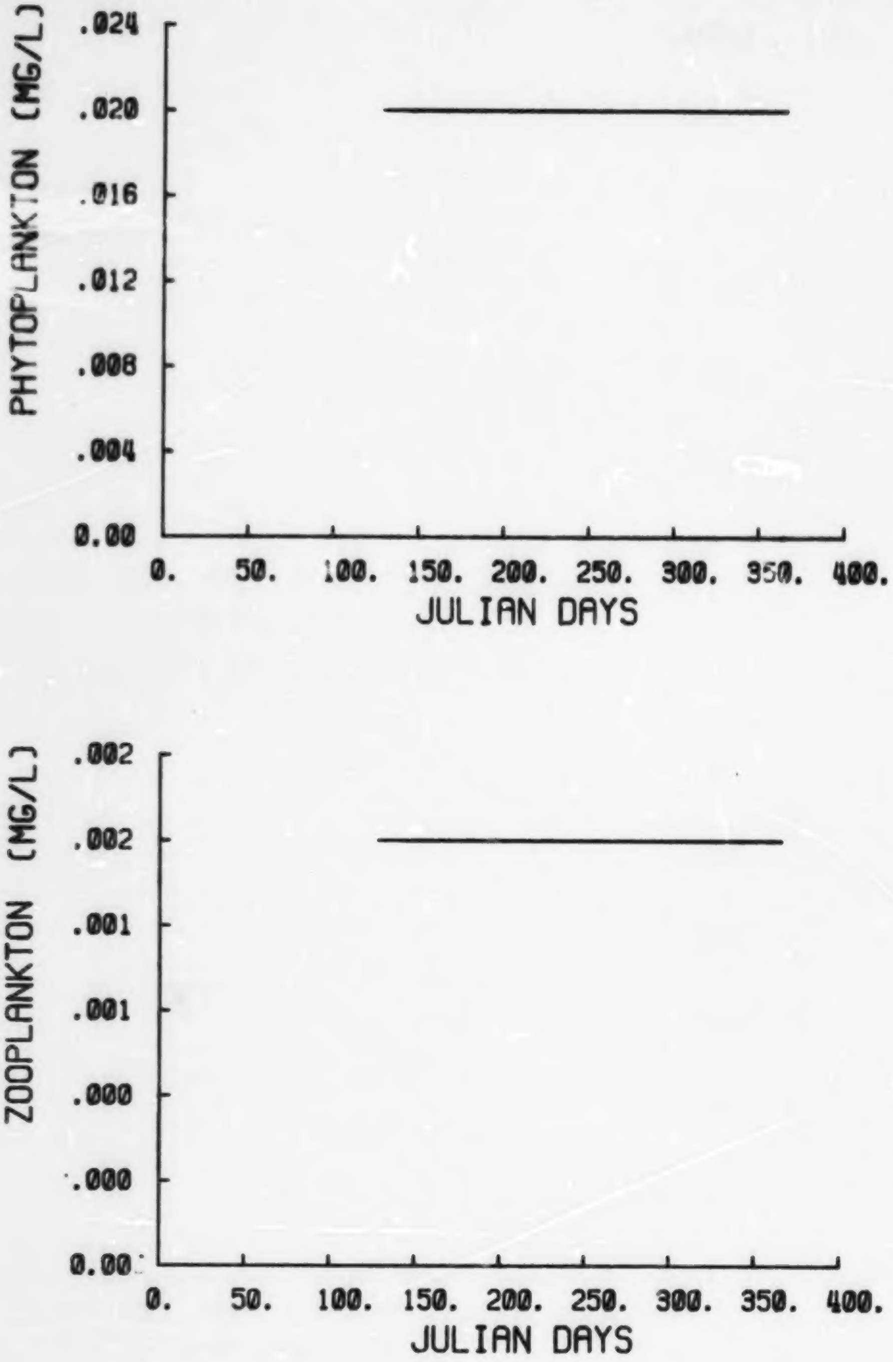

FIGURE A-27. Tributary 3-Plytoplankton and Zooplankton, 1968

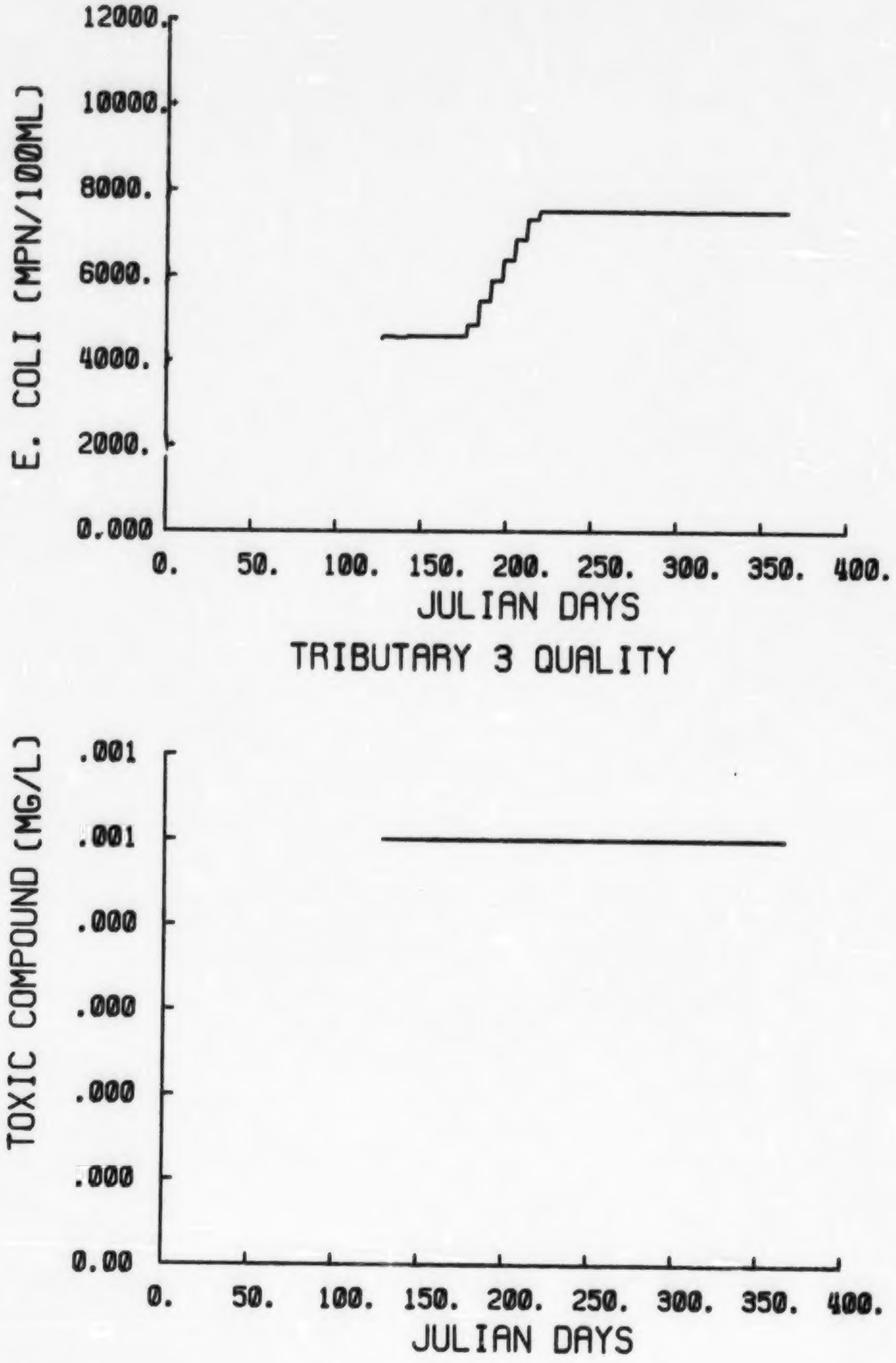

FIGURE A-28. Tributary 3-*E. coli* and Toxic Compound, 1968